AD-A091 955 DESIGN STUDY FOR GROUND-BASED ATMOSPHERIC LIDAR SYSTEM (U) GENERAL ELECTRIC CO PHILADELPHIA PA SPACE DIV R L FRANKLIN ET AL. 29 SEP 80 AFGL-TR-80-0264 1/3

UNCLASSIFIED F19628-80-C-0062 F/G 4/1 NL

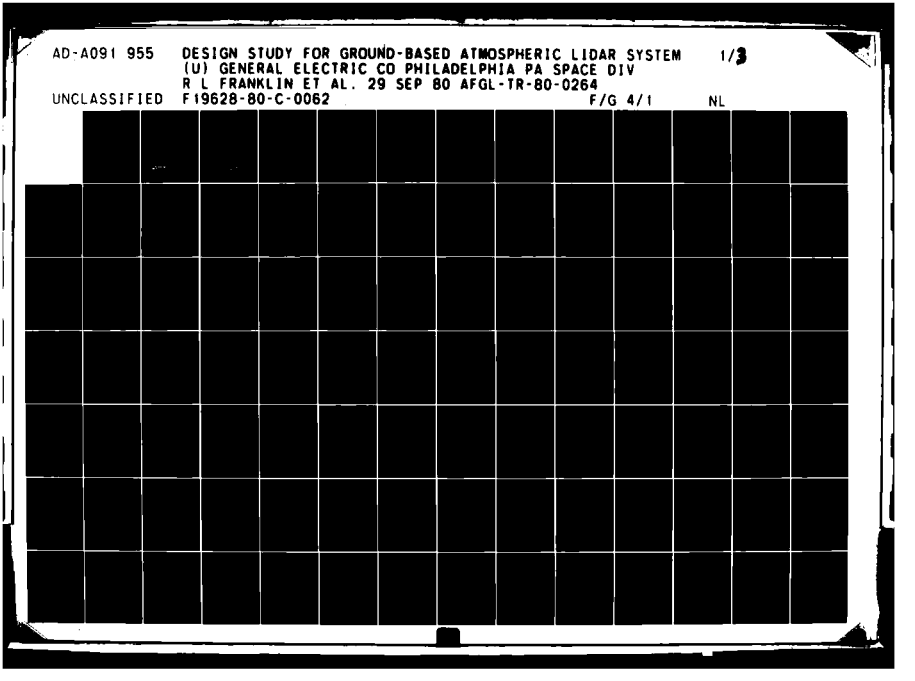

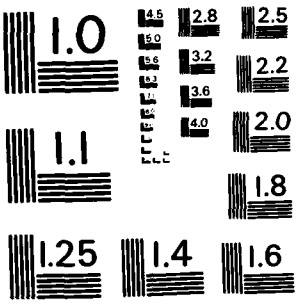

AFGL-TR-80-0264

DESIGN STUDY FOR GROUND-BASED ATMOSPHERIC LIDAR SYSTEM

R.L. Franklin
G.W. Rathke
L.W. Springer

General Electric Company
Space Division
P.O. Box 8555
Philadelphia, PA 19101

Final Report
29 February 1980 - 29 September 1980

29 September 1980

Approved for public release; distribution unlimited

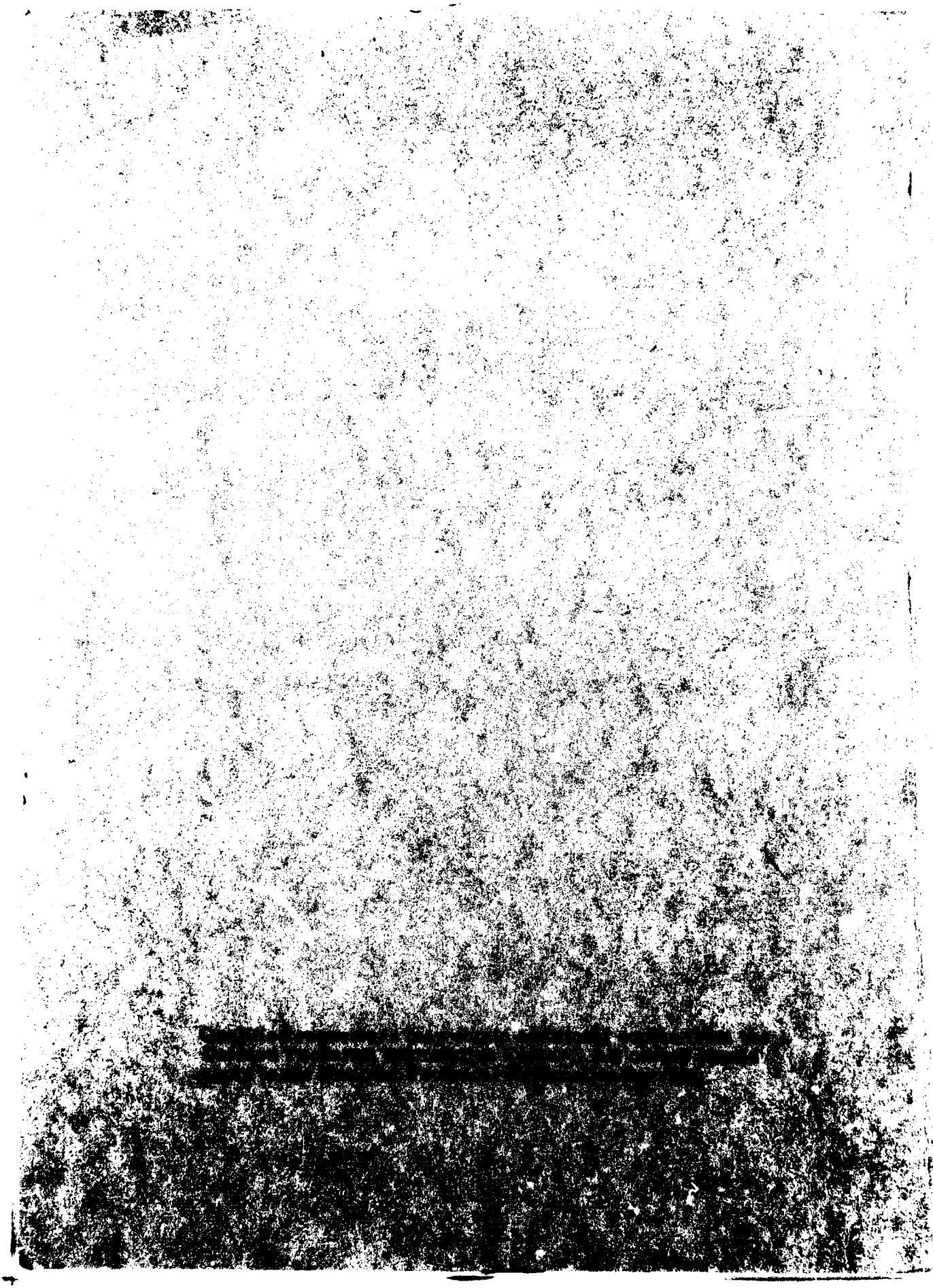

UNCLASSIFIED

SECURITY CLASSIFICATION OF THIS PAGE (When Data Entered)

REPORT DOCUMENTATION PAGE	READ INSTRUCTIONS BEFORE COMPLETING FORM
1. REPORT NUMBER: AFGL-TR-80-0264	2. GOVT ACCESSION NO.: AD-A091 955
	3. RECIPIENT'S CATALOG NUMBER:
4. TITLE (and Subtitle): DESIGN STUDY FOR GROUND-BASED ATMOSPHERIC LIDAR SYSTEM	5. TYPE OF REPORT & PERIOD COVERED: FINAL REPORT 29 FEB. 1980 TO 29 SEPT. 1980
	6. PERFORMING ORG. REPORT NUMBER:
7. AUTHOR(s): R.L. Franklin, G.W. Bethke, L.W. Springer	8. CONTRACT OR GRANT NUMBER(s): F19628-80-C-0062
9. PERFORMING ORGANIZATION NAME AND ADDRESS: General Electric Company, Space Division, P. O. Box 8555, Philadelphia, PA 19101	10. PROGRAM ELEMENT, PROJECT, TASK AREA & WORK UNIT NUMBERS: 62101F, 669004AJ
11. CONTROLLING OFFICE NAME AND ADDRESS: Air Force Geophysics Laboratory, Hanscom AFB, Massachusetts 01173, Monitor/Joseph McIsaac/LKB	12. REPORT DATE: 29 SEPTEMBER 1980
	13. NUMBER OF PAGES: vi + 236
14. MONITORING AGENCY NAME & ADDRESS (if different from Controlling Office)	15. SECURITY CLASS. (of this report): UNCLASSIFIED
	15a. DECLASSIFICATION/DOWNGRADING SCHEDULE

16. DISTRIBUTION STATEMENT (of this Report)

Approval for public release; distribution unlimited.

17. DISTRIBUTION STATEMENT (of the abstract entered in Block 20, if different from Report)

18. SUPPLEMENTARY NOTES

19. KEY WORDS (Continue on reverse side if necessary and identify by block number)

Measurement of Atmospheric Molecular Density
Transmitter Section (includes Laser, Beam Expander and 45° Mirror)
Receiving Telescope (receives scattered light from atmospheric measurements)
Detector Assembly Package
Data Collection and Data Reduction

20. ABSTRACT (Continue on reverse side if necessary and identify by block number)

The Ground-Based Atmospheric Lidar System (G-BALS) is a two-color lidar configuration which provides simultaneous measurements of light backscatter from laser wavelengths at 532 nm (green) and 355 nm (near UV). Light scatter measurements are implemented through photon counting for both the Rayleigh and Mie scatter phenomena. The system includes on-site data processing/reduction to obtain atmospheric molecular density and haze characteristics in the altitude region from 20 to 97 kilometers.

DD FORM 1 JAN 73 1473 EDITION OF 1 NOV 65 IS OBSOLETE

UNCLASSIFIED

SECURITY CLASSIFICATION OF THIS PAGE (When Data Entered)

SUMMARY/CONCLUSION

A preliminary design is presented herein for a Ground-Based Atmospheric Lidar System (G-BALS). The G-BALS is a two-color lidar configuration which provides simultaneous measurements of light backscatter from laser wavelengths at 532 nm (green) and 355 nm (near UV). Light scatter measurements are implemented through photon-counting detection of light scattered by both the Rayleigh (gas molecules) and Mie (aerosol/particulate haze) phenomena. The system includes on-site data processing/reduction to obtain atmospheric molecular density and haze scatter characteristics in the altitude region from 20 to 97 kilometers.

The G-BALS preliminary design configuration is capable of measurements up to 97 kilometers in altitude due to a self-imposed telescope size limitation of 36 inches in diameter. This limitation is based on the results of a trade study which included "cost versus size" as one of the selection criteria for the telescope definition. Therefore, if sufficient program funds are available for the follow-on Critical Design Review (CDR) and hardware phase, the G-BALS measurement capability can be extended to 100 kilometers in altitude by increasing the telescope size to 54 inches in diameter. Measurement of atmospheric density from 20 to 100 kilometers in altitude is the primary objective of the system capability.

Techniques are also included to achieve G-BALS secondary objectives that detect and measure particulates, minor species concentrations, gas temperatures and wind characteristics.

There are no new technology requirements for the G-BALS described herein. All subsystems utilized in assembling the system are in the "state-of-the-art" technology categories and are commercially available.

In summary, the G-BALS preliminary design effort has addressed all the technical areas and meet all objectives identified in the Statement-of-Work issued by the Air Force Geophysics Laboratory (AFGL). The G-BALS preliminary design configuration is ready to proceed into the Critical Design Review (CDR) phase and subsequent operational hardware phase.

PREFACE

This document is the final report for the Design Study of a Ground-Based Atmospheric Lidar System, which was performed by the Electro-Optics and Sensors Subsection of the General Electric Company's Space Division. The study was performed under Contract No. F19628-80-C-0062 for Mr. Joseph P. McIsaac, Contract Manager, Air Force Geophysics Laboratory, Hanscom Air Force Base, Massachusetts.

The following individuals at General Electric contributed to this design study effort:

R. L. Franklin	Program Manager
Dr. G. W. Bethke	Senior Physicist and Principal Investigator
L. W. Springer	Electronic Engineer
C. G. Clay	Computer Systems Engineer
R. P. Estes	Designer
C. G. Hunt	Designer

AD-A091 955

The following are blank pages:

ii, 4, 8, 12, 51, 53, 67, 118, 120, 128,

140, 148, 154, 160, 164, 198, 214, 223 & 227.

TABLE OF CONTENTS

TABLE OF CONTENTS (continued)

1.0 INTRODUCTION

1.0 INTRODUCTION

The data contained herein presents the final results of a preliminary design study of a Ground-Based Atmospheric Lidar System (G-BALS). General Electric Company, Space Division was awarded a seven-month, preliminary design study on 29 February 1980 by the Air Force Geophysics Laboratory (AFGL), Hanscom Air Force Base, Massachusetts.

Primary tasks pursued to accomplish this effort and meet the objectives stated in Section 3.0 were:

a) Preform trade studies/analysis.

b) Develop system design requirements.

c) Prepare preliminary design drawings/plans and specifications.

As stated in the previous Summary paragraph, the primary objectives of this study have been accomplished and a preliminary design of a baseline lidar system has been completed.

This final report is organized and presented in a manner to facilitate the understanding of definitions, capabilities, design features, and performance specifications of all major subsystems. These subsystems are then assembled to form the overall lidar system.

A brief description of each section contained in the final report follows.

Section 2.0 states the primary and secondary objectives of the design study and program plans/tasks which were implemented to accomplish this effort.

Section 3.0 describes the approach that GE implemented to arrive at an optimum and cost effective system based on the guidelines established by AFGL during the study.

Section 4.0 describes the overall lidar system and is further sub-sectioned to describe each subsystem. Each subsystem is described by a specification and a preliminary design drawing. Specific model numbers and recommended vendors are also identified for selected subsystems which are purchased as off-the-shelf units (i.e., laser, beam expander, etc.). Notations are made where off-the-shelf items require additional features to be added or modified to meet performance requirements of the Ground-Based Atmospheric Lidar System.

Section 5.0 describes several safety features. A radar system is recommended for overhead detection of aircraft which would automatically deactivate the laser before any aircraft entered the lidar field-of-view. Various safety considerations for on-site personnel are also included.

Section 6.0 depicts and recommends an alignment technique and describes a step-by-step procedure to implement the total alignment initially. Subsequent "quick check" features are included for verification prior to operational usage.

Section 7.0 outlines a test and calibration procedure for G-BALS.

Section 8.0 covers cleanliness and periodic cleaning requirements of optical elements.

Section 9.0 identifies on-site G-BALS facility requirements such as water, power, thermal protection, minimum floor area and access. In addition, various Ground Support Equipment (GSE) that are envisioned at this time are identified.

Section 10.0 briefly describes transportability considerations.

Section 11.0 lists all the trade studies and their results that were utilized by GE and AFGL to arrive at a baseline G-BALS configuration which is presented in this final report.

Section 12.0 lists several sources of perturbations and interferences that would impact the final measurements/results of the data collected by the G-BALS.

Section 13.0 discusses secondary objectives of the baseline G-BALS. These secondary objectives include detection and measurements of particulates, species concentration, gas temperature, and wind characteristics.

An Appendix section includes supplemental data.

Data presented in the following sections are arranged in a format in which a summarizing or pictorial presentation is provided on the right hand page (odd numbered) with the corresponding detailed narrative contained on the facing left hand page (even numbered). A publication fashioned in this manner has proven to be most useful to facilitate the understanding and use of this data in technical and management presentations.

2.0 OBJECTIVES

2.0 OBJECTIVES

The task of General Electric's design study team has been to investigate, design, and submit plans, drawings and/or prints for the development and fabrication of a ground-based lidar system. The primary objective of this lidar system will be the measurement of atmospheric molecular density in the altitude region from 20 to 100 kilometers. Secondary objectives can include the detection and measurement of particulates, minor species concentrations, gas temperature, and winds.

Table 2-1 lists general system and task requirements including various categories of design considerations that are addressed in relation to system performance.

TABLE 2-1

2.0 GENERAL SYSTEM AND TASK REQUIREMENTS

1) Measure atmospheric molecular density at altitudes of 20-100 km, with the following goals:

	Altitude	
Goals	20 km	100 km
Accuracy	4%	10%
Altitude resolution	0.5 km	2.5 km
Measurement time	5 min	15 min

2) Calibration techniques and procedures.

3) Test, evaluation and set-up time and procedures.

4) Data processing technique and procedures.

5) Operational constraints:
   a) eye safety;
   b) environmental factors;
   c) operational/general safety;
   d) instrumentation limitations (power, thermal, etc.).

6) Equipment configuration/definition:
   a) laser/transmitter-type, power, size, stability, reliability, availability, etc.;
   b) optics/receiver-type, configuration, size, simplicity, sturdiness, etc.;
   c) detector/data interface - counters, microprocessor, realtime storage, etc.;
   d) off-the-shelf or existing equipment concept where feasible.

7) Perturbations:
   a) clouds, aerosols, daylight;
   b) signal/noise levels;
   c) background discrimination.

8) Cleanliness/maintenance.

9) Transportability.

3.0 DESIGN APPROACH

3.0 DESIGN APPROACH

The design of this ground-based atmospheric lidar system (G-BALS) is based on simultaneous measurement of light back-scattered from two laser wavelengths, at 532 nm (green) and at 355 nm (near UV), The light at each wavelength is scattered by both the gas molecules (Rayleigh scattering) and the aerosol/particulate haze (Mie scattering). Since the Rayleigh and Mie scatter phenomena vary differently with wavelength, the making of scatter measurements at two wavelengths allows the two effects to be separated during data reduction. The atmospheric density profile is then directly obtained from the Rayleigh scatter information.

Due to the very low signal levels obtained from the highest altitudes, photon counting detection techniques are employed along with digital data processing. For little added cost, the system even has the capability for "on-site" data reduction to rapidly yield atmospheric density and haze scatter coefficients as a function of altitude.

Within the limits permitted by the system performance requirements, cost minimization was stressed. The use of both wavelengths from the same laser reduces laser costs as well as eliminating the added problems of synchronizing or tying to two separate laser systems. Because large telescopes are extremely expensive and increase in cost with approximately the cube of their diameter, the use of relatively expensive high efficiency optical coatings throughout will actually save money by allowing use of a smallest receiving telescope. The use of commercial components, a stationary site, and fixed vertical pointing considerably reduces component, structural, and facilities costs. A conservative design philosophy was followed so as to reduce risk.

3.0 DESIGN APPROACH

- Use Two-Color Lidar Concept
  - Laser wavelengths used:

    532 nm (green)
    355 nm (near UV)
  - Measure Rayleigh (gas) plus Mie (haze) backscatter at both wavelengths.
  - Permits analytical separation of gas (density) and haze effects.
- Photon Counting Detection
- Digital Data Processing
- Capability for On-Site Data Reduction
- Minimize Cost
  - Both laser wavelengths are from same laser.
  - Maximum efficiency optics throughout, to reduce required telescope size.
  - Stationary lidar site.
  - Fixed vertical pointing direction only.
  - Conservative design to reduce development uncertainties.
  - Extensive use of commercially available components and sub-systems.

4.0 SYSTEM DESCRIPTION

4.0 SYSTEM DESCRIPTION

4.0.1 Simplified Optical Block Diagram

Briefly, the G-BALS is to use an up-collimated Neodymium:YAG frequency doubled and tripled laser beam as the two-wavelength light source, a large aperture compound reflecting telescope as the lidar receiver, and an array of photomultiplier tube (PMT) detectors with beam splitters and narrow band filters for spectral isolation.

As detailed in Section 4.1, a two-color laser output is to be used, this being supplied by a commercially-available Nd:YAG laser which is capable of simultaneous large outputs at both 532 nm (green) and 355 nm (near UV) at a 10 pps repetition rate. Figure 4.0-1 illustrates how the laser output will pass through a laser energy monitor WE and then through an upcollimating beam expander to decrease laser beam divergence. After leaving the beam expander, the laser beam will reflect off adjustable flat mirror FM so as to become parallel to the adjacent receiver telescope axis. This adjustable mirror is the means by which the lidar laser is boresighted to the lidar receiver.

For eye safety, a small microwave radar transceiver system is also recommended so as to allow automatic abort of laser system output when an aircraft nears the laser beam.

(continued)

4.0.1 SYMBOLS FOR SIMPLIFIED OPTICAL DIAGRAM

(See Figure 4.0-1, next page)

BS beam splitter with large T and small R

CL collimating lens

DL detector lens

DM dichroic mirror (transmit green and reflect UV)

FU UV bandpass interference filter

FG green bandpass interference filter

FM flat mirror

FS field stop (at telescope focus)

NF neutral filter (to adjust PMT sensitivity)

PM primary mirror

PMT photomultiplier tube detector, together with its amplifier/discriminator for photon counting

PS shutter wheel position sensor

R reflectance

RL relay lens

SM secondary mirror

SW shutter wheel

T transmittance

UV ultraviolet

WE combination window and laser energy monitor

WT telescope focus window

4.0.1 Simplified Optical Block Diagram (continued)

After the backscattered laser light plus any background light is reflected off the receiver primary mirror PM to the secondary mirror SM, the light is focused through the telescope indoor/outdoor window WT onto field stop FS. This focus is also near shutter wheel SW(A). After passing through FS, the now diverging light is collimated by lens CL and then directed to several detectors PMT-1 through PMT-6 via a dichroic mirror DM, flat mirror FM, bandpass filters FG and FU, a series of beam splitting mirrors BS, some intensity-adjusting neutral filters NF, detector lenses DL, and in some cases also through relay lenses RL.

Dichroic mirror DM is a "long pass" type which transmits the green light to 532 nm bandpass filter FG, and which reflects the near UV light to 355 nm bandpass filter FU. The purpose of the four beam splitters BS is to apportion the light between the three PMT's, which are provided for each wavelength, in such a manner that each PMT is used at an optimum light intensity during its assigned lidar altitude interval.

Shutter wheel SW(A) covers field stop FS during relatively intense lidar signals from altitudes below 20 km, protecting the light-sensitive PMT's. Shutter wheel SW(B) is on the same shaft as SW(A), but with a different angular adjustment such that it protects the two most sensitive (highest altitude) detectors from lidar signals originating below 40 or 50 km altitude.

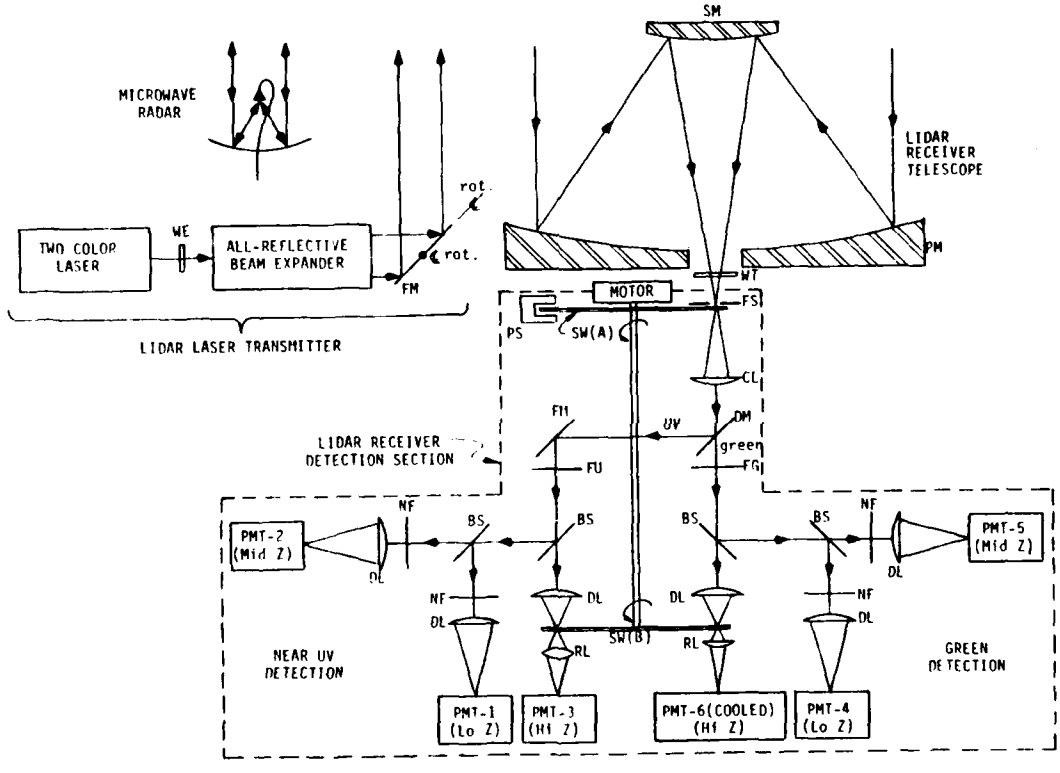

Figure 4.0-1. Simplified Optical Block Diagram of G-BALS

4.0.2 Simplified System Electronic Block Diagram

The weak lidar signals detected by the PMT's are to be measured by photon counting techniques. Thus each PMT output is processed by its own amplifier/discriminator. The discriminator outputs are then switched by multiplexers to a fast multichannel counter plus data processing and storage.

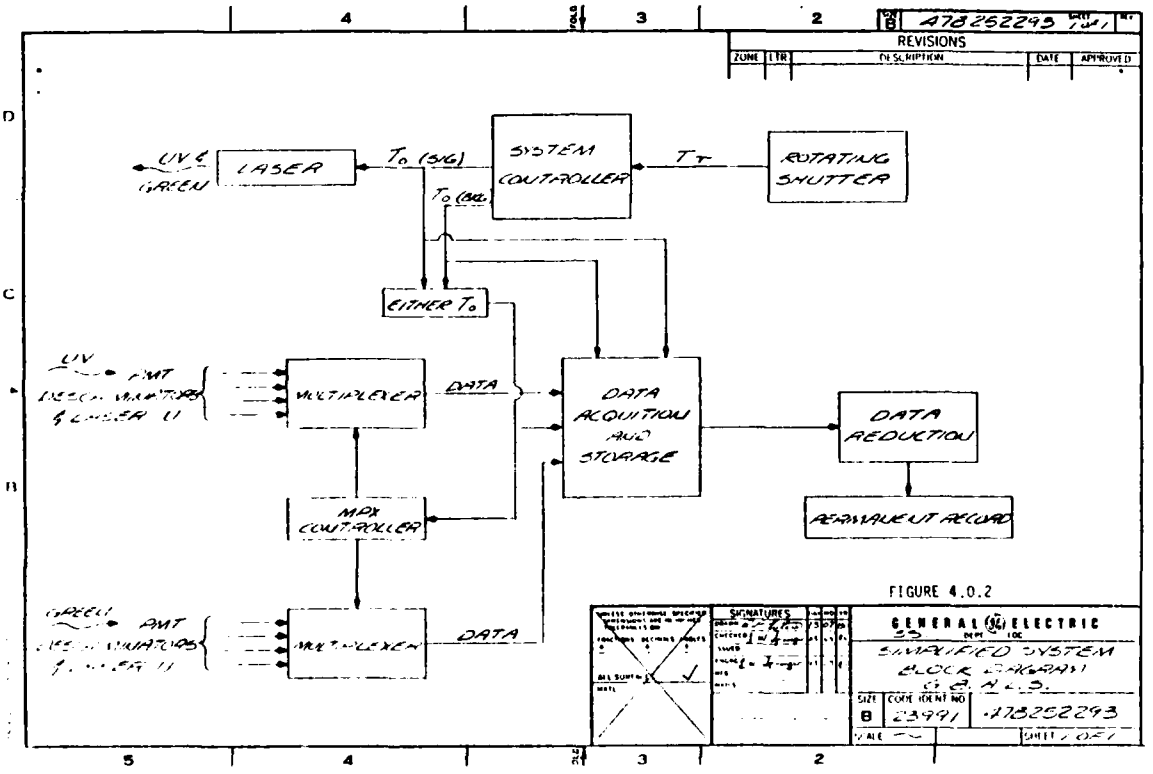
REVISIONS
ZONE
LTR
DESCRIPTION
DATE
APPROVED
UV & GREEN
LASER
T_o (S/G)
T_o (REF)
SYSTEM CONTROLLER
T_T
ROTATING SHUTTER
EITHER T_o
UV
PMT
MULTIPLEXER
DATA
DATA ACQUITION AND STORAGE
DATA REDUCTION
MPX CONTROLLER
EQUIVALENT RECORD
GREEN
PMT
MULTIPLEXER
DATA
SIGNATURES
GENERAL ELECTRIC
SIMPLIFIED SYSTEM BLOCK DIAGRAM
U.S.
SIZE
CODE IDENT NO
A78252293
SCALE
SHEET 1 OF 1

FIGURE 4.0.2

4.0.3 G-BALS Installation

Figure 4.0.3 presents an overall arrangement and installation of the total G-BALS. All the individual subsystems that are utilized within the system, and shown on Figure 4.0.3, are discussed in detail in the following pages of Section 4.0.

Figure 4.0.3 is a reduced copy of an original larger size drawing. Portions that are illegible should be referred to the original issue which is supplied under separate cover. The reduced copy was utilized to facilitate the reader's review.

The lidar support structure is intended to minimize the distance and structural complexity between those lidar optical subsections which have the largest impact on stability of overall lidar system alignment. Thus a compact tightly linked re-enforced structure supports and/or positions the lidar transmitter components (laser, beam expander, and beam-directing mirror) as well as the receiving telescope and detection system. Aluminum is used in all critical locations to reduce thermally-induced twisting effects which result from the differential expansion of dissimilar materials.

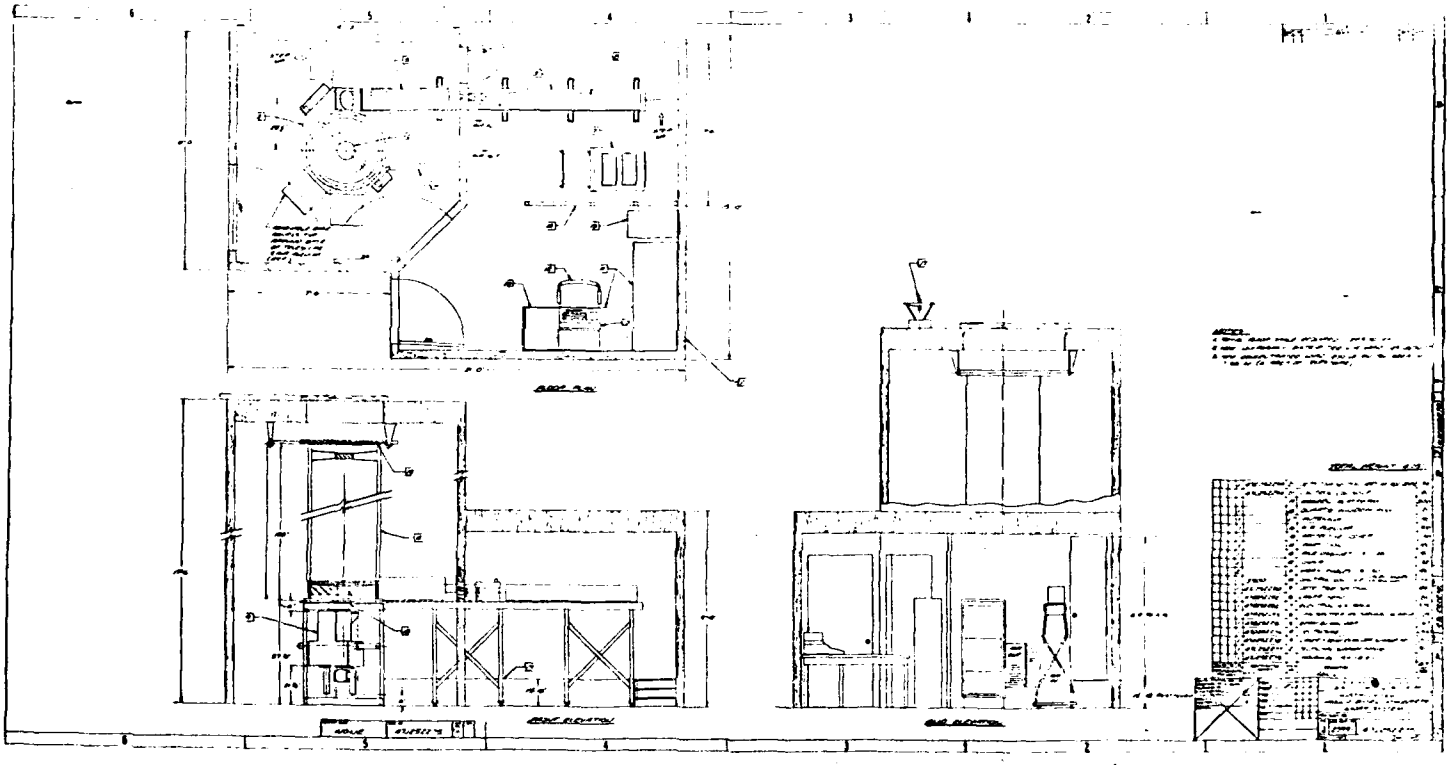

FIGURE 4.0.3

4.0.4 Installation Temperature Zones

Most of the PMT detectors, the various interference filters, the laser optical head, and some of the data processing electronics require a moderate and relatively constant ambient temperature and non-extreme humidity. Yet the fairly large output aperture of the laser beam expander, and expecially the very large receiving telescope aperture, would require uneconomically large optical windows. Thus the lidar/housing layout is such that indoor/outdoor temperature walls are located between the laser head and beam expander, and also between the receiving telescope and the receiver detection section which is below the telescope.

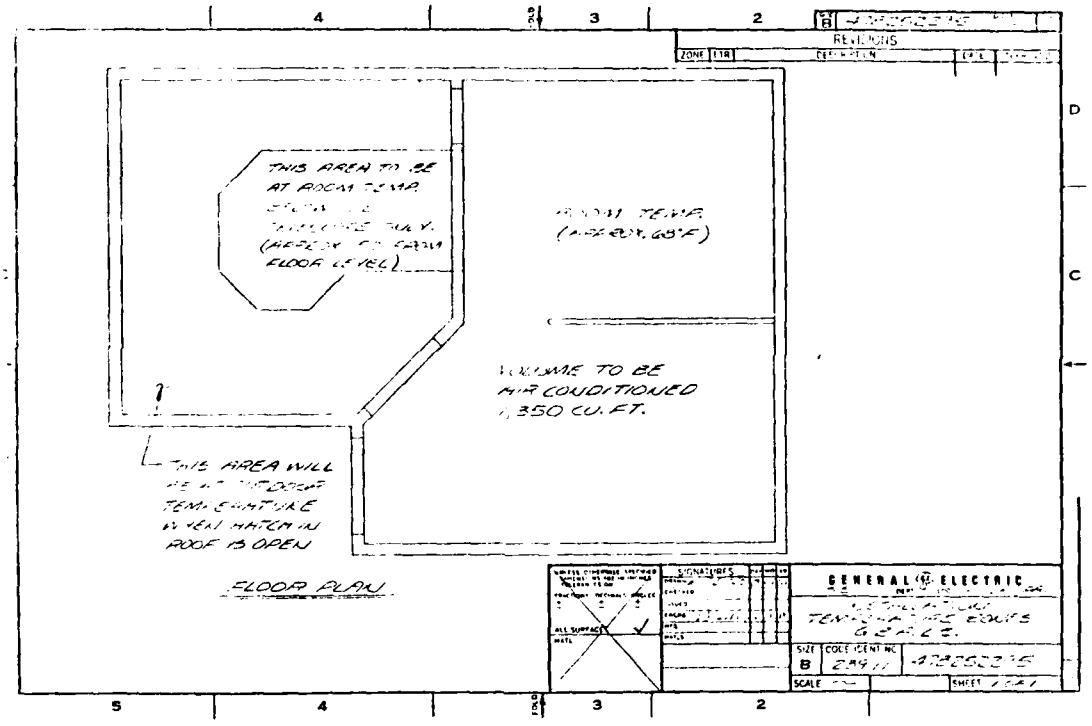
4
3
2
REVISIONS
ZONE
LTR
DESCRIPTION
D
C
THIS AREA TO BE
AT ROOM TEMP.
(APPROX. 68°F)
FLOOR LEVEL).
VOLUME TO BE
AIR CONDITIONED
1,350 CU. FT.
THIS AREA WILL
BE AT OUTDOOR
TEMPERATURE
WHEN HATCH IN
ROOF IS OPEN
FLOOR PLAN
GENERAL ELECTRIC
TEMPERATURE EQUIPS
GE
SIZE
B
SCALE
SHEET
5
4
3
2

FIGURE 4.0.4

4.0.5 Transmitter Layout

The laser output beam passes through a differential rotator (perhaps located on or in the laser head), through the laser time reference/energy monitor which also forms the inside/outside temperature window for the laser beam, and then through the laser beam expander/divergence reducer. After expansion, the laser beam is re-directed (boresighted) parallel to the receiver telescope line of sight by the adjustable beam deflecting flat mirror. The fixed autocollimator is adjusted parallel to the expanded lidar beam and is used for lidar system alignment and alignment checks (see Section 6.0).

Note that both Figure 4.0-5 and Figure 4.0-3 (GE Drawing 47J252275) show the receiver detection assembly to be oriented so its optical plane is vertical and at a 45^{0} angle to the plane which includes the receiver telescope axis and the transmitter adjustable mirror. The reason for this is given in Section 4.4.

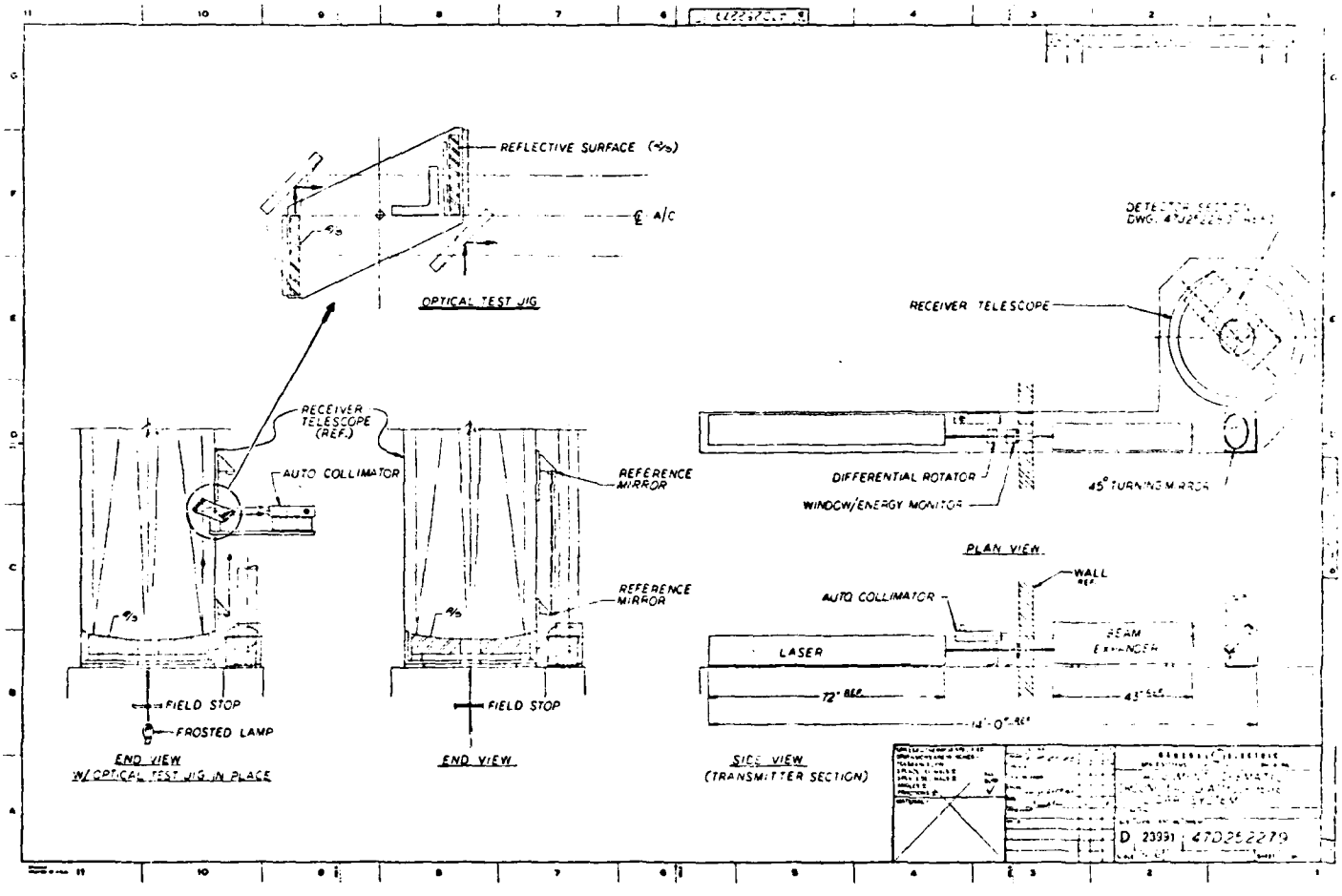
REFLECTIVE SURFACE (4/5)
℄ A/C
OPTICAL TEST JIG
RECEIVER TELESCOPE (REF.)
AUTO COLLIMATOR
REFERENCE MIRROR
REFERENCE MIRROR
FIELD STOP
FROSTED LAMP
END VIEW W/ OPTICAL TEST JIG IN PLACE
FIELD STOP
END VIEW
RECEIVER TELESCOPE
DIFFERENTIAL ROTATOR
WINDOW/ENERGY MONITOR
45° TURNING MIRROR
PLAN VIEW
WALL
AUTO COLLIMATOR
LASER
BEAM EXPANDER
72" REF.
45° REF.
14'-0" REF.
SIDE VIEW (TRANSMITTER SECTION)
D 23991
47D252279

FIGURE 4.0.5

4.1 Laser

4.1.1 Dimensional Outline of Laser Head

The commercially-available laser is designed for a laboratory type environment, and for a stable horizontal orientation. Although, in principle, the laser head internal optics could operate in any varying orientation, to do so with success would require the design and construction of a special much more rigid laser head baseplate.

Figure 4.1-1 presents a dimensional outline of the laser head.

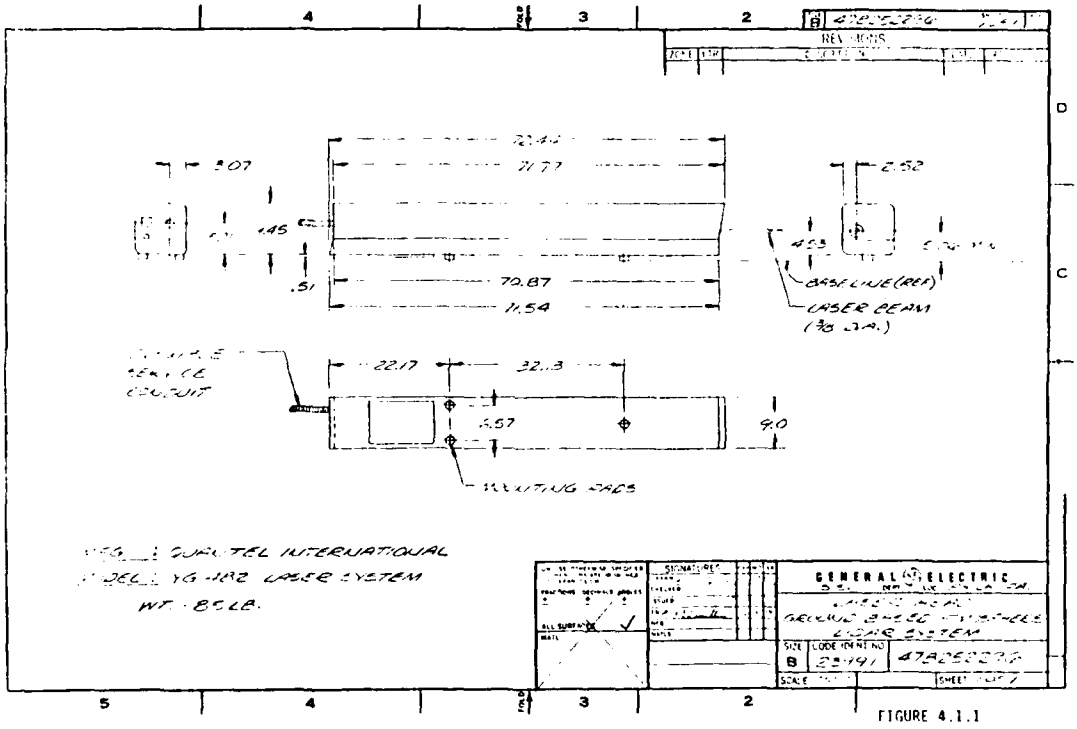
REVISIONS
5.07
1.45
.51
22.46
21.77
70.87
11.54
2.52
4.53
BASE LINE (REF)
LASER BEAM
(3Ø DIA.)
22.17
32.3
4.57
9.0
MOUNTING PADS
GENERAL ELECTRIC
SIZE
B
SCALE

FIGURE 4.1.1

4.1.2 Optical Schematic of Laser Head

The laser head internal structure and optics normally include all components shown in Figure 4.1-2 except for the 1/2 wave plate and the HeNe alignment laser. The half-wave plate plus an external differential rotator plate have been specified (see Table 4.1-1) to provide the desired polarization for both output wavelengths. Although the laser head as supplied by Quantel International includes an alignment laser holder and beam directing optics for the alignment laser output, the Spectra Physics or Coherent Radiation Model 136 alignment laser must be purchased separately.

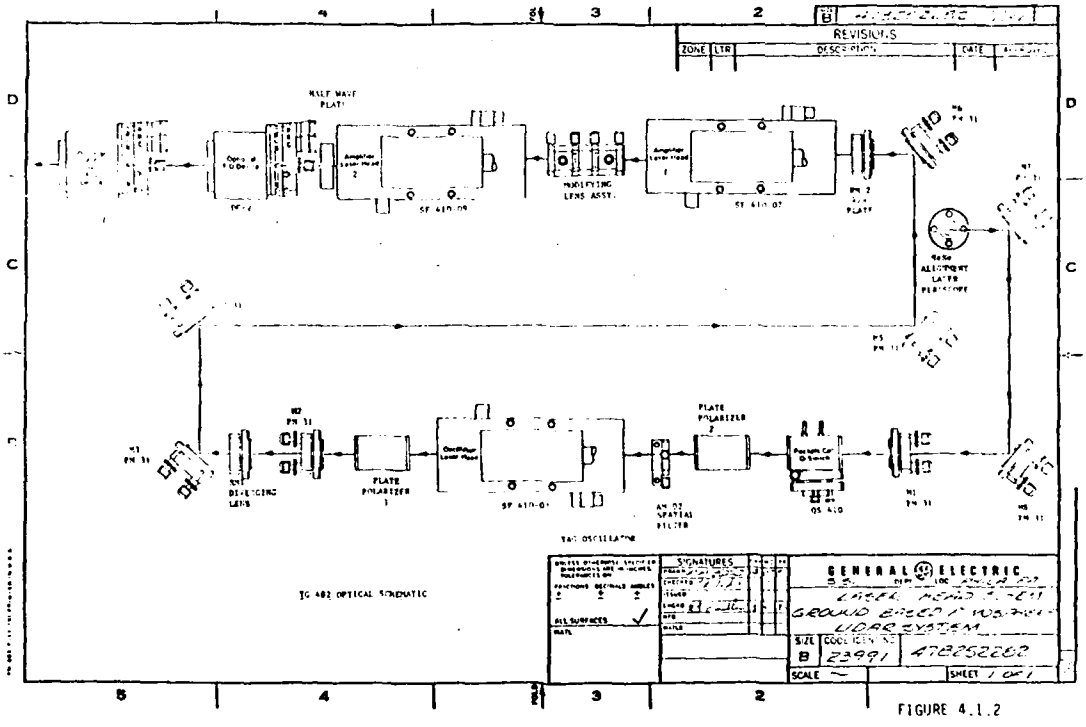
REVISIONS
ZONE
LTR
DESCRIPTION
DATE
HALF WAVE PLATE
DIVERGING LENS
PLATE POLARIZER 1
PLATE POLARIZER 2
TAC OSCILLATOR
TG 482 OPTICAL SCHEMATIC
SIGNATURES
GENERAL ELECTRIC
SIZE
B
SCALE
SHEET 1 OF 1

FIGURE 4.1.2

4.1.3 Laser Power Supply Electronics Rack

Figure 4.1-3 shows the laser power supply rack containing all non-optical laser components including Pockels cell electronics, laser control module, flashlamp power supply plus capacitors, and the closed cycle water cooling system water pump plus water:water heater exchanger. As indicated in Table 4.1-1 (follows), the cabling between laser rack and laser head limits their separation to 13 feet maximum.

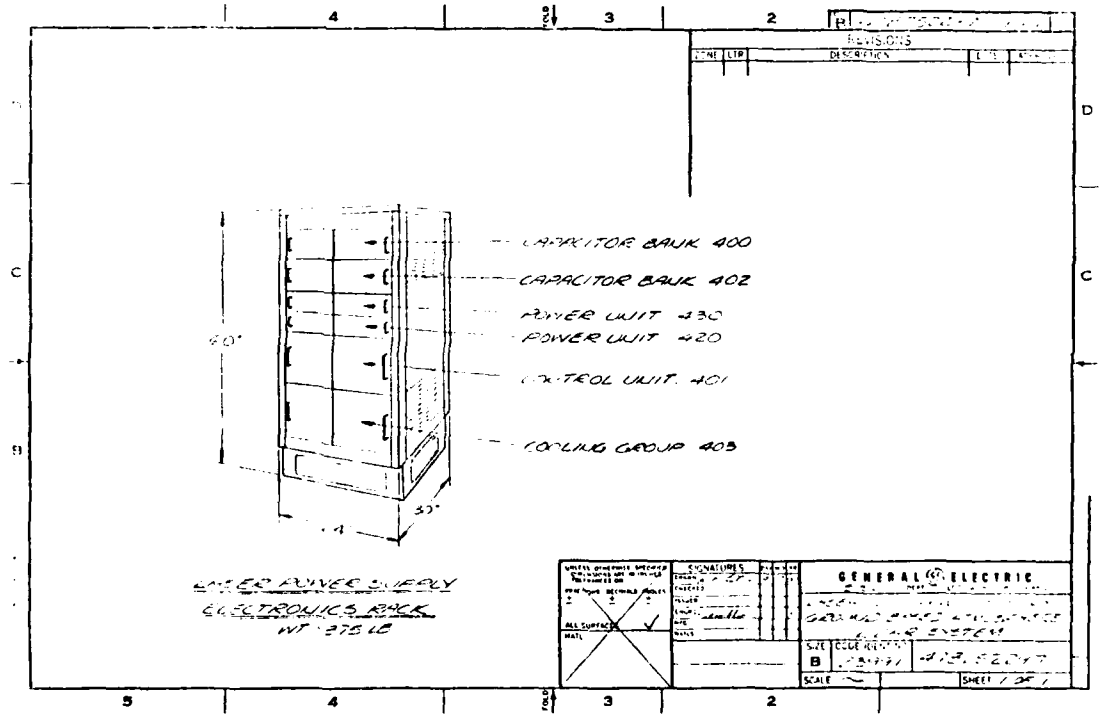
CAPACITOR BANK 400
CAPACITOR BANK 402
POWER UNIT 430
POWER UNIT 420
CONTROL UNIT 401
COOLING GROUP 403
40"
30"
24"
LASER POWER SUPPLY
ELECTRONICS RACK
WT 375 LB
GENERAL ELECTRIC

FIGURE 4.1-3

4.1.4 Laser Specifications

Specifications for the YG-482-THG laser are all standard except for those related to modification of the output polarization angle. It is desirable for both desired output wavelengths (532 nm and 355 nm) to be polarized the same and horizontal to permit optimizing the reflective coating on the laser beam deflecting adjustable mirror and any other lidar non-perpendicular mirrors. The most durable and highest efficiency coatings are of the dielectric type, but their reflectivity is a strong function of wavelength, angle of reflection, and polarization angle. Thus the coating must be not only peaked for the wavelength of interest at the intended angle of incidence, but also for the incident beam polarization angle which is preferably perpendicular to the plane of reflection. The requirement of double peaked reflection and anti-reflection coatings (for the laser's two wavelengths) makes the optimum performance conditions even more difficult to meet.

As to facility requirements, the electric power consumption varies during the 10 pps cycle time, 25 amps being the peak current. Although the laser catalog lists the external cooling (tap) water requirement as 15-25^{o}C, the manufacturer has advised that for this highest power laser version, it is preferable if the external cooling water temperature is under 20^{o}C. Because the laser system contains water, it must not be subject to freezing temperatures at any time.

While the laser will operate at ambient air temperatures in the 50-95^{o}F range, the laser head must be optically aligned for the ambient temperature of use within a $\pm$3^{o}F range. If the ambient air temperature changes by more than 3^{o}F from the laser head alignment temperature, then the laser must be re-aligned. Thus it is preferable to operate the laser in a controlled stable environment.

4.1.4 TABLE 4.1-1. LASER SPECIFICATIONS

Laser Manufacturer	Quantel International
Model number	YG-482-THG
Lasing medium	Neodymium:YAG (pulsed)
Fundamental wavelength	1064 nm
Q-switch method	Pockels cell
Maximum repetition rate	10 pulses per second
Simultaneous outputs at 10 pps	
At 1064 nm	0.45 J/pulse
At 532 nm	0.40 J/pulse
At 355 nm	0.22 J/pulse
Pulse length	15 ns (all wavelengths)
Beam diameter	9.5 mm (3/8 inch)
Beam divergence	∿0.6 mrad. full angle
Spectral width	∿0.1 cm^{-1}
Output polarization	Linearly polarized
At 1064 nm	90° angle (vertical)
At 532 nm	45° angle
At 355 nm	135° angle
Internal cooling	Deionized water (closed loop)
Modification of Output Polarization of Laser	
Desired pol. angle (532 nm)	0° angle (horizontal)
Desired pol. angle (355 nm)	0° angle (horizontal)
Extra components required	
In laser head	1/2 wave plate*
In laser beam	Differential rotator*
Facility Requirements for Laser	
External water required	Tap water ok
temperature	<20°C
flow	2 gallons/minute
Power required	208 VAC, 3 phase, 25 amps
Weight, head	120 lb.
Weight, power supply	500 lb.
Max. separation, head: PS	13 feet
Ambient temp. limits (operation)	50°-95°F (but const. ± 3°F)
Ambient temp. limits (storage)	35°-100°F

*Needs special double peaked anti-reflection coatings.

4.2 Laser Transmitter

4.2.1 Beam Expander

The laser beam expander has the primary purpose of reducing the laser beam divergence so as to permit use of a relatively small lidar receiver field-of-view.

Since the G-BALS laser will emit two wavelengths of interest, the beam expander must perform well at both wavelengths. This could be accomplished with refractive achromatic optics, except good achromatic performance is difficult and expensive to achieve in the UV. Thus an all-reflective beam expander design was chosen. Furthermore, the off-axis feature of the chosen expander has the additional advantage of no efficiency-reducing central obscuration.

As indicated in the specification list of Table 4.2-1, this design expands the beam and reduces its divergence by 15 times. Special laser-resistant double peaked dielectric reflectance coatings should be applied to both optical surfaces to permit the use of high energy laser pulses, and also to provide high optical efficiency.

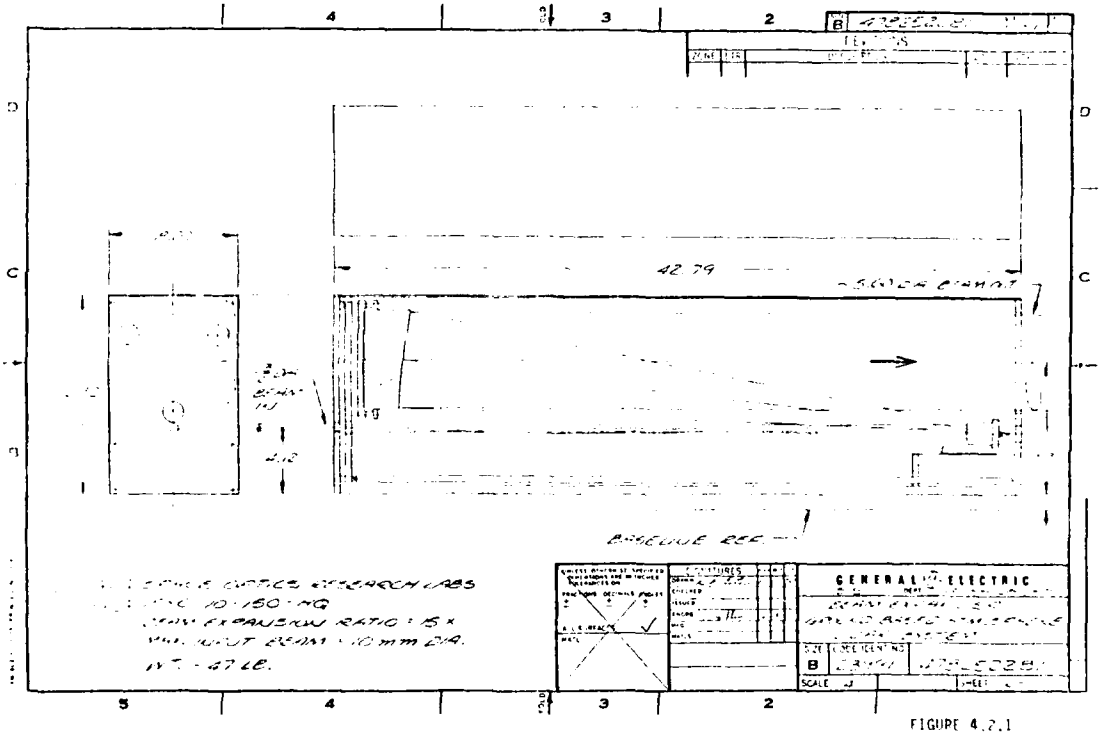

FIGURE 4.2.1

4.2.2 Transmitter Adjustable Mirror

The lidar transmitter beam-deflecting flat mirror and adjustable mount re-directs both the expanded laser beam and the transmitter auto-collimator line-of-sight along the receiving telescope line-of-sight. All alignment adjustments between lidar transmitter and receiver are easily made by means of this mirror. As indicated in Table 4.2-1, this mirror is also to use a special double-peaked dielectric coating for highest reflectivity at the laser wavelengths. Since the light angle of incidence is 45^{0} and the laser polarization is to be horizontal at both wavelengths, the coatings must be specified as optimized for "S-polarization" (perpendicular to the plane of reflection).

This assembly consists of a mounting stand (Dwg. 47C252298), a commercially available 10-inch diameter mirror cell, and a 10-inch diameter by 1.75-inch thick "first surface" flat mirror. The overall assembly dimensions are approximately 11.00" W x 11.00" D x 12.00 H, and its total weight will be approximately 29 lb.

The mirror is contained by the mirror mount at three points and in turn the mirror mount is fastened to the mounting stand by three screws, springs, and thumbwheels. This arrangement allows for the 2-axis adjustment of the mirror by turning the thumbwheels until the mirror is in its required position. Vertical adjustment of the mirror assembly is to be made by shimming between the mounting stand and the telescope support frame (Dwg. 47D252277). After initial mirror positioning, no further adjustments should be necessary.

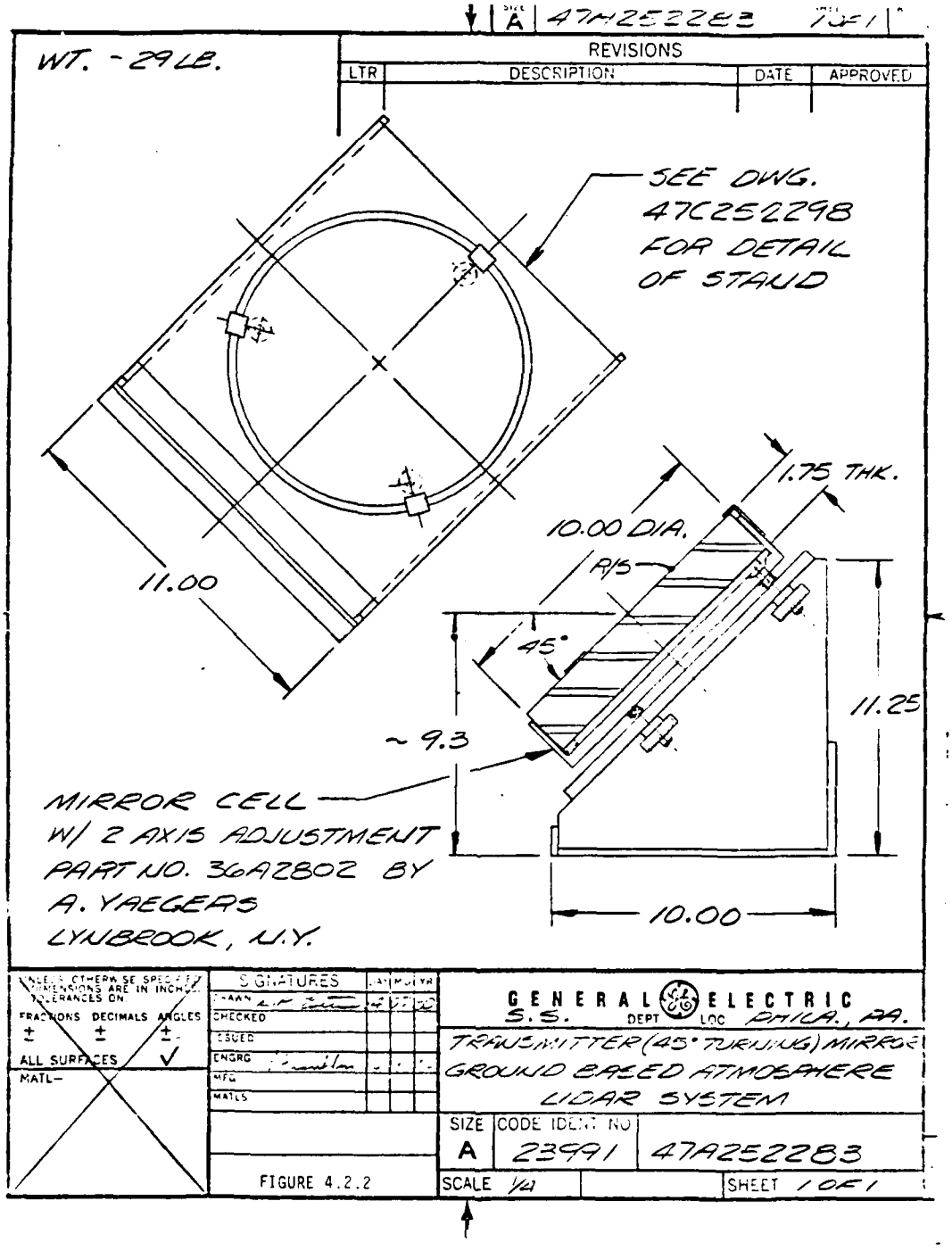
SIZE A 47M252283 SHEET 1 OF 1
WT. - 29 LB.
REVISIONS
LTR
DESCRIPTION
DATE
APPROVED
SEE DWG. 47C252298 FOR DETAIL OF STAND
11.00
1.75 THK.
10.00 DIA.
R/5
45°
11.25
~ 9.3
MIRROR CELL W/ 2 AXIS ADJUSTMENT PART NO. 36A2802 BY A. YAEGERS LYNBROOK, N.Y.
10.00
UNLESS OTHERWISE SPECIFIED DIMENSIONS ARE IN INCHES TOLERANCES ON FRACTIONS DECIMALS ANGLES ± ± ± ALL SURFACES √ MATL—
SIGNATURES
DRAWN
CHECKED
ISSUED
ENGRG
MFG
MATLS
GENERAL ELECTRIC
S.S. DEPT LOC PHILA., PA.
TRANSMITTER (45° TURNING) MIRROR
GROUND BASED ATMOSPHERE
LIDAR SYSTEM
SIZE A
CODE IDENT NO 23991
47A252283
SCALE 1/1
SHEET 1 OF 1

FIGURE 4.2.2

4.2.3 Laser Window/Output Energy Monitor

This combination window and laser energy monitor supplies not only the output energy of each laser pulse at both 355 nm and 532 nm, but also the time-zero for each lidar system shot. The optical phenomenon upon which this energy monitor functions is the measurement of light internally scattered from the entire laser beam by the window material. The detectors are best located to the side at an angle which is perpendicular to both the laser beam and the beam's (horizontal) plane of polarization. Such an energy monitor design is durable, stable, and removes only a negligible amount of energy from the laser beam.

To reduce the number of electrical groundloops, electrical insulating materials should be used in contact with the photodiode detectors and also the BNC electrical connectors. Such connectors can be isolated from the monitor metal structure through proper use of Mylar shims and Nylon screws. The thin Nylon spacer indicated in Figure 4.2-3 between each detector and its narrow band filter can be replaced with a neutral density filter which adjusts monitor sensitivity as desired.

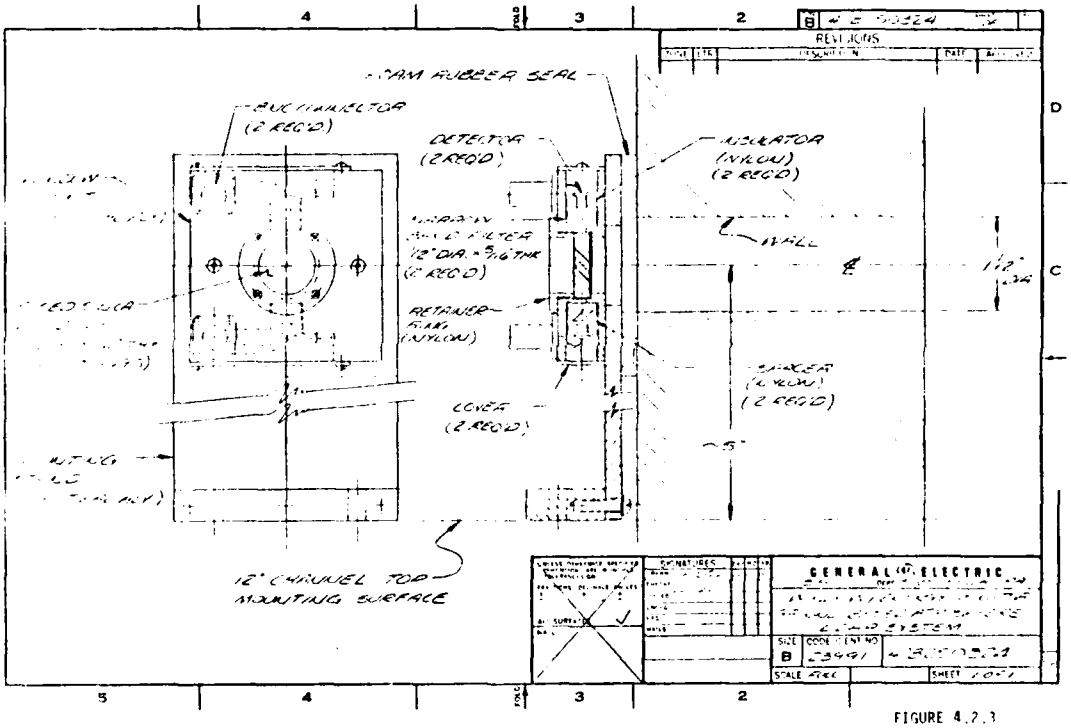
FOAM RUBBER SEAL
(2 REQ'D)
DETECTOR
(2 REQ'D)
INSULATOR
(NYLON)
(2 REQ'D)
WALL
1 1/2"
38
RETAINER
PLATE
(NYLON)
(2 REQ'D)
5"
(2 REQ'D)
12" CHANNEL TOP
MOUNTING SURFACE
REVISIONS
GENERAL ELECTRIC

FIGURE 4.2.3

4.2.4 Lidar Transmitter Specifications

Table 4.2-1 lists lidar transmitter specifications for the laser window/output energy monitor, laser beam expander, and adjustable beam deflecting mirror.

4.2.4 TABLE 4.2-1. LIDAR TRANSMITTER SPECIFICATIONS

Laser Output Energy Monitor	
Location	On window in laser beam
Window material	Fused silica*
Window transmission (AR coated*)	>99% at 355 and 532 nm
Detector	
for 532 nm	Si photodiode (PIN - 5D)
for 355 nm	Si photodiode (PIN - 5 UV)
Wavelength selection, each det.	Narrow band filter, each det.
Beam Expander	
Manufacturer	Space Optics Research Labs.
Model number	15XC-10-150-HQ
Type	All-reflective* off-axis
Beam obscuration	None
Optical quality	1/5 wave at 630 nm
Beam expansion	15 times
Maximum input beam diameter	10 mm (.394 inch)
Output aperture	6 inches diameter
Throughput efficiency*	98% at 355 and 532 nm
Expanded laser beam	
beam diameter	5.6 inches
beam divergence	.04 mrad. full angle
Beam Deflecting Mirror	
Type	Flat to 0.1 wave
Size	10 inches diameter
Angle of incidence & reflectance	45°
Reflectivity (S-polarization)*	99%

*Special double-peaked dielectric coatings on all optical surfaces.

4.3 Receiving Telescope

4.3.1 Telescope Preliminary Specifications

To minimize construction and mounting costs, the lidar system and its receiver telescope are to have a fixed vertical orientation whether in use or not. Since the receiving telescope is to not only have a large aperture but is also to be used at both 355 nm in the near UV and at 532 nm in the visible green, a reflector design was chosen. The Dall Kirkham compound reflector design meets the performance requirements consistent with relatively low cost and compactness.

Although an f/2 or f/3 primary mirror (PM) would allow a somewhat shorter telescope and smaller central obscuration, the PM is tentatively specified as f/4 to reduce the optical labor costs. A PM of Pyrex-type glass is relatively cheap and sufficient for the required performance, but availability of large blanks in that material is sometimes a problem. The Cervit or Zerodur PM material has better thermal properties and is more readily available in large sizes, but it is more expensive.

An overall (effective) f-number greater than f/20 causes the telescope focal length and thus required field stop diameter (0.2 mrad) to increase to a physical size which overly increases the shutter wheel opening time (see Section 4.4). Less than f/15 results in too large a central obscuration.

The resolution upper limit was chosen as 0.025 mrad (5 arc-seconds). This can be compared with the transmitter expanded laser beam divergence of 0.04 mrad full full angle and the anticipated lidar field stop diameter of about 0.2 mrad. The 1 mrad field-of-view requirement for the specified telescope resolution allows for later expansion of the lidar field stop if desired.

The telescope mirror coatings are specified for high reflectivity at 355 nm and 532 nm, consistent with the size of each mirror. Although these coatings will cost more than the usual Aℓ(SiO) coatings, the increased reflectivity compared with Aℓ(SiO) will more than compensate for the additional coating expense. This situation results from the significantly higher telescope cost that would result if the use of the less efficient Aℓ(SiO) coatings were compensated for by suitably increasing telescope aperture to yield the same overall throughput. For a given design, large telescope costs tend to be proportional to the aperture cubed.

(continued)

TABLE 4.3-1

4.3.1. PRELIMINARY

TELESCOPE SPECIFICATION
FOR
LIDAR SYSTEM

Use: Fixed vertical position only for ground-based atmospheric density measurements for wavelengths of 355 nm and 532 nm. Protected laboratory environment during non-operating periods. Exposed to temperatures of -20°F to +120°F during operating periods.

Type: Dall Kirkham, compound reflector telescope including: primary and secondary mirrors, mirrors' cells, and all support structure. Include mounting points (but no mount) for vertical use.

Primary Mirror:

Diameter: 36 inches with center hole to pass telescope focus

Material: Pyrex, Zerodur or equivalent

f/number: f/4

Secondary Mirror:

Diameter: 10 inches maximum (minimum obscuration)

Material: Cervit or Zerodur

Effective f Number:

f/15 to f/20 (overall telescope)

Resolution (Blur Circle):

5 arc sec (.025 mrad) within a 0.001 radian field-of-view (full angle) at focal point.

Focal Point Location:

12 $\pm$ 1.0 inches aft of telescope primary structure.

Coatings:

(1) Primary Mirror:

(a) Enhanced metal coating with R $\geq$ 95% at 355 nm and R > 90% at 532 nm.*

(b) Durability should be such that surface can be cleaned with reasonable care.

*R = Reflectance

(continued)

4.3.1 Telescope Specifications (continued)

As to structural design, the solid enclosure requirement is to ease the problem of keeping the PM clean. It is desirable to minimize tube outside diameter to allow the lidar laser beam axis to be as close as possible to the receiver axis. Such an arrangement improves laser beam:receiver field-of-view overlap at measurement altitudes, and also eases transmitter:receiver alignment (see Section 6.0).

Ambient temperature changes will cause the telescope PM:secondary mirror (SM) distance to change, moving the telescope focus. If it is assumed that the only thermal effect is change of PM:SM distance due to the all-aluminum structure, the focus should move by about 16 times the PM:SM distance change (see Section 4.4), or 0.24 inch per 10^{o}F change in temperature. This yields a focus position change of 3.34 inches for the full -20^{o}F to $+120^{o}$F specified operating range. The field stop and detection section position will be adjustable to correct for this focus shift (see Section 4.4).

4.3.1 TABLE 4.3-1 (CONTINUED)

(2) Secondary Mirror:

(a) Dielectric double peaked reflecting coating, with R > 99% at both 355 nm and 532 nm (R = Reflectance).

(b) Durability should be such that surface can be cleaned and wiped with reasonable care.

Structure:

(a) Aluminum, and enclosed in an aluminum dust shield.

(b) Size: Less than 42 inches outside diameter by 144 inches maximum length.

(c) Mounting Points (Tie-Down): As required near primary mirror.

(d) Finish: Anodize or equivalent (Black).

(e) Reasonable access to clean primary and secondary mirrors.

Weight:

(TBD) pounds. (Cost effective design for laboratory use, i.e., not for flight.)

FOR DELIVERY

HARDWARE

Quantity	Name
1	Telescope as per specification
2	End dust covers
1	Lifting and handling fixture
1 (set)	Shipping containers

DOCUMENTATION

Item No.	Title
1	Program Plan and Schedule
2	Acceptance Tests Procedures (Foucault and collimator/optical flat)
3	Acceptance Tests Results
4	One set design drawings (reproducibles)
5	Installation and Maintenance (cleaning and alignment) manual
6	Letter Progress Reports (Monthly)
7	All Analysis (stress, thermal, computer print-outs, etc.)

4.3.2 36-Inch Telescope

Figure 4.3-1 shows the lidar receiving telescope structural design.

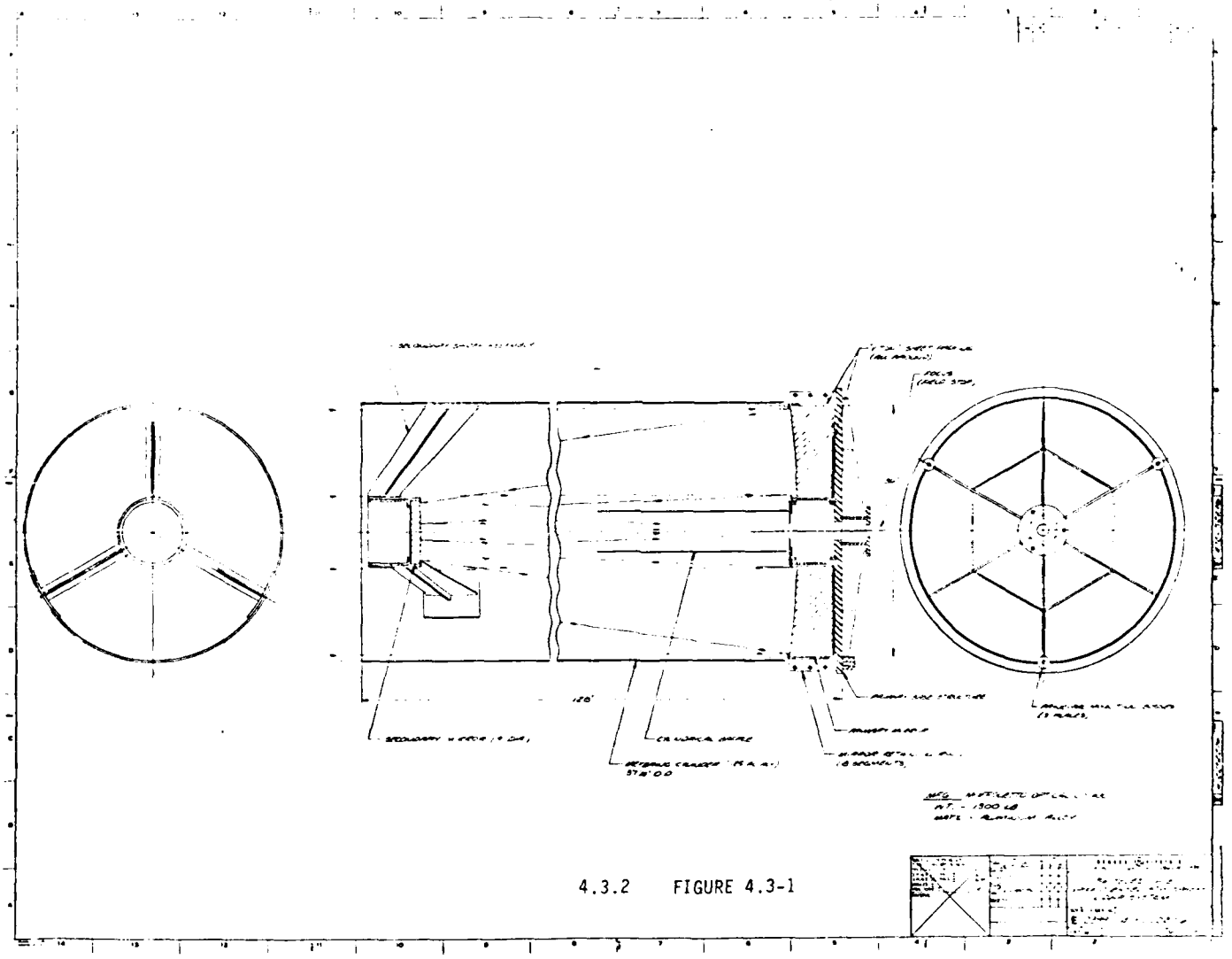

4.3.2 FIGURE 4.3-1

4.4 Receiver Detection Assembly

4.4.1 Detector Section

The receiver detection optical concept has already been described in Section 4.0 and illustrated with Figure 4.0-1. Here, the detector section assembly drawing (Figure 4.4-1) illustrates how the optical components and detectors can be fitted together along with numerous light baffles and manual shutters for each detector. This particular configuration of Figure 4.4-1 resulted from the use of a two-wheel rotating shutter system, and the desire to keep direction-changing reflections to a minimum (reduce light losses) and optical path length to a minimum (minimize effect of the slight spreading of the collimated beam from lens item 10).

The detector section is packaged in an inverted "T" shaped enclosure. The enclosure measures 30" W x 30" H x 12.3" D and weighs 64 lbs including the cover.

The enclosure (item 2) is made up entirely of 6061-T6 aluminum alloy. The base plate or back plate, which will have all the optical components mounted to it, will be 0.375 plate and all the side walls are 0.25 plate. The cover (item 3) will be 0.125 sheet and be reinforced as required. All corner joints are rabbet-type joints bolted as required to form a stiff and light tight enclosure. The cover will be equipped with 1/4-turn fasteners for easy and fast removal. The enclosure interior and exterior are to have all the required mounting holes for the hardware to be packaged. Those threaded holes which are subject to wear due to frequent equipment adjustments will have stainless steel threaded inserts. Also as part of this box will be a series of interior light baffles which will divide the interior into a number of individual sections. The baffles will be removable as required. The bottom side of the box which will receive four PMT's will be reinforced with an angle running 30" side to side. The top and bottom of the enclosure will support the shutter wheel assembly (item 4).
The only opening in the enclosure will be at the top which will have an interchangeable aperture plate (item 46).

The entire enclosure and associated parts are to have a black anodized finish to prevent surface reflections. Exterior surfaces to be alodined only.

(continued)

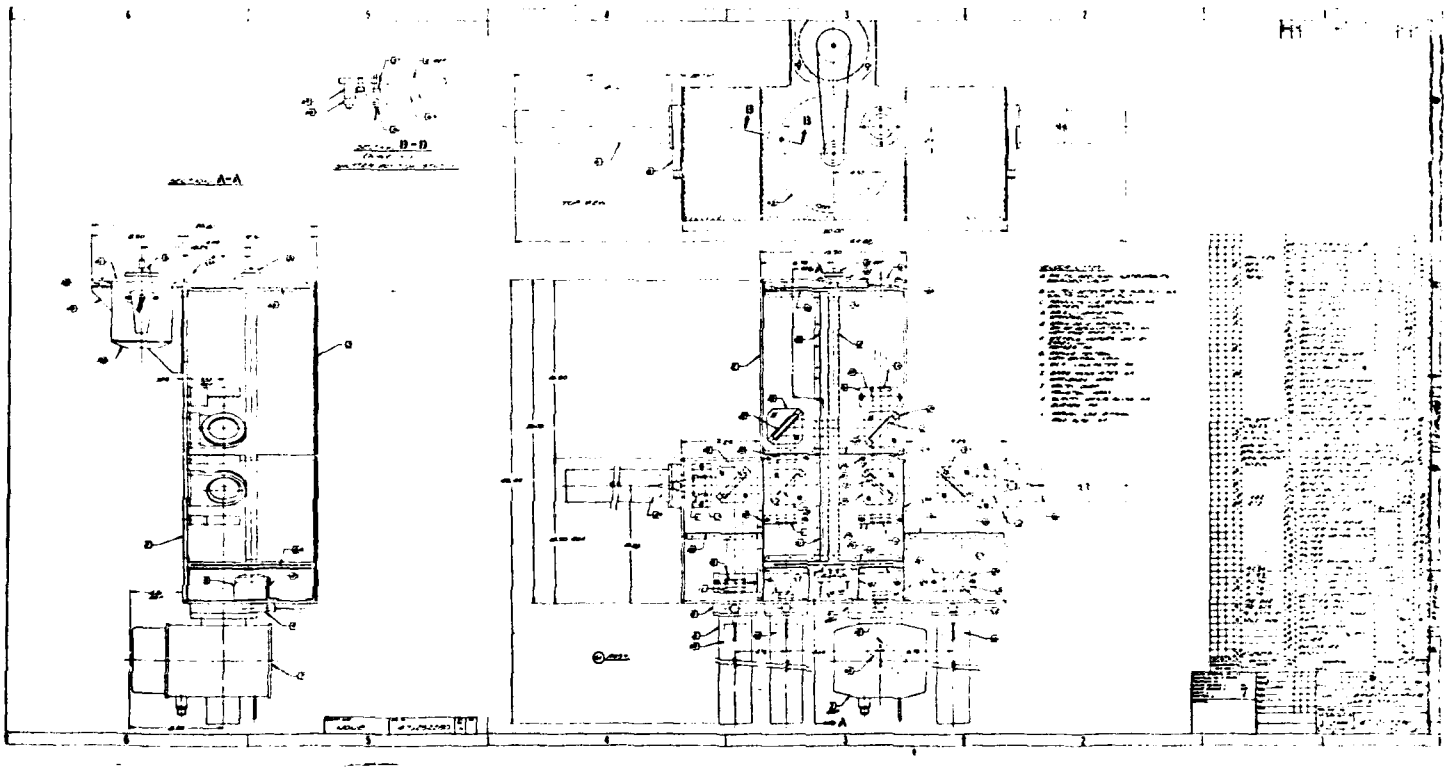

FIGURE 4.4.1

4.4.1 Detector Section (continued)

Not shown in Figure 4.4-1 but previously shown in Figure 4.0-1 and listed in Table 4.4-1 is the small window WT which is in the thermal separation interface between the telescope base and the detection section. Also not shown here but indicated in the telescope Section 4.3 and detailed later in this section is the method by which thermal changes in receiving telescope focus are compensated.

A reduced copy of the original issue Drawing 47J252280 is shown as Figure 4.4-1. Portions of the figure, at this reduced size, are illegible. However, the reduced copy insertion was considered prudent to facilitate the reader's review and understanding of G-BALS. If greater detail is desired, the reader should refer to the original full size drawing issue which is provided under separate cover.

4.4.2 Orientation of the Receiver Detection Assembly

As briefly indicated in Section 4.0 and shown in Figures 4.0-3 and 4.0-5, the lidar detector section (Figure 4.4-1) is to be oriented so its optical plane is vertical and at a 45^{o} angle to the plane which includes both the receiver telescope axis and the transmitter adjustable mirror. This detector section orientation is designed to avoid a variation of lidar system sensitivity depending on the degree of backscatter depolarization.

The laser output at both wavelengths is to be linearly polarized in the horizontal direction which, after reflection off the transmitter adjustable mirror, is polarized in the plane which includes the receiving telescope axis. While the atmospheric Rayleigh (gas) scattering and spherical particle (Mie) scattering show little depolarization, non-symmetric particulates as well as any multiple scattering can produce backscattered light which is significantly depolarized. Unfortunately, any non-perpendicular reflector such as the 45^{o} dichroic mirror DM (item 21, Figure 4.4-1) in the detector section, will show different reflectance for a polarization vector or vector component parallel to the plane of incidence (P-component) than for a polarization vector component perpendicular to the plane of incidence (S-component). Thus the lidar system sensitivity (and calibration) could vary with the degree of backscatter depolarization. This would invalidate the lidar data reduction and resulting atmospheric density values.

The G-BALS design avoids this problem by orienting the detector section as indicated above, such that the first non-perpendicular reflecting surface (DM) has its plane of incidence at 45^{o} to the polarization angle of the outgoing laser beam. Then the backscattered light which is still polarized the same as ($I(\|)$) as well as any perpendicular to ($I(\perp)$) the laser beam polarization angle, are both at 45^{o} to the DM plane of incidence. Now both $I(\|)$ and $I(\perp)$ are vectorially split equally between S-type and P-type reflection components, resulting in equal lidar system sensitivity to $I(\|)$ and $I(\perp)$. Thus the lidar system sensitivity is independent of backscatter depolarization.

4.4.3 Receiving System Optical Specifications

Table 4.4-1 is a specifications summary for all the receiving system optical elements. The letter symbols are the same as those used and illustrated in block diagram Figure 4.0-1, while the letter I in the focal length column indicates that all flat mirrors and windows have infinity focal lengths. Letter-identified footnotes as used in Table 4.4-1 are as follows:

(a) Item numbers are those used in Figure 4.4-1 (GE assembly drawing 47J252280).

(b) Optical materials are BC=BK-7 borosilicate crown glass, FS=fused silica, PG=Pyrex glass or equivalent, ZD=Zerodur or equivalent.

(c) R=reflective coating, AR=anti-reflective coating, NC=not coated, A:(LiF)=LiF-enhanced A. coating, ID=single peaked hard dielectric coating, 2D=double peaked hard dielectric coating, (45^{o})=used at 45^{o} angle to optical axis.

(d) For more information on items 21, 15, and 20 see Table 4.4-2, "Some Receiver Optical Specification Details"

Optical efficiencies for the neutral density filters, items 16-19, have been only tentatively specified. These optical elements (or their absence) will be used to obtain the desired sensitivity ratios (altitude ranges) between PMT detectors, and will depend on the PMT and other optical efficiencies as actually obtained from the suppliers. The optical efficiency value pairs listed for each beam splitter refer to net transmittance and reflectance at the indicated wavelength.

4.4.3 TABLE 4.4-1. RECEIVING SYSTEM OPTICAL SPECIFICATIONS

Type of Item	Symbol	Item No. (a)	Opt. Matl. (b)	Diam. (in)	Focal Length (cm)	Qty.	Wavelength of use (nm) 532	355	Type Coating (c) No. Surfs. Coated	R or AR	Coating Matl.	Opt. Eff. 532 nm	355 nm
Telescope mirror	PM	-	PG/ZD	36	366	1	x	x	1	R	Al (LiF)	.90	.95
Telescope mirror	SM	-	ZD	9	-	1	x	x	1	R	2D	.99	.99
Tel. focus window	WT	-	FS	2	1	1	x	x	2	AR	2D	.99	.99
Lens	CL	10	FS	2	25	1	x	x	2	AR	2D	.99	.99
Lens	DL	11	FS	2	10	3	-	x	2	AR	1D	-	.995
Lens	PL	13	FS	1.5	3.8	1	-	x	2	AR	1D	-	.995
Lens	DL	12	BC	2	10	3	x	-	2	AR	1D	.995	-
Lens	RL	14	BC	1.5	5	1	x	-	2	AR	1D	.995	-
Dichroic mirror	DM	21	?	3	1	1	x	x	2	-	(d)(45°)	.9	.99
Flat mirror	FM	22	PG	3	1	1	-	x	1	R	1D (45°)	-	.99
Bandpass filter	FG	15	?	2	1	1	x	-	-	-	(d)	.60	0
Bandpass filter	FU	20	?	2	1	1	-	x	-	-	(d)	0	.25
Beamsplitter	BS	23	BC	3	1	1	x	-	0	-	NC (45°)	.90/.097	-
Beamsplitter	BS	57	FS	3	1	1	x	-	1	AR	1D (45°)	.96/.045	-
Beamsplitter	BS	58	FS	3	1	2	-	x	1	AR	1D (45°)	-	.95/.047
Neutral filter	NF	16	?	2	1	1	x	-	0	-	NC	1?	-
Neutral filter	NF	17	?	2	1	1	x	-	0	-	NC	.4?	-
Neutral filter	NF	18	?	2	1	1	-	x	0	-	NC	-	.5?
Neutral filter	NF	19	?	2	1	1	-	x	0	-	NC	-	1?

4.4.4 Some Receiver Optical Specification Details

Since the receiver telescope specifications (see Table 4.3-1) only approximately define the telescope effective focal length (540-720 inches), the desired field-of-view of 0.2 mrad results in a required field stop diameter of 0.27-0.36 cm.

The G-BALS bandpass interference filters FG and FU are specified with wide enough pass bands so as to allow relatively good peak transmittances. Good transmittance is important for obtaining lidar measurements to high altitudes. The less advanced technology for producing UV bandpass filters is responsible for the poorer bandpass and transmittance specifications for the 355 nm filter. Interference filters typically show a thermally-induced band center shift of (0.003% of band center wavelength)/^{o}C, which will allow their use through the detection section's maximum allowed ambient temperature range of 10^{o} to 35^{o}C (see Section 9.0). If significantly narrower bandpass filters are ever desired to reduce signal background for improved daytime measurements, then receiver efficiency will suffer reduced lidar nighttime measurement range; also thermally controlled filter cells may be necessary.

4.4.4 TABLE 4.4-2. SOME RECEIVER OPTICAL SPECIFICATION DETAILS

Receiving Telescope		
Type	Dall Kirkham reflector	
Collecting aperture	36 inches diameter (91.4 cm)	
Aperture area obscured	7%	
Effective focal length	∿600 inches (∿15 m)	
Field of view	0.2 mrad full angle	
Detector Assembly Field Stop (FS)		
Item number*	46	
Hole diameter	∿0.3 cm	
Dichroic Mirror (DM)		
Item number*	21	
Diameter	3 inches	
Angle of use	45°	
Type	Long wavelength transmitting	
Coating characteristics		
side one	99% reflect at 355 nm >85% transmit at 532 nm	
side two	AR (antirefl.) coat for 532 nm	
Interference Filters		
Symbols	FG	FU
Item numbers*	15	20
Diameter	2 inches	2 inches
Number of cavities	3	3
Transm. peak wavelength	532 nm	355 nm
Passband width (FWHH)	2.5 nm	5.0 nm
Peak transmittance	$\geq$ 60%	$\geq$ 25%
Off-band rejection	$\leq$ .001%	$\leq$ .001%
Rejection range	Far UV to >800 nm	
Angle of use	Perpendicular to radiation	
Design temperature	$20^{o}C$	

*Item number used in Figure 4.4-1 (GE Drawing #47J252280).

4.4.5 Lidar Receiver Detection Specifications

The RCA-8850 and Varian VPM-152S detectors to be used were primarily chosen for their combination of high quantum efficiency, low background, fast response, relatively good photo-electron collecting efficiency, and good first dynode gain.

A good first dynode gain is important for photon counting detection methods because it allows one to better discriminate against dark counts and also results in very stable photon counting sensitivity. With good first dynode gain, photon counting methods show less sensitivity to drift than do current measurement detection methods.

It should be noted that the typically quoted photo-cathode quantum efficiencies (QE) are often not achieved in practice due to imperfect electron-collection efficiency by the first dynode. The linear focused PMT's chosen here are both estimated to have first dynode collection efficiencies of about 0.9. The RCA-8850 PMT has such a high first dynode gain that it is estimated to have a counting efficiency of one, for an overall efficiency of 0.9 x (QE). Since the VPM-152S PMT has a less high first dynode gain, its counting efficiency is estimated as 0.9, for an overall efficiency of 0.81 x (QE) = 28.4% at 532 nm.

TABLE 4.4-3

4.4.5 LIDAR RECEIVER DETECTION SPECIFICATIONS

PHOTOMULTIPLIER TUBE (PMT) DETECTORS SELECTED

PMT item numbers[a]	62	61	60	59
Altitude range detected	hi Z	mid, low	hi Z	mid, low
Wavelength detected (nm)	532	532	355	
PMT manufacturer	Varian	RCA	RCA	
PMT model number	VPM-152S	8850	8850	
Quantity	1	2	3	

PMT CHARACTERISTICS AND REQUIREMENTS

PMT model	VPM-152S	RCA-8850
Dynode structure	linear focused	linear focused
Cathode type	GaAsP	bialkali
Cathode quantum eff. (typ.)		
at 355 nm	40%	32%
at 532 nm	35%	10%
Cathode diameter (mm)	5	46
Dark counts		
at +20° and 22°C	5000	170 (20)[b]
at -20°C	10	NA
Volts for 10^6 gain	6000	1700
PMT housing recomm.		
manufacturer	Products for Research	Pac. Prec. Instrum.
model no.	TE-157TS-RF	3262/AD6
housing dimensions (in.)	8.6 x 12.9 x 7.8	3 diam. x 14.6
special features	cooled	contains A-D
Ampl. - Discriminator (A-D)		
recomm. model.	PPI #AD6	PPI #AD6
location of A-D	near housing	in housing

Notes:

a) For item number definition, see Figure 4.4-1 (GE Dwg. #47J252280).
b) As reduced with use of PR-411 magnetic defocusser.

4.4.6 Shutter Wheel System reatures

A synchronized pair of rotating shutter wheels will protect the PMT detectors from the relatively intense near-range lidar signals. This protection is desirable because exposure to high light levels just before low level measurements will increase PMT dark current and can temporarily decrease PMT sensitivity or even damage it.

Figure 4.4-1 (GE drawing 47J252280) shows how two shutter wheels (items 63 and 64) are mounted on a common shaft (item 4) and driven, through a 1:2 geared belt (item 33), by a 3450 rpm electric motor (item 30). Use of a constant voltage transformer plus variable autotransformer will allow stable but somewhat adjustable shutter speed. At a nominal 7000 rpm, the shutter wheel will uncover the 3 mm field stop FS (item 46) in 32 microseconds (4.8 km lidar range interval). Shutter wheel A (item 63) will be set to unblock FS by an altitude (Z) of 20 km, while wheel B (item 64) will unblock the two highest altitude-sensing PMT's by Z=50 km.

An LED source (item 36) plus double photodiode detector (item 37) senses shutter wheel A position, and provides a timing trigger pulse for firing the lidar laser.

4.4.6 SHUTTER WHEEL SYSTEM FEATURES

Purpose

- Protect detectors from relatively intense low altitude lidar signal.

General Concept

- Rotating shutter wheels.
- Use shutter wheel position sensor to determine laser firing time.

More Details[a]

- Use two shutter wheels on common shaft.
- Shutter wheel A blocks all detectors during signals from altitude (Z) <20 km.
- Shutter wheel B blocks highest altitude detectors (2) for Z <50 km.
- Both shutter wheels are identical but rotationally displaced as necessary.
- Shutter wheel diameters $\approx$ 11 inches.
- Couple drive motor to wheels via geared belt and 1:2 pulley ratio.[a]
- Use 1/2 HP 3450 rpm drive motor.[a]
- Stabilize drive with constant voltage transformer.
- Provide some rpm adjustment with variable autotransformer.
- Shutter wheel speed approximately 7,000 rpm.
- Use large diameter hollow shaft to avoid resonant vibration.
- LED - photodiode pair[a] detects shutter wheel position.

[a]See Figure 4.4-1 (GE Drawing #47J252280).

4.4.7 Shutter Wheel System Specifications and Useage

Table 4.4-4 details shutter wheel and position sensor design and performance characteristics.

Mechanical dynamics are analyzed in Appendix A. Characteristics considered include wheel drag and required drive power, shaft resonance, bearing strength and loads, and shutter wheel stress.

TABLE 4.4-4

4.4.7 SHUTTER WHEEL SYSTEM SPECIFICATIONS AND USEAGE

TYPE SHUTTER SYSTEM	Two rotating shutter wheels		
SHUTTER WHEEL DESCRIPTION[a] (BOTH WHEELS)			
Number open slots	three per wheel		
Open slot length	45° each		
Diameter outside edge	11 inches approx.		
Radius of use	5.0 inches		
Distance of axis from opt. plane	2.50 inches		
SHUTTER WHEEL USE			
Wheel speed	adjust to 7,200 rpm maximum		
Laser shot timing	once per 12 wheel revolutions		
Background opportunities	35 maximum per laser shot		
Wheel rpm	6900	7000	7200
Wheel rps	115	116.7	120
Shutter openings/sec.	345	350	360
Laser shots/sec.	9.58	9.72	10
SHUTTER A			
Item number[a]	63		
PMTs protected	all		
Full open altitude	20 km		
SHUTTER B			
Item number[a]	64		
PMTs protected	high altitude PMTs (items 60 and 62)[a]		
Full open altitude	50 km approximately		
POSITION SENSOR DESCRIPTION[a]			
Sensor item numbers[a]	36-39		
Angular location	135° before optical axis		
Edge-emitting LED source	RCA #C30123		
Position - sensing photodiode	UDT # PIN Spot/2D		

[a]See Figure 4.4-1 (GE Drawing #47J252280).

4.4.8 Detector Section Vertical Height Adjustment Detail (Figure 4.4-2, Dwg. #47D252299)

This mechanical assembly allows for the vertical height adjustment of the detector section (Figure 4.4-1, Dwg. 47J252280) to compensate for the thermal expansion of the telescope (Dwg. 47E252276). The detector section will be adjustable ± 2.0 inches from its nominal position, the nominal position to be determined by the position of the telescope focus at an ambient temperature of about $50^{o}F$. Assuming temperatures of $-20^{o}F$ to $+120^{o}F$, the change in primary-to-secondary mirror distance due to expansion of the telescope structure will be:

$$12.1 \times 10^{-6} \text{ in/in/}^{o}F \ (120 \text{ in})(-88^{o}F) = -0.128 \text{ in.}$$

and

$$13.0 \times 10^{-6} \text{ in/}^{o}F \ (120 \text{ in})(52^{o}F) = 0.081 \text{ in.}$$

But the telescope focus moves (sec. mirror magnification)^2 times more than the mirror:mirror distance change. Thus for a $140^{o}F$ temperature range, the focus moves

$$(4)^2 \times (0.128 + 0.081) = 16 \times 0.209 = 3.34 \text{ inches.}$$

Thus, an adjustment of ± 2" for the detector section will compensate for any movement in the telescope due to thermal expansion. Some degree of adjustment is also required to initially set the detector section field stop at the telescope focus.

Adjustment of the vertical location of the detector section will be made manually by the operation of a hand crank which will be located at the outside of the telescope support frame structure which will be totally enclosed. The hand crank will operate a scissors jack which will raise and lower the detector section as required.

As shown on Drawing 47D252299 the detector section will have four linear bearing assemblies (items 6, 7, and 8) mounted to its rear (vertical base) plate, the bearing assemblies will ride vertically on two 1-inch diameter shafts (item 4) which will be mounted to a frame assembly (item 2) by means of four shaft hangers (item 5).

(continued)

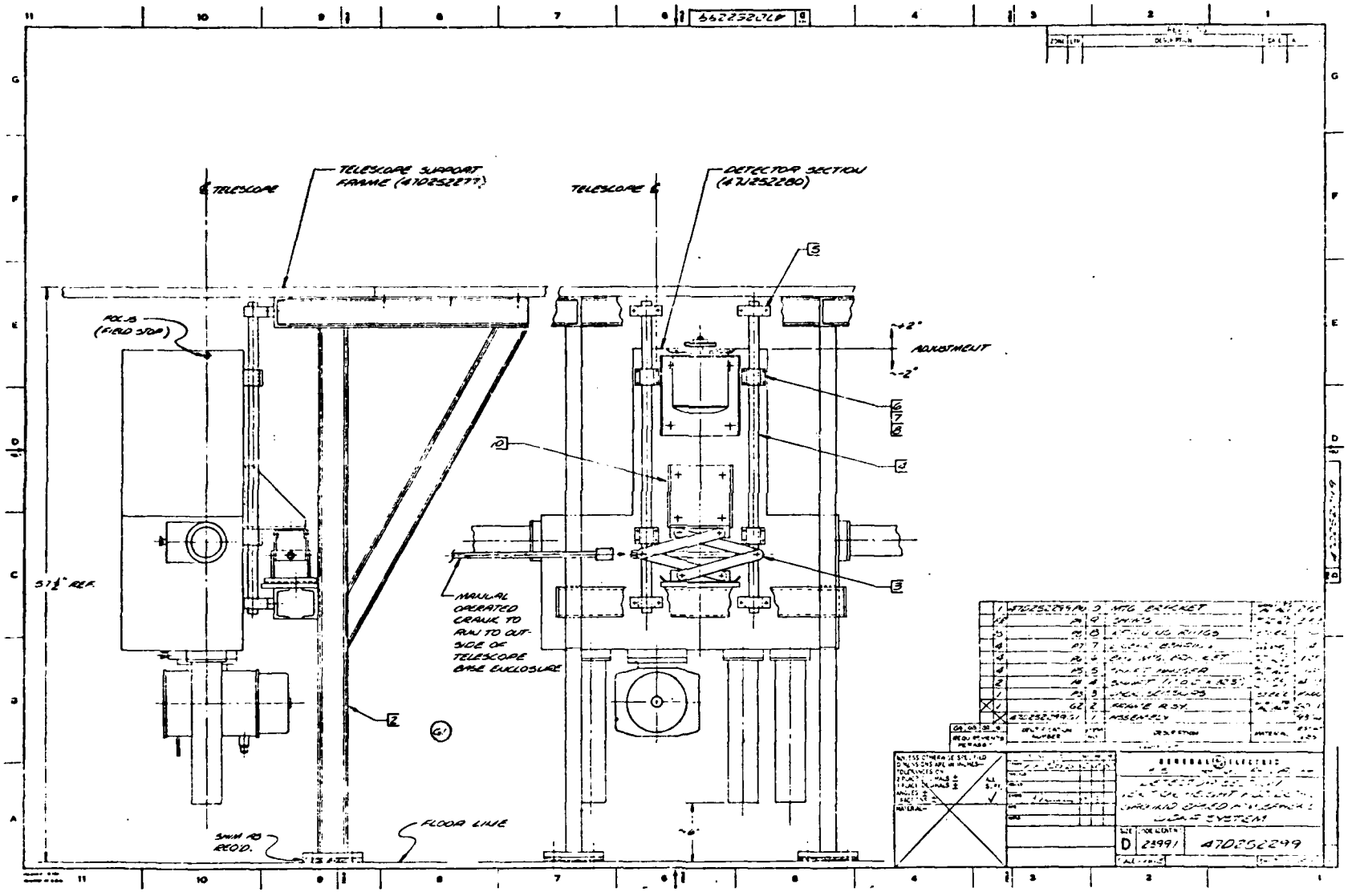

4.4.8 Figure 4.4-2

4.4.8 (continued)

The frame assembly will be constructed of 3-inch aluminum channel welded to form the support frame for both the detector section and the scissors jack. This support frame will be mounted under the enclosed telescope support frame and anchored to the floor in two places. The entire adjustment section excluding the detector section will weigh approximately 94 lbs.

The loads on the linear bearings will be minimal, approximately 25 lb in the radial direction. The radial load is due to the detector section being cantilevered out from its support shafts. The linear bearings are rated at 200 lbs each, which is well above the actual loads they will support.

4.5 Control and Data Acquisition

4.5.1 Basic Requirements

The Altitude of interest and the Time/Lidar run were defined in the SOW. The Altitude will determine when data will be acquired and the maximum time/Lidar run will effect how much memory is necessary to store the acquired data.

The maximum number of laser shots/sec. is defined by the Laser manufacturer and cannot exceed 10 pps. It has been determined that a maximum of 10 background measurements for every 1 laser shot will be adequate to gather atmospheric background data.

The dwell time/channel will directly affect the range resolution and its limit is defined in the statement of work.

The dead time while switching channels was arbitrarily chosen so as to minimize the loss of information while switching from one channel to the next.

4.5.1 BASIC LIDAR REQUIREMENTS

- Altitude of Interest - 20 km to 100 km
- Time/Lidar Run - ≈15 min (maximum)
- Number of Laser Shots - 10 pps - 9000/Run
- Background Measurements - 1 to 10/Laser Shot
  - 10 to 100/Sec.
  - 9,000 to 90,000/Run
- Dwell Time/Channel - ≤4 μsec
- Dead Time (Time to Switch Channels) - <100 nsec

4.5.2 Derived Requirements

The time of interest is arrived at by making use of the minimum and maximum altitude of interest in conjunction with the speed of light. This results in a time of approximately 130 μsec to 670 μsec after the emission of light from the laser.

The maximum number of counts/channel/run must be estimated in order to properly size the data memory. Assuming a maximum count rate of 20 counts/μsec, a dwell time of 2 μsec/ch, and 9000 laser shots/run then:

20 count/laser shots μsec • 2 μsec/ch • 9000 laser shots/run

This yields 360,000 counts/ch run.
Therefore a data memory with the capacity of 2^{19} would be adequate. This means a 19 bit wide memory.

The number of channels is based on a system using two energy detectors, one for λ_1 and one for λ_2, and six detectors. If one assumes a dwell time of 2 μsec/ch and you begin from T_0 then:

$$T_{100km} = 670 \text{ μsec}$$

$$\frac{670 \text{ μsec}}{2 \text{ μsec/ch}} = 335 \text{ channels}$$

Therefore

Data Channels	335	λ_1 Laser Shot
	335	λ_2 Laser Shot
	335	λ_1 Background Measurement
	335	λ_2 Background Measurement
	1340	Data Channels

The number of channels used to collect laser energy information from each laser shot is arbitrarily set at 500 ch/λ. This gives us 1 msec to gather the energy data. Then the total number of channels necessary would be:

1340	Data Channels
500	Energy λ_1
500	Energy λ_2
2340	

4.5.2 DERIVED REQUIREMENTS

- Time of Interest - 130 to 670 μsec after lasing

- Number of Counts/Channel - 360,000 or 2^{19} maximum

- Number of Channels Necessary -

- Data	335	λ_1	Laser
	335	λ_2	Laser
	335	λ_1	Background
	335	λ_2	Background
	500	λ_1	Energy
	500	λ_2	Energy
Total Channels	2340		

4.5.3 Simplified System Block Diagram

This simplified diagram relates to logistical control and functional subsystems necessary to realize a Lidar system.

System timing will be initiated and synchronized by the rotating shutter. This will determine when we have an opportunity for an event. The system Controller must then make a decision whether the event should be a laser shot, a background shot, or nothing at all.

Information relative to timing and nature of the event must be sent to both the multiplex controller and the data acquisition and storage subsystem.

The multiplexer in conjunction with the multiplex controller will determine what data is sent to the Data Acquisition and Storage subsystem. After the completion of a Lidar run, the data must be reduced and some type of permanent record made.

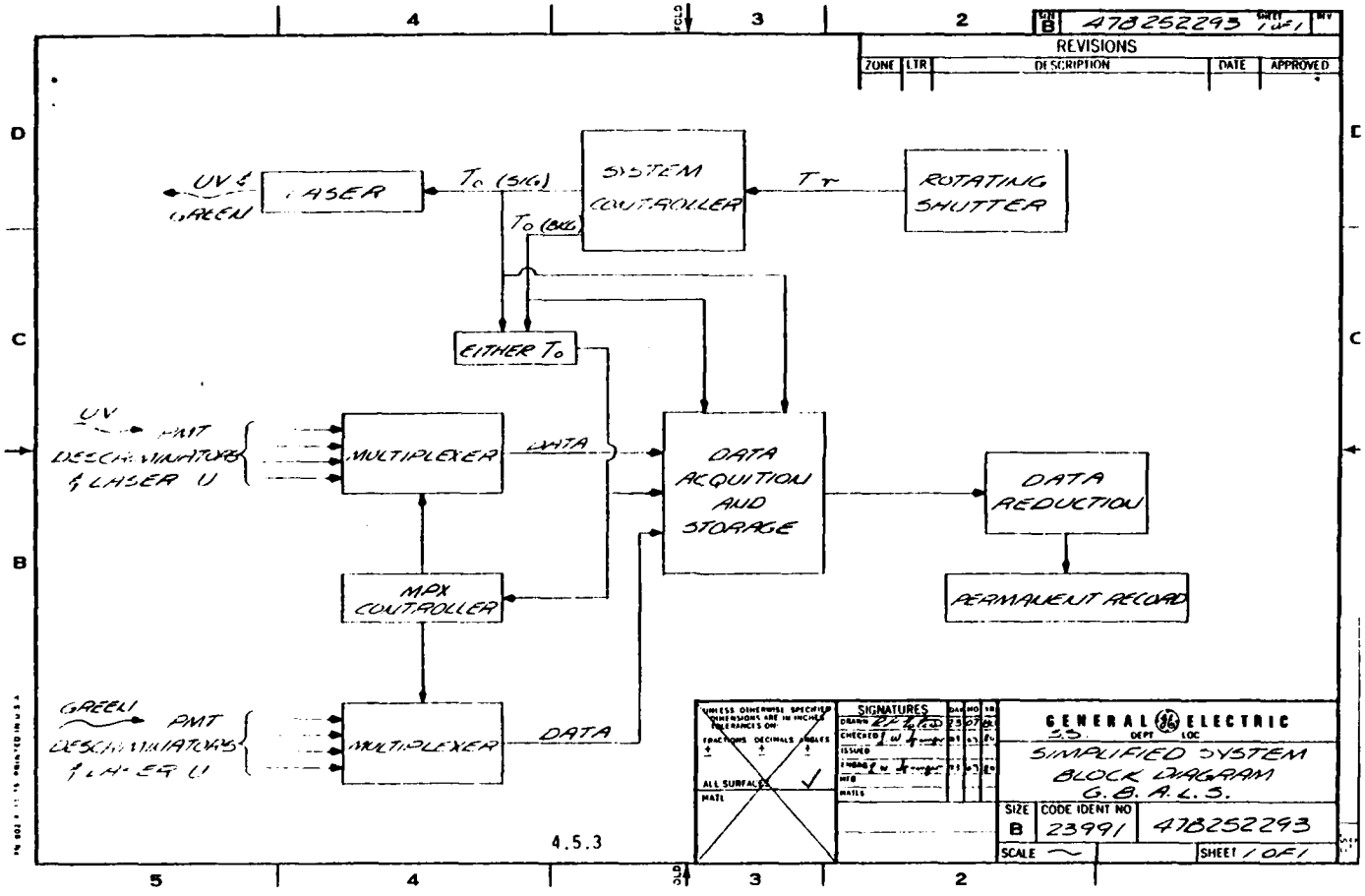
4
3
2
SIZE B 478252293 SHEET 1 OF 1 REV
REVISIONS
ZONE LTR DESCRIPTION DATE APPROVED
D
C
B
UV & GREEN
LASER
T_o (SIG)
T_o (BKG)
SYSTEM CONTROLLER
T_T
ROTATING SHUTTER
EITHER T_o
UV PMT DESIGNATORS & LASER U
MULTIPLEXER
DATA
DATA ACQUITION AND STORAGE
DATA REDUCTION
PERMANENT RECORD
MPX CONTROLLER
GREEN PMT DESIGNATORS & LASER U
MULTIPLEXER
DATA
4.5.3
UNLESS OTHERWISE SPECIFIED DIMENSIONS ARE IN INCHES TOLERANCES ON FRACTIONS DECIMALS ANGLES ALL SURFACES MATL
SIGNATURES
DRAWN
CHECKED
ISSUED
MFG
MATLS
GENERAL ELECTRIC
55 DEPT LOC
SIMPLIFIED SYSTEM BLOCK DIAGRAM G.B.A.L.S.
SIZE B CODE IDENT NO 23991 478252293
SCALE ~ SHEET 1 OF 1
5
4
3
2

4.5.4 Data Acquisition and Storage (DAS)

The main function of the DAS System is to count the number of events presented to it and store these events in a memory which can be correlated with respect to T_o. These events must be stored in a cumulative fashion so as to reflect the total count of a Lidar Run.

The Le Croy Model 3521 Multi-channel Scaling module fits this application. It has a maximum counting rate of 100 mHz, with a minimum dwell time of 1 μsec/channel for each unit. This means since we will have two of these units that our minimum dwell time per channel will be 2 μsec. This directly relates to range resolution. The dead time between channels is negligible resulting in no loss of data while switching. To realize all these capabilities it must be operated in the DMA mode, i.e., free from processor control. This is easily accomplished with an onboard DMA controller.

All necessary functions of the 3521 can be externally controlled. This is necessary in our situation so we can synchronize the counter to T_o.

The standard memory width and depth is more than adequate for our needs and is easily expandable by a factor of eight.

4.5.4 DATA ACQUISITION & STORAGE (DAS)

FUNCTION

- Acquire Data Rapidly
- Store Data in Proper Time Slot
- Be Able to Add Data From Many Shots
- Be Externally Controllable

SOLUTION - LeCroy Model 3521 Multi-Channel Scaling Module

SPECIAL FEATURES

- 100 mHz Counting Rate
- 1 μsec dwell time/channel/unit
- 5 nsec dead time
- DMA compatible
- 8000 channel capacity standard
- 24 bit word standard
- Externally or internally controlled
- Data stored can be cumulative

4.5.5 Electronic Control Block Diagram

After the system has been reset and the start button depressed, initiation begins with the detection of the first shutter sync pulse. This pulse is derived from the shutter wheel and a photodiode/LED combination. The pulse is passed through the shaper and delay circuit. This circuit sharpens the pulse and provides a variable delay for timing. The pulse is then passed on to the system controller.

The function of the system controller is to determine if the system is in a go condition. If so it then counts the number of pulses received from the shutter. Depending on the number received it will either do nothing, send a signal to make a background run, or finally send a signal to fire the laser. Each time the laser is fired an internal counter is incremented and compared with the front panel setting for the number of laser shots. The laser continues to fire, with background shots being taken in between laser shots, until the preset number has been reached. The system controller then stops firing.

Each time a laser trigger or a background trigger is sent out, the 3521's and the multiplexer controller are reset and readied for the next shot.

The system clock runs at a crystal controlled frequency of 500 kHz and is used to increment the 3521's address and to increment the counter in the MPX controller. It is started by the detection of laser output or a delayed signal from the background trigger. This forces the system to be synchronized with the laser output.

If a fire laser trigger appears the address controller is automatically enabled. This adds an address offset into the 3521's, and the laser shot data will be stored separately from background shot data.

The MPX controller counts the number of clock pulses from T_0 and compares them with three front panel set points which determines when the MPX will switch detectors.

Data is presented to the 3521's via the multiplexers.

The energy from the two wavelengths is independently monitored by two photodiodes. This information is then properly amplified and digitized using a voltage-to-frequency converter. The digitized signal is then presented to the multiplexer and in turn the 3521's for storage.

It should be pointed out that two fiber optic links are used in the system. These are used to couple signals to the laser console, a large source of noise. The fiber optics completely eliminate any ground loops between the laser console and the control console.

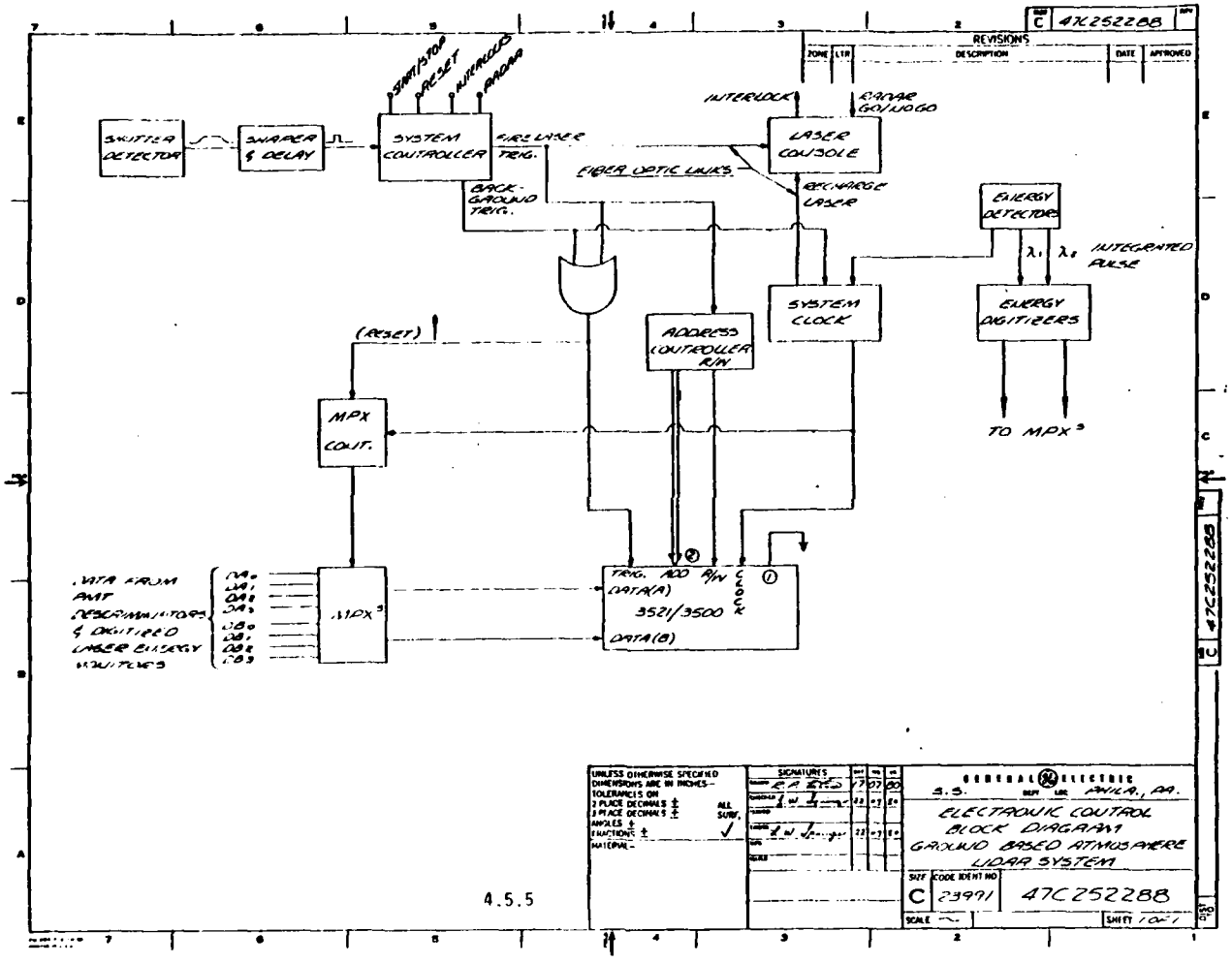
47C252288
REVISIONS
ZONE LTR DESCRIPTION DATE APPROVED
SWITCH DETECTOR
SHAPER & DELAY
SYSTEM CONTROLLER
START/STOP
RESET
INTERLOCKS
RADAR
FIRE LASER TRIG.
BACK-GROUND TRIG.
INTERLOCK
RADAR GO/NO GO
LASER CONSOLE
FIBER OPTIC LINKS
RECHARGE LASER
ENERGY DETECTOR
λ1 λ2 INTEGRATED PULSE
ENERGY DIGITIZERS
SYSTEM CLOCK
ADDRESS CONTROLLER RAM
(RESET)
MPX CONT.
TO MPX'S
DATA FROM ANT DISCRIMINATORS & DIGITIZED LASER ENERGY MONITORS
MPX'S
TRIG. ADD R/W
DATA(A)
3521/3500
DATA(B)
CLOCK
UNLESS OTHERWISE SPECIFIED DIMENSIONS ARE IN INCHES
TOLERANCES ON
2 PLACE DECIMALS ±
3 PLACE DECIMALS ±
ANGLES ±
FRACTIONS ±
MATERIAL
ALL SURF. ✓
SIGNATURES
GENERAL ELECTRIC
S.S. ANCLA., AA.
ELECTRONIC CONTROL BLOCK DIAGRAM GROUND BASED ATMOSPHERE LIDAR SYSTEM
SIZE C
CODE IDENT NO 23991
47C252288
SCALE
SHEET 1 OF 1
4.5.5

4.5.5-1 System Timing

This diagram shows how individual signals are related to others, with respect to time. It is not all inclusive, but rather shows those events in time that are critical. The purpose is to show sequential events and therefore the pulse widths are not necessarily to scale.

Two different events are shown on the diagram, one is a laser shot and the other a background shot. In both cases the shutter sync signal initiates the event. A shaped shutter sync is generated with the proper delay to assure an aperture open condition during the time of interest. For both the laser shot and the background shot, reset signals are generated and presented to both the multiplex controller and the 3521's. This readies them for the upcoming shot. If the laser is to be fired, then the address control is enabled and information sent to the 3521's to modify their base address. It it is a background shot, then the address controller is left disabled and the beginning address of the 3521's will not be modified.

To achieve an accurate T_0 for a laser shot, the actual laser pulse is used to start the system clock. The clock has an inherent 2.6 μsec delay and we add another 1.4 μsec of delay so that the clock starts exactly 4 μsec after lasing, it is then exactly 2 channels late. This loss of time is not significant since useful data is not obtained for 130 μsec after laser firing. Since the offset in time is known quite accurately, then it can easily be accommodated in the data reduction software.

During a background shot there is no laser pulse to initiate the clock and a delayed pulse is generated which closely approximates the proper T_0.

Paragraphs 4.5.5-1 through 4.5.5-8 discuss each system function in detail.

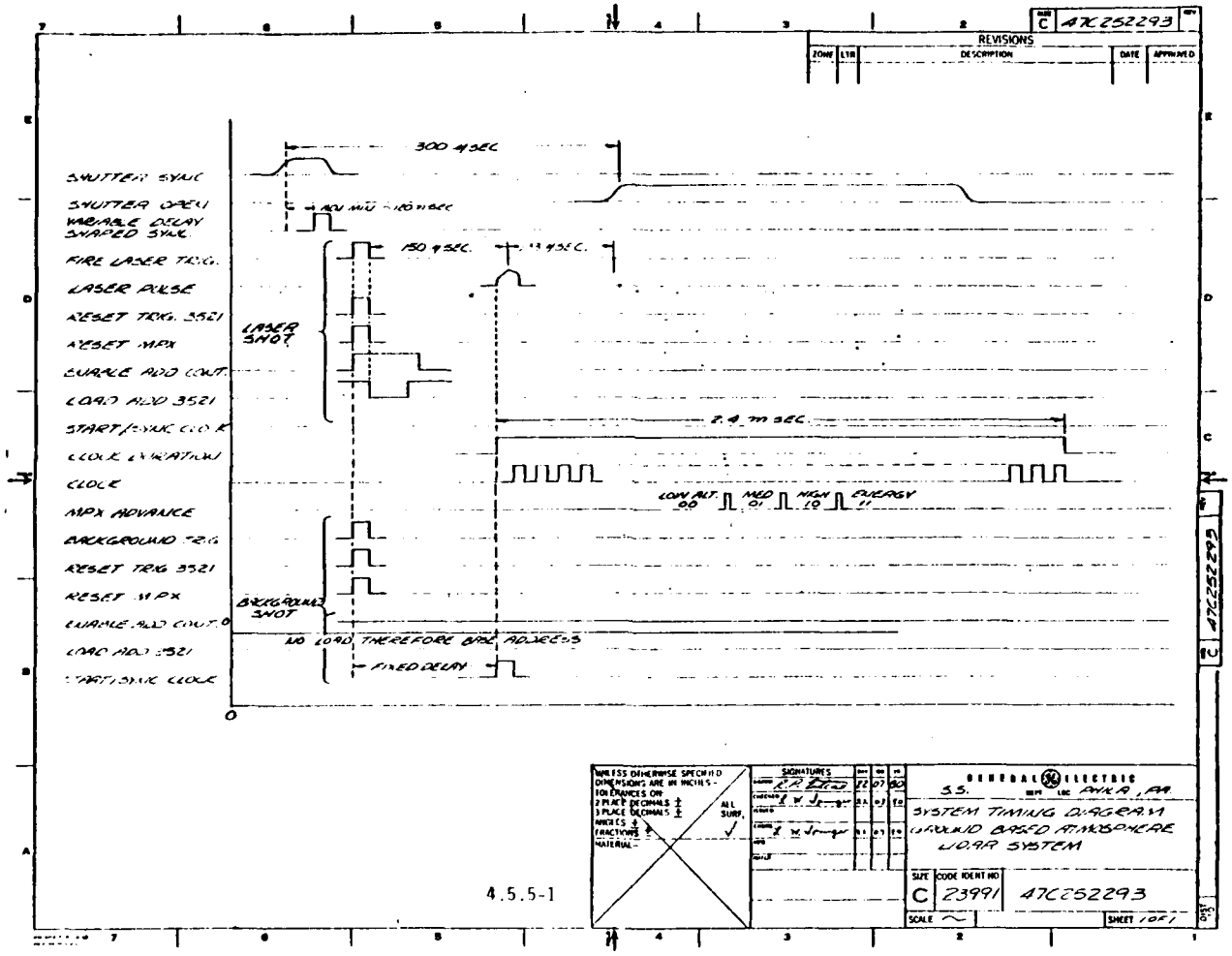
C 47C252293
REVISIONS
ZONE LTR DESCRIPTION DATE APPROVED
300 μSEC
SHUTTER SYNC
SHUTTER OPEN
VARIABLE DELAY SHAPED SYNC
FIRE LASER TRIG.
LASER PULSE
RESET TRIG. 3521
RESET MPX
LASER SHOT
BURST ADD COUNT
LOAD ADD 3521
START/SYNC CLOCK
CLOCK OSCILLATION
CLOCK
MPX ADVANCE
BACKGROUND TRIG
RESET TRIG 3521
RESET MPX
BACKGROUND SHOT
BURST ADD COUNT
LOAD ADD 3521
START/SYNC CLOCK
150 μSEC.
13 μSEC.
2.4 m SEC.
LOW ALT. 00
MED 01
HIGH 10
ENERGY 11
NO LOAD, THEREFORE BASE ADDRESS
FIXED DELAY
UNLESS OTHERWISE SPECIFIED DIMENSIONS ARE IN INCHES - TOLERANCES ON 2 PLACE DECIMALS ± 3 PLACE DECIMALS ± ANGLES ± FRACTIONS ± MATERIAL -
ALL SURF. ✓
SIGNATURES
GENERAL ELECTRIC
S.S. AMES, IA
SYSTEM TIMING DIAGRAM
GROUND BASED ATMOSPHERE LIDAR SYSTEM
SIZE C
CODE IDENT NO 23991
47CE52293
SCALE
SHEET 1 OF 1
4.5.5-1
C 47C252293

4.5.5-2 Shutter Sync Shaper and Delay Circuit

This circuit consists of only one IC, which is a dual monostable flip-flop with Schmitt trigger inputs.

Operation of the circuit is as follows: A relatively slow rising pulse is received from the rotating shutter wheel. This shutter sync pulse is generated substantially ahead of the actual shutter opening, approximately 300 μsec. The signal is fed to the Schmitt trigger input of one of the flip-flops. Two things result; first the Schmitt trigger input substantially sharpens the leading edge of the pulse and secondly the monostable flip-flop generates a square pulse of variable length. The variable length of the pulse is used to set the delay of the circuit. This pulse is then fed to the input of the second flip-flop. On the negative transition of the first pulse the second flip-flop is triggered and delivers an output pulse of fixed width. This output is then used as a sync pulse for other events.

The minimum delay that can be realized from this circuit is approximately 120 nsec.

For a more detailed circuit see drawing #47B252284 - Electrical Schematic.

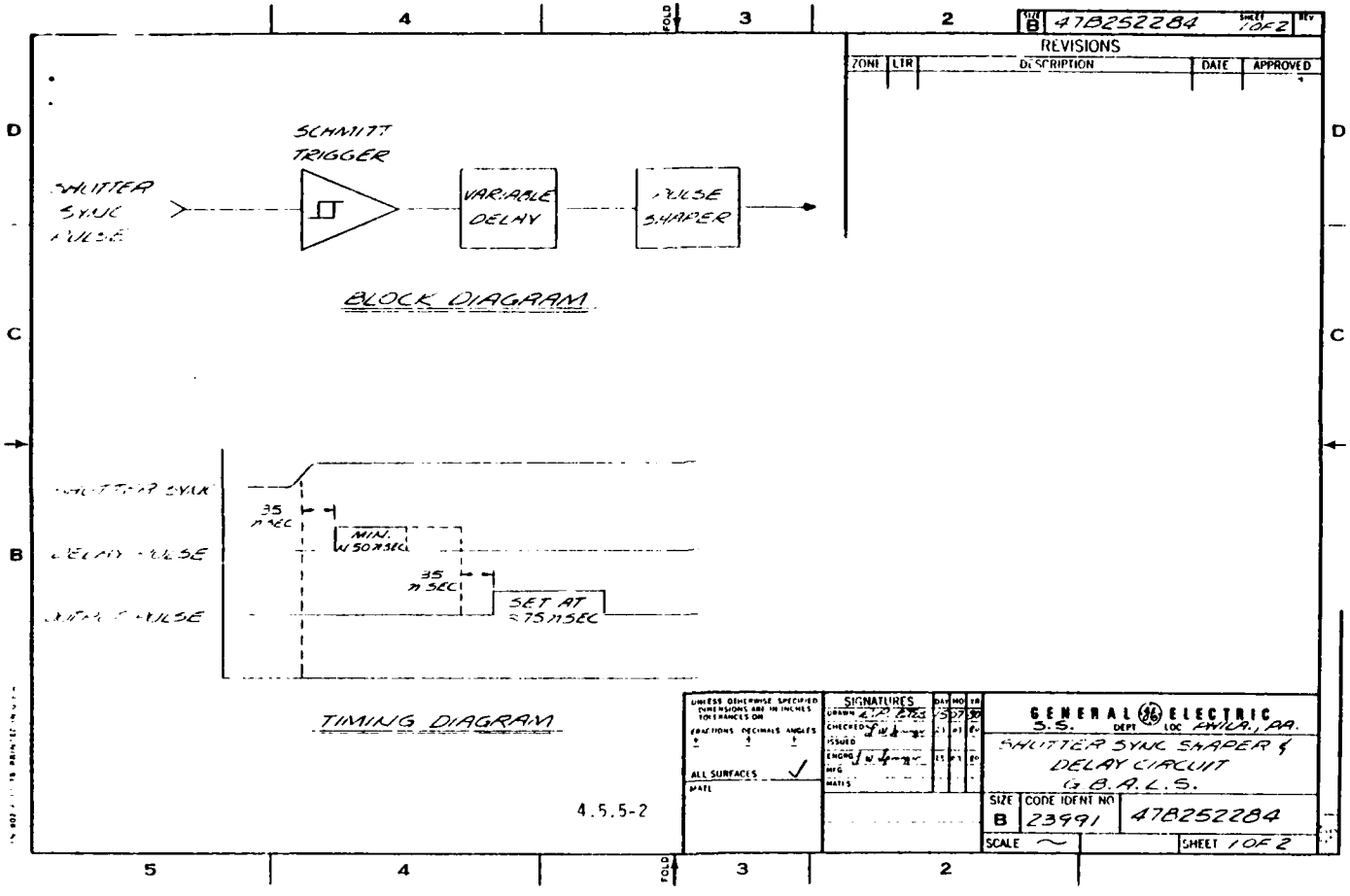
4
3
2
B 47B252284 SHEET 1 OF 2 REV
REVISIONS
ZONE LTR DESCRIPTION DATE APPROVED
D
C
B
SCHMITT TRIGGER
SHUTTER SYNC PULSE
VARIABLE DELAY
PULSE SHAPER
BLOCK DIAGRAM
SHUTTER SYNC
35 μSEC
MIN. W 50 μSEC
DELAY PULSE
35 μSEC
SET AT ≈75 μSEC
OUTPUT PULSE
TIMING DIAGRAM
4.5.5-2
UNLESS OTHERWISE SPECIFIED DIMENSIONS ARE IN INCHES TOLERANCES ON FRACTIONS DECIMALS ANGLES ALL SURFACES MATL
SIGNATURES
DRAWN
CHECKED
ISSUED
ENGRG
MFG
MATLS
GENERAL ELECTRIC
S.S. DEPT LOC PHILA., PA.
SHUTTER SYNC SHAPER & DELAY CIRCUIT
G.B.A.L.S.
SIZE B CODE IDENT NO 23991 47B252284
SCALE SHEET 1 OF 2
5
4
3
2

4.5.5-3 System Controller

The system controller can be separated into three major sections; the shutter opportunity counter/control, laser shot counter/control, and reset circuitry, including start/stop functions and power-up inhibit circuitry.

Circuit operation begins when power is turned on. This causes two separate circuits to output a pulse which inhibits circuit operation by disabling the input gate. By pressing the reset button all circuits are cleared and primed for operation. However, the input gate is still disabled since the start button must be pressed after the reset button. Assuming all external interlocks have been closed, the circuit is now ready to begin operation. By pushing the start/stop button once, the input gate is enabled and shutter sync pulses are fed to the divide-by-two circuit, then every other pulse clocks the 24-bit shift register. The high which was previously loaded into bit 1 of the shift register is now shifted sequentially from left to right down the register. The number and timing of background shots is determined by accessing the parallel outputs of the register. As shown on the drawing, background shots will occur from the 6th through the 17th clock pulse. This can be changed as desired. The 18th bit of the shift register is fed through a pulse generator and fires the laser. As can be seen this happens once every 18 clock pulses or once every 36 shutter sync signals. An explanation is in order to explain why there is a laser pulse every 18th clock pulse or every 36th shutter pulse. Because of shutter wheel speed and the number of openings in the shutter wheel there are 345 openings or opportunities per second. The divide-by-2 circuit gives us 172.5 clock pulse/sec and divide that by 18 yields 9.58 laser shots/sec. This is just under the manufacturers 10 shots/sec for the laser.

The decade counter is incremented every time the laser fires and its output presented in BCD. The output of the decade counter is fed to a 16-bit magnitude comparator which compares the laser shots to the number set on the front panel thumbwheel switch designated "Number of Laser Shots". When the number of laser shots equals the set number the input gate is disabled and an "End of Run" light is energized.

The process can be stopped and restarted any time during the run by again pressing the start/stop button. A radar control is easily implemented, which could automatically stop and restart the process.

Speed is not critical in any of the above functions, therefore standard TTL circuits are used throughout.

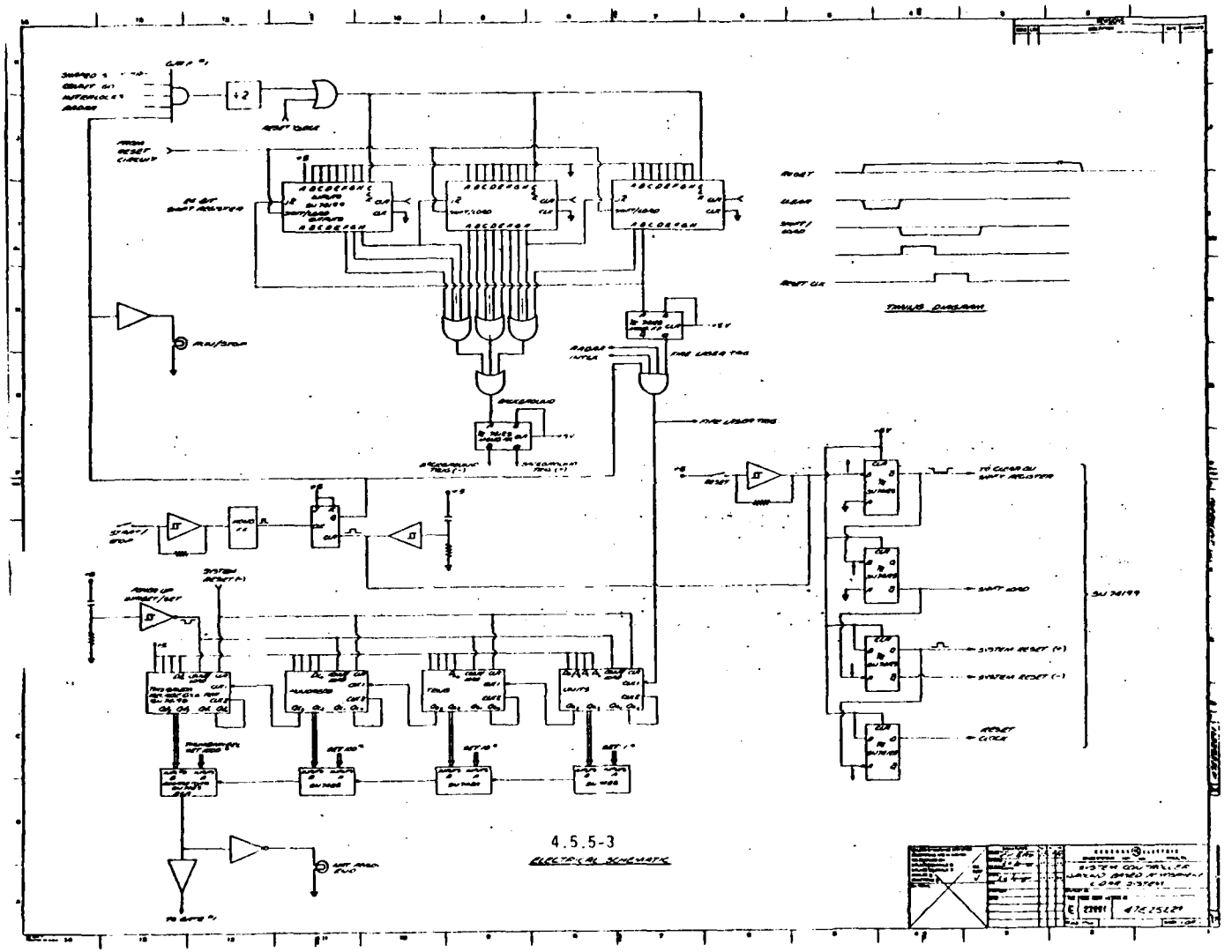

4.5.5-3
ELECTRICAL SCHEMATIC

4.5.5-4 Multiplex Controller

The multiplex controller provides address information to the multiplexer for proper time/channel control.

The controller consists of three major sections; a 3-digit decade counter, three-twelve bit magnitude comparators, and an address decoder.

Circuit operation begins when a reset pulse is received from either the background trigger or the fire laser trigger. Operation of the circuit is the same in either case. When the system clock starts it is fed through a shaper to the 3-digit decade counter. The BCD output of this is fed to three separate 12-bit magnitude comparators. The comparator continually samples this information and compares it with three preset values; a medium altitude start, a high altitude start, and an energy start. When the count equals a set point an output pulse is generated which causes the address decoder to be incremented by one, thereby switching channels on the multiplexer.

In this circuit speed is essential to minimize dead time when switching inputs. This circuit will result in switching times of less than 100 nsec, including the switching time of the multiplexer itself, which is 12 nsec. If necessary a three-fold improvement could be realized by the use of more complex and consequently more expensive circuitry.

For a more detailed circuit drawing refer to the electrical schematic drawing #47C252289.

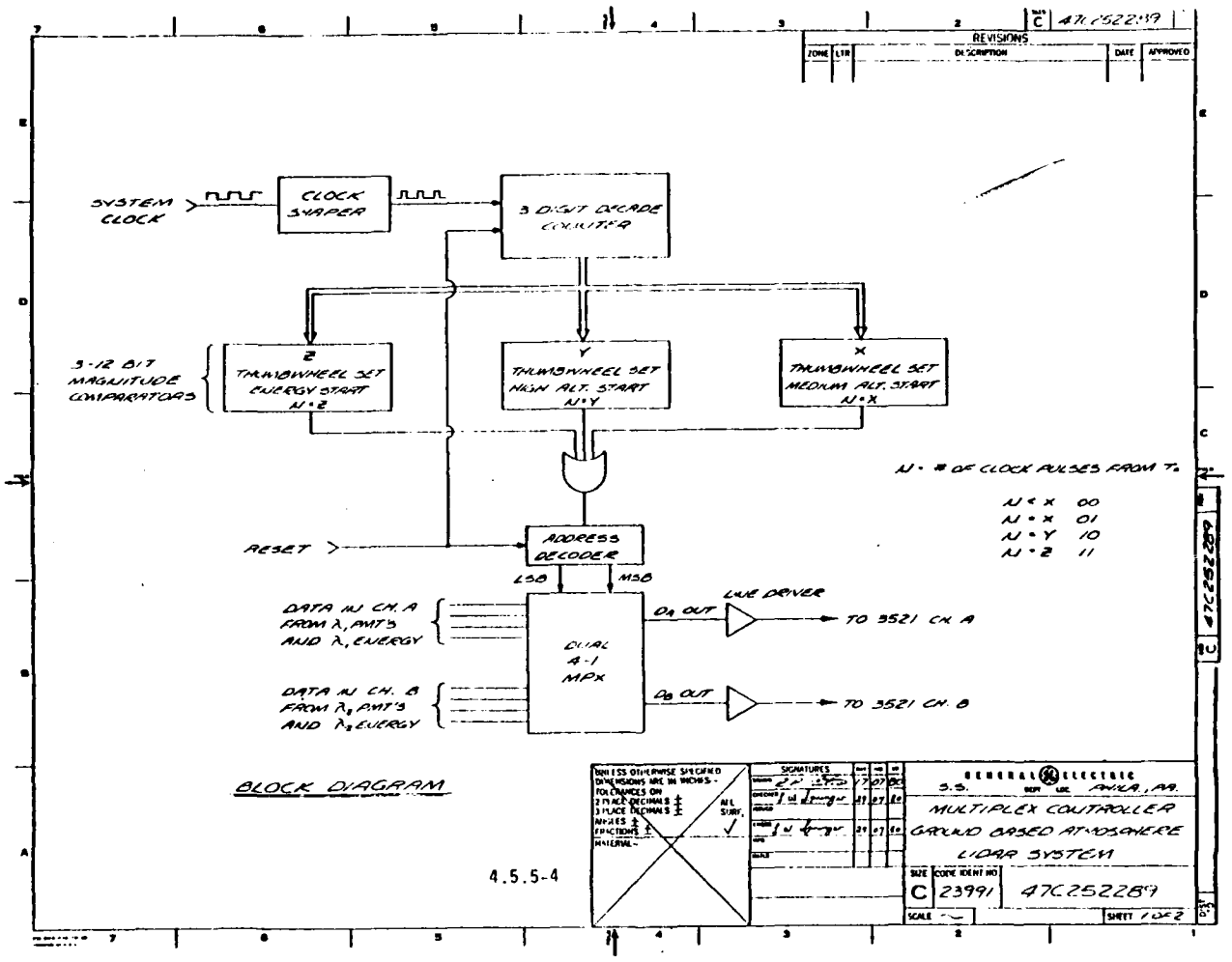
47C252289
REVISIONS
ZONE LTR DESCRIPTION DATE APPROVED
SYSTEM CLOCK
CLOCK SHAPER
3 DIGIT DECADE COUNTER
3-12 BIT MAGNITUDE COMPARATORS
Z THUMBWHEEL SET ENERGY START N=Z
Y THUMBWHEEL SET HIGH ALT. START N=Y
X THUMBWHEEL SET MEDIUM ALT. START N=X
N = # OF CLOCK PULSES FROM T0
N < X 00
N = X 01
N = Y 10
N = Z 11
RESET
ADDRESS DECODER
LSB
MSB
DATA IN CH. A FROM λ1 AMT'S AND λ1 ENERGY
DATA IN CH. B FROM λ2 AMT'S AND λ2 ENERGY
DIGITAL 4-1 MPX
DA OUT
DB OUT
LINE DRIVER
TO 3521 CH. A
TO 3521 CH. B
BLOCK DIAGRAM
4.5.5-4
UNLESS OTHERWISE SPECIFIED DIMENSIONS ARE IN INCHES
FOR CHANGES ON
2 PLACE DECIMALS ±
3 PLACE DECIMALS ±
ANGLES ±
FRACTIONS ±
MATERIAL
ALL SURF. ✓
SIGNATURES
GENERAL ELECTRIC
S.S. ANNA, PA.
MULTIPLEX CONTROLLER
GROUND BASED ATMOSPHERE
LIDAR SYSTEM
SIZE C
CODE IDENT NO 23991
47C252289
SCALE
SHEET 1 OF 2

4.5.5-5 System Clock

The lidar system requires synchronization between the laser pulse T_0 and the LeCroy channel advance. Usually the LeCroy system uses an internal clock to advance its channels and although this signal is available to the user, it is not capable of being externally synchronized; therefore, the need for an external clock.

The circuit shown in the schematic uses a single I.C. for the clock generator. It is basically a voltage controlled oscillator which can be operated in a crystal controlled mode, resulting in good stability. The ability of this device to be externally gated on and at the same time synchronized makes it particularly suited to this application. The fundamental frequency of the crystal is 500 kHz thereby allowing the required 2 μsec dwell time for the LeCroy 3521's.

The circuit operation differs somewhat between a laser shot and a background shot, this difference will be explained after brief explanation of the circuit.

The clock generator itself has a 2.6 μsec inherent delay, and added to this is a fixed delay of 1.4 μsec. This results in a 4 μsec delay of the clock which is an even multiple of the clock frequency. As long as the delay is known and is consistent it presents no problem since data gathering does not begin until $(T_0 + 130)$ μsec.

During a laser shot the output of the laser is used to trigger the clock generator. This is coupled into the circuit which generates the previously described 1.4 μsec delay. After the delay a pulse of 2 msec is fed to an "and" gate. This pulse along with a "go" from the comparator circuit generate an enable signal for the clock. The clock pulses are then buffered and fed to both the 3521's and the multiplex controller. The clock continues to run until the number of pulses is equal to the preset number fed into the comparator. This is a front panel thumbwheel switch to be labeled "maximum channel count". The process is repeated for each subsequent laser or background shot.

When a background shot is required it is necessary to generate a pseudo T_0 signal which has approximately the same delay from the shutter sync pulse as does the laser output. This pulse is generated by the use of a suitable delay circuit. The timing for a background shot is not critical, and after the delay the operation of the circuit is exactly the same as that of a laser shot.

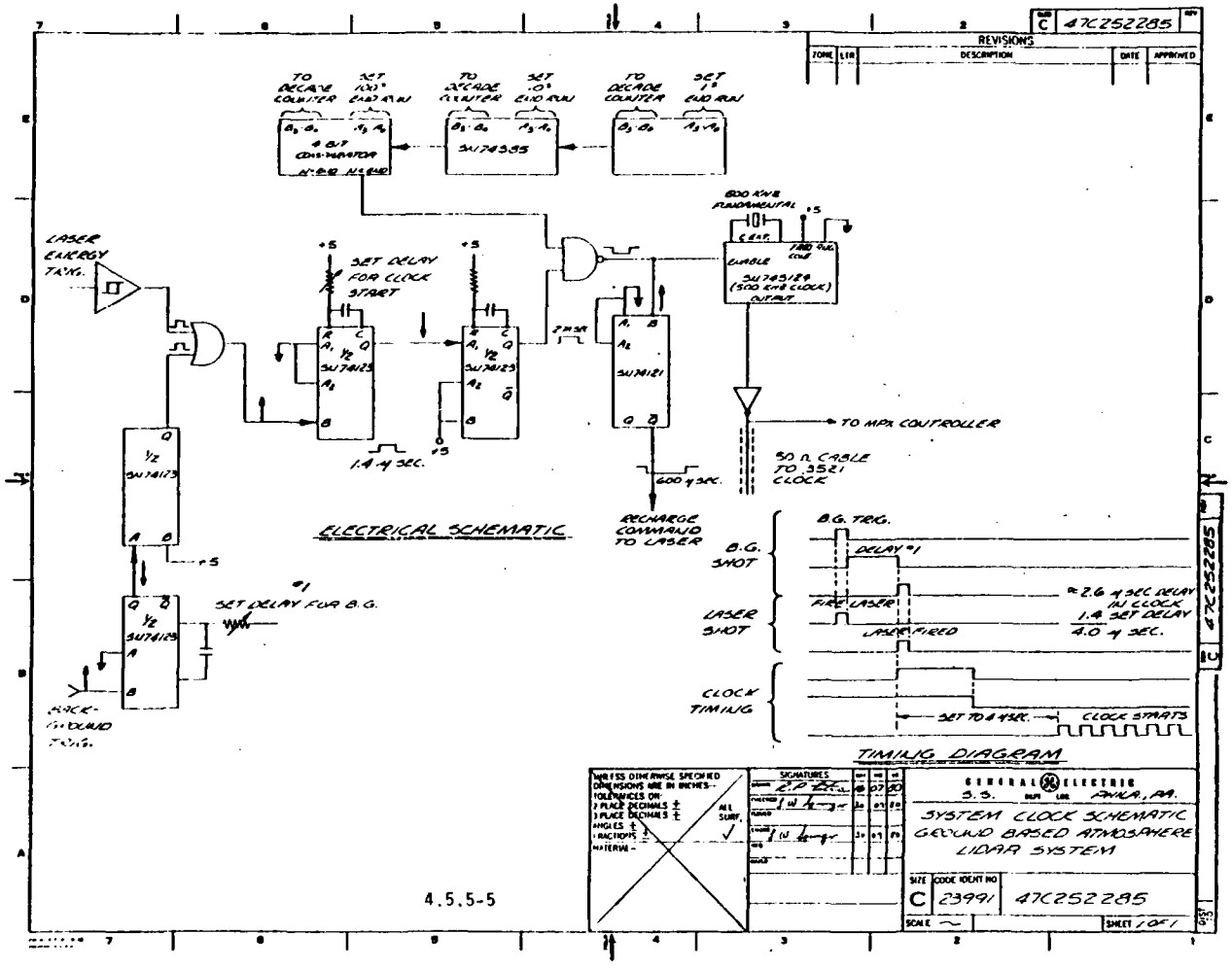
C 47C252285
REVISIONS
ZONE LTR DESCRIPTION DATE APPROVED
TO DECADE COUNTER
SET 100's END RUN
TO DECADE COUNTER
SET 10's END RUN
TO DECADE COUNTER
SET 1's END RUN
4 BIT COMPARATOR
SN74S85
LASER ENERGY TRIG.
+5
SET DELAY FOR CLOCK START
SN74123
1.4 μ SEC.
SN74121
600 KHz FUNDAMENTAL
CRYSTAL
CABLE
SN74S189 (500 KHz CLOCK) OUTPUT
TO MPX CONTROLLER
50 Ω CABLE TO 3521 CLOCK
600 μ SEC.
RECHARGE COMMAND TO LASER
ELECTRICAL SCHEMATIC
SET DELAY FOR B.G.
#1
BACK-GROUND TRIG.
B.G. TRIG.
B.G. SHOT
DELAY #1
FIRE LASER
≈ 2.6 μ SEC DELAY IN CLOCK
1.4 SET DELAY
4.0 μ SEC.
LASER SHOT
LASER FIRED
CLOCK TIMING
SET TO 4 μSEC.
CLOCK STARTS
TIMING DIAGRAM
UNLESS OTHERWISE SPECIFIED DIMENSIONS ARE IN INCHES
TOLERANCES ON:
2 PLACE DECIMALS ±
3 PLACE DECIMALS ±
ANGLES ±
MACHINE
MATERIAL
ALL SURF.
SIGNATURES
GENERAL ELECTRIC
S.S. DEPT. LOC. ANAHEIM, CA.
SYSTEM CLOCK SCHEMATIC
GROUND BASED ATMOSPHERE
LIDAR SYSTEM
SIZE C
CODE IDENT NO 23991
47C252285
SCALE ~
SHEET 1 OF 1
4.5.5-5

4.5.5-6 Address Controller

During any lidar run there will be both laser shots and background shots. Separate storage locations must be provided and properly accessed for the two different types of data. This is the function of the address controller.

In the basic LeCroy 3500 system there are 8000 data storage locations. Upon initial set up, each of the 3521 scalers is given a base address where it begins to store its data. The address is then incremented by one channel each time it receives a clock pulse. By use of the proper control lines and the address bus of the 3521's this base address can be modified. The resulting address that the 3521's use to store data then would be the base address plus the modifying address. In this way we separate the background shot data from the laser shot data.

The circuit allows one to modify the base address by as much as 2048 by properly setting the internal switches, which represents bits 0 through 11 of the address lines.

The rest of the circuit is there to provide timing for both the address modifier and the 3521's. The base address of the 3521's is modified when a laser event occurs,otherwise (background shot) the circuit is disabled and no modifying address is presented to the 3521's.

For a more detailed drawing of the address controller see drawing #47B252287, "Address Controller Schematic Diagram".

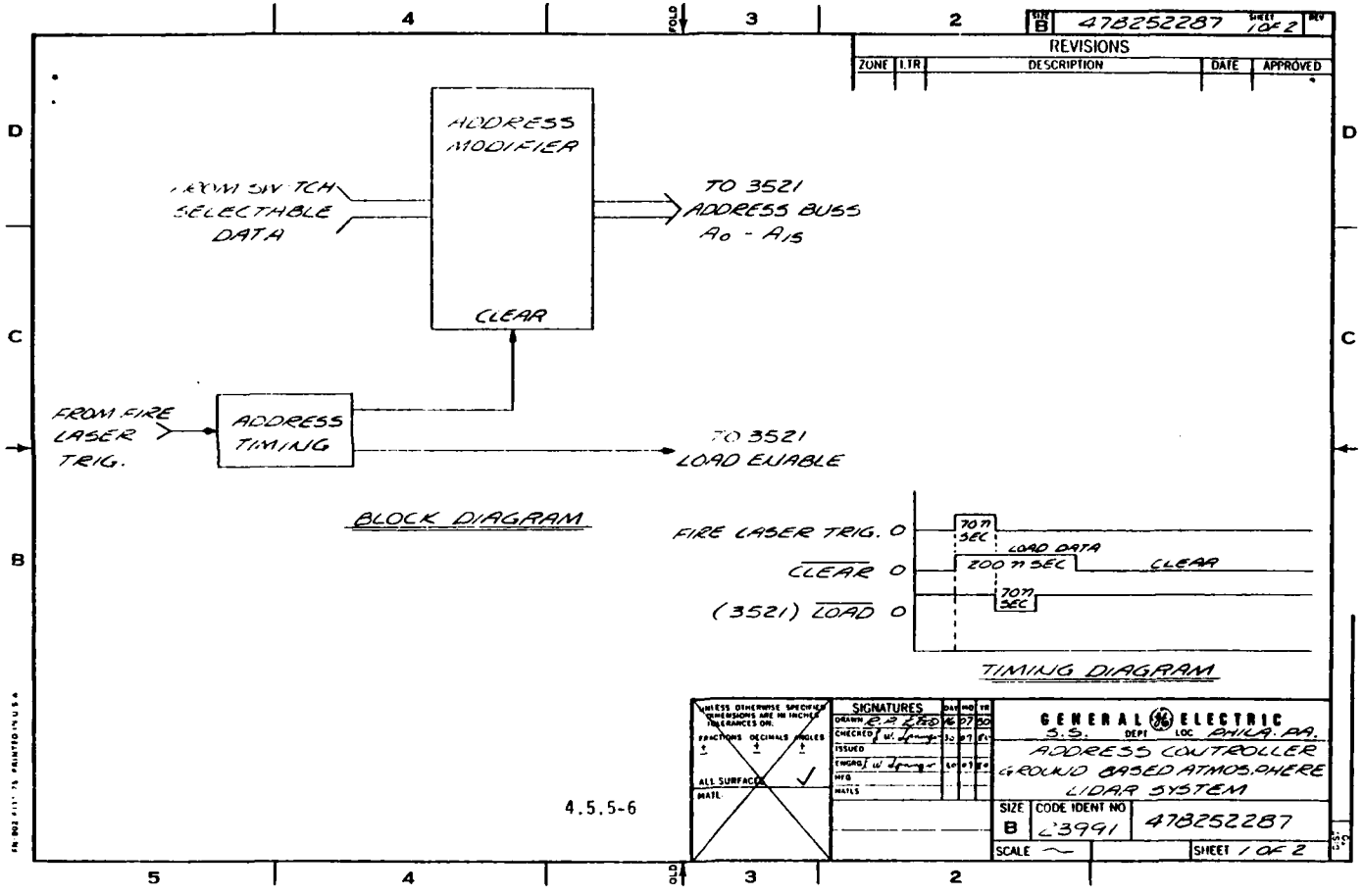
SIZE B 478252287 SHEET 1 OF 2 REV
REVISIONS
ZONE | LTR | DESCRIPTION | DATE | APPROVED
ADDRESS MODIFIER
TO 3521 ADDRESS BUSS A0 - A15
CLEAR
FROM FIRE LASER TRIG.
ADDRESS TIMING
TO 3521 LOAD ENABLE
BLOCK DIAGRAM
FIRE LASER TRIG. 0
CLEAR 0
(3521) LOAD 0
70 ?? SEC
LOAD DATA
200 ?? SEC
CLEAR
TIMING DIAGRAM
SIGNATURES
DRAWN
CHECKED
ISSUED
ENGRG
MFG
MATLS
GENERAL ELECTRIC
S.S. DEPT LOC PHILA. PA.
ADDRESS CONTROLLER
GROUND BASED ATMOSPHERE
LIDAR SYSTEM
SIZE B CODE IDENT NO 73991 478252287
SCALE SHEET 1 OF 2
4.5.5-6

4.5.5-7 Energy Monitor

The energy monitor serves two purposes, first it serves to monitor the energy of the laser pulse and secondly it is used to generate the T_0 pulse for the electronics. Two monitoring circuits are required; one for the UV and one for the green.

The circuit itself is very simple and consists of a fast photodiode connected to a power supply through a load resistor. One output is coupled directly from the photodiode and is used as a T_0 signal, the other is fed to an integrator for use as an energy monitor. This circuit is not new and has previously been used successfully on other GE lidar systems.

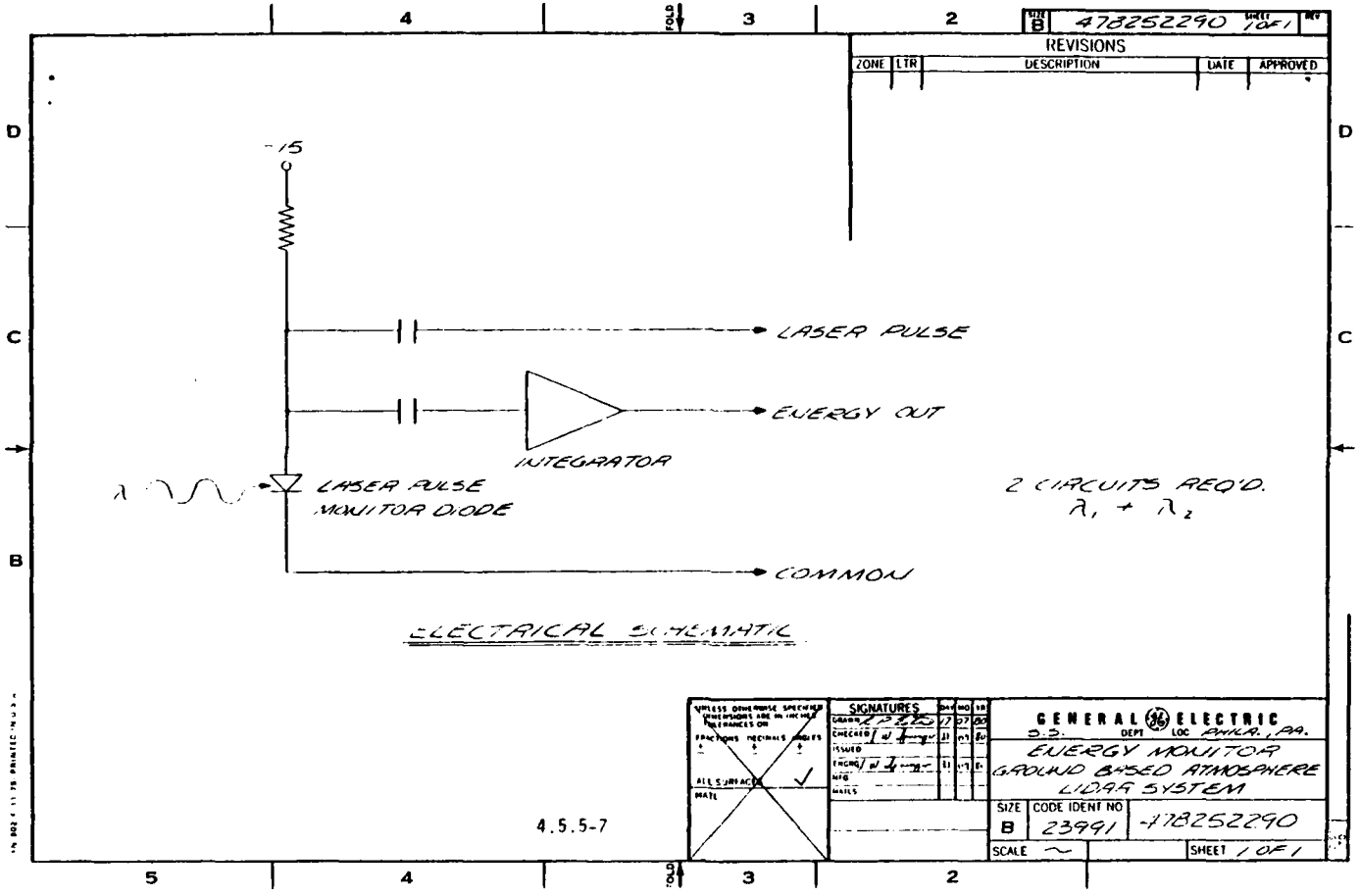
4
3
2
SIZE B 478252290 SHEET 1 OF 1 REV
REVISIONS
ZONE LTR DESCRIPTION DATE APPROVED
D
C
B
15
LASER PULSE
ENERGY OUT
INTEGRATOR
LASER PULSE MONITOR DIODE
COMMON
2 CIRCUITS REQ'D.
λ1 + λ2
ELECTRICAL SCHEMATIC
4.5.5-7
SIGNATURES
GENERAL ELECTRIC
U.S. DEPT LOC ANKA., PA.
ENERGY MONITOR
GROUND BASED ATMOSPHERE
LIDAR SYSTEM
SIZE B
CODE IDENT NO 23991
478252290
SCALE ~
SHEET 1 OF 1
5
4
3
2

4.5.5-8 Energy Digitizer

The energy digitizer is used to convert the analog energy signal to digital form so that it can be stored in the 3500 system.

Analog information from the energy monitor circuit is presented to the track and hold amplifier. At the proper time a pulse is sent to the T/H amplifier, which for the length of the pulse causes it to track the analog input signal. After the pulse again returns to zero the analog input is locked into the amplifier. With the proper voltage conditioning it is fed to a voltage-to-frequency converter. This device delivers a frequency output which is proportional to the input voltage. The maximum frequency is 1 MHz and the minimum usable frequency for our system is 1 kHz. The output of the V/F converter is then fed to a pulse shaper, and then directly to the multiplexer, which at the proper time delivers it to the scaler.

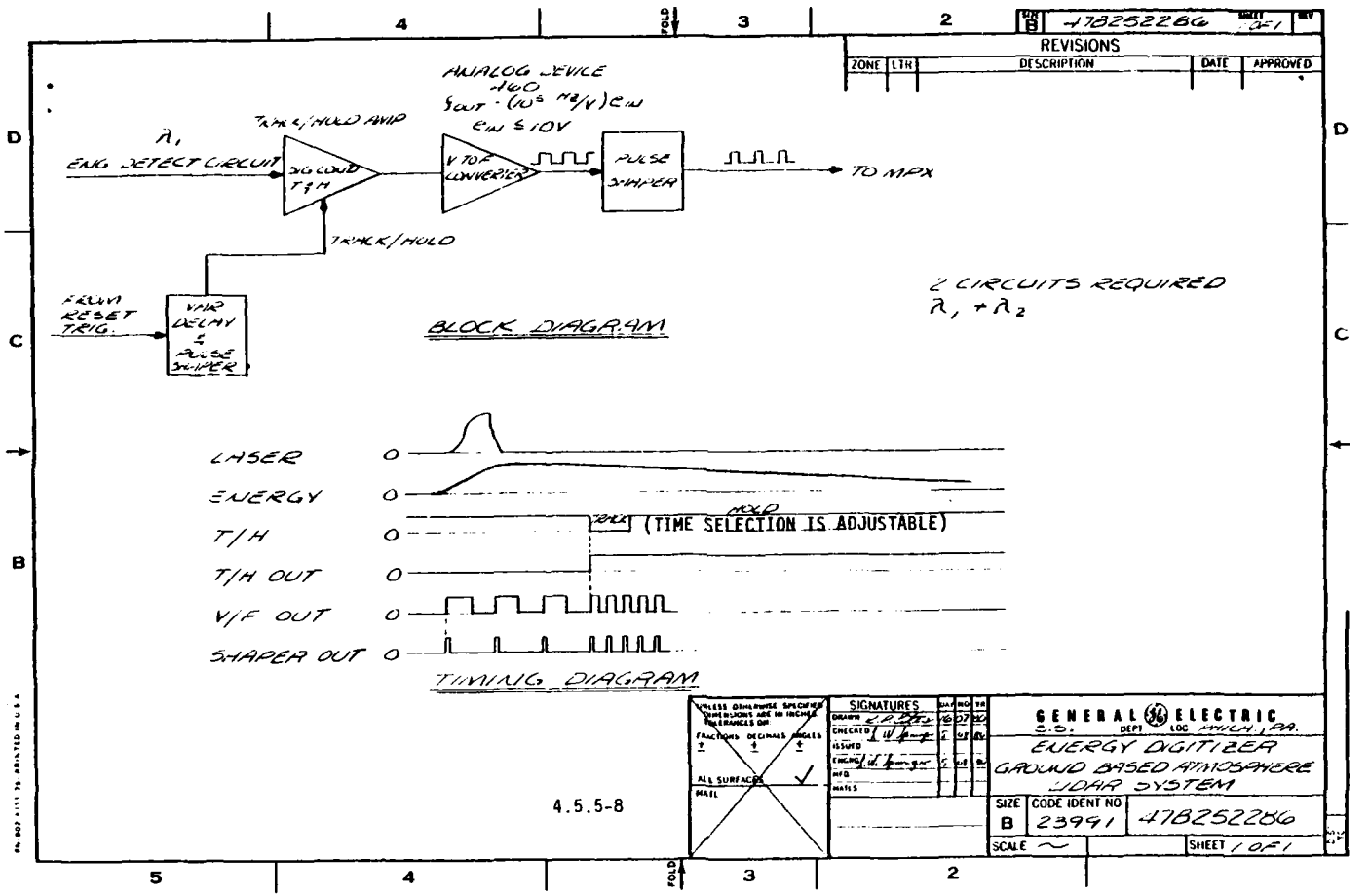
SIZE B 4782522B6 SHEET 2F1 REV
REVISIONS
ZONE LTR DESCRIPTION DATE APPROVED
ANALOG DEVICE 460
$V_{OUT} = (10^5 \text{ Hz/V}) e_{IN}$
$e_{IN} \leq 10V$
λ_1
ENG DETECT CIRCUIT
TRACK/HOLD AMP
20 LOUD T&H
V TO F CONVERTER
PULSE SHAPER
TO MPX
TRACK/HOLD
FROM RESET TRIG.
VAR DELAY & PULSE SHAPER
BLOCK DIAGRAM
2 CIRCUITS REQUIRED
$\lambda_1 + \lambda_2$
LASER
ENERGY
T/H
T/H OUT
V/F OUT
SHAPER OUT
0
MAX
MIN
(TIME SELECTION IS ADJUSTABLE)
TIMING DIAGRAM
4.5.5-8
SIGNATURES
DRAWN
CHECKED
ISSUED
ENGR
MFG
MATLS
GENERAL ELECTRIC
S.D. DEPT LOC MICH, PA.
ENERGY DIGITIZER
GROUND BASED ATMOSPHERE
LIDAR SYSTEM
SIZE B
CODE IDENT NO 23991
4782522B6
SCALE
SHEET 1 OF 1

4.5.6 LeCroy System 3500

The LeCroy system 3500 is a high performance acquisition and control system.

In G-BALS it provides housing, power, and some control of the two 3521 multi-channel scalers. The control functions related to the MCS units are limited to initialization, DMA, and data storage.

The 3500 system is very versatile and with the addition of optional equipment G-BALS can make good use of many other functions, resulting in a completely self-contained Lidar system. These options will be discussed individually and finally a complete system shown.

AD-A091 955 DESIGN STUDY FOR GROUND-BASED ATMOSPHERIC LIDAR SYSTEM (U) GENERAL ELECTRIC CO PHILADELPHIA PA SPACE DIV R L FRANKLIN ET AL. 29 SEP 80 AFGL-TR-80-0264 2/3

UNCLASSIFIED F19628-80-C-0062 F/G 4/1 NL

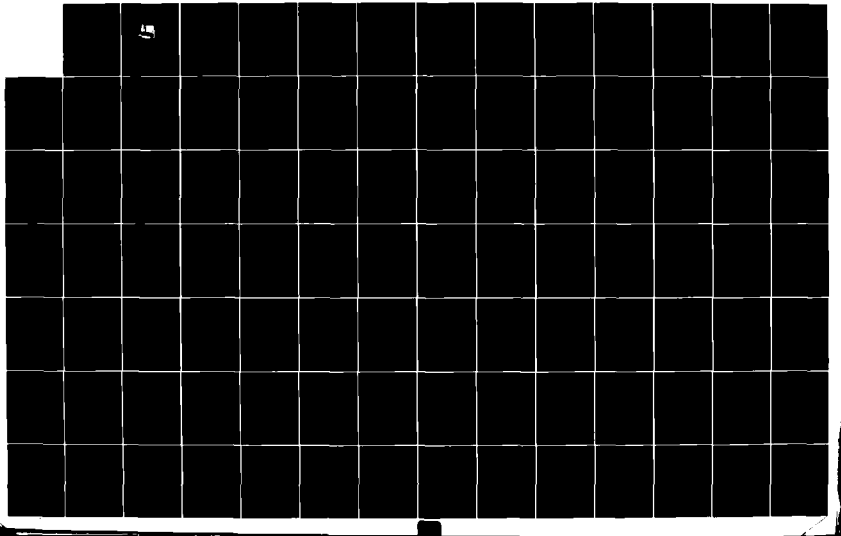

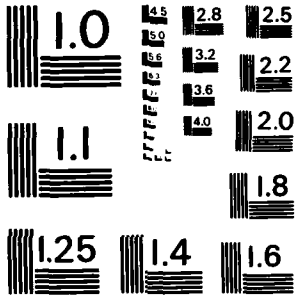

4.5.6 LE CROY SYSTEM 3500

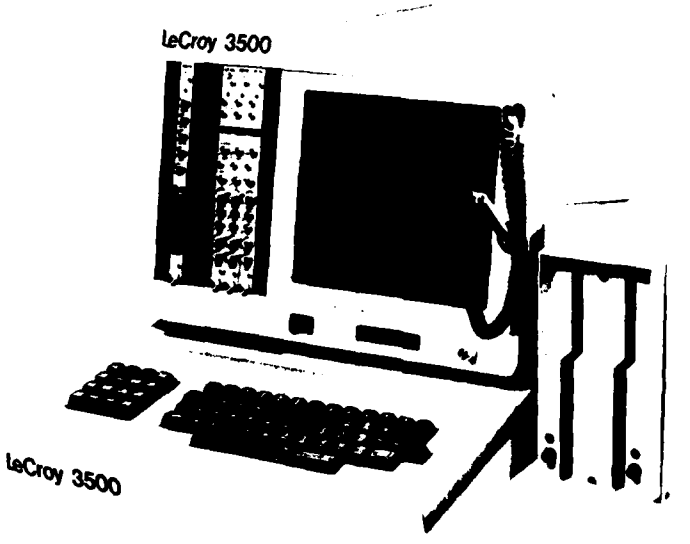

Functions Provided

- Initialization of 3521's
- DMA control for 3521's
- Provide memory for data
- Serialized data dump (RS-232)
- Normalization and display of data
- High density data storage via floppy disc
- Complete data reduction
- Hard copy via plotter/printer

4.5.6-1 Dual-Drive Floppy Disc

The LeCroy Model 3921 Dual-Drive Floppy Disc is an accessory for LeCroy's 3500 system. It is a random access memory device that records and retrieves data on two removable flexible diskettes. It provides 273 Kilo-bytes per drive of data or program storage in IBM 3740 format. Model 3921 consists of a dual-drive disc unit, a disc controller interface, a diskette containing software, which includes LeCroy's system 3500 operating system, and the users choice of Fortran or Basic Software, and two spare diskettes for data and/or user program storage. By the addition of the dual-drive floppy disc the 3500 system becomes in essence a fully programmable mini-computer.

With the addition of this device the Lidar system can be made completely independent of a host computer. Contact was made by GE with the appropriate LeCroy personnel. It was determined that all calculations necessary to reduce the raw data can be made by the LeCroy 3500 system using an appropriate Fortran program. It should be possible to put the Fortran translator, the 3500 operating system, and the Lidar program all one disc. This will leave 273 Kilo-bytes available for permanent storage of data. If the data were stored in raw form this would result in approximately 17 lidar runs per diskette, assuming 32 bit format (24 bit data and 8 bit identification). Of course as many diskettes can be used as necessary.

4.5.6-1 DUAL-DRIVE FLOPPY DISC

OPTIONAL ACCESSORY FOR 3500 SYSTEM

- PROVIDES
  - Two floppy disc drives and controller
  - 273 Kilo-bytes/drive of storage
  - Fortran programming
  - Complete data reduction
  - Permanent data storage
  - Reduced data displayed on CRT
    - Tabular
    - Curves
    - Run number
    - Etc.

4.5.6-2 Printer/Plotter

The LeCroy Model 3931 Printer/Plotter will provide the user with a permanent hard copy of Lidar results. Anything that is presented on the 3500 CRT can be easily dumped to the printer/plotter. The Model 3931 directly interfaces with the existing RS232 port and therefore needs no special interface board.

4.5.6-2 PRINTER/PLOTTER

- LeCroy Model 3931
- Provide hard copy
- Direct CRT screen dump
- Compatible with existing RS 232 port

4.5.7 System 3500 Architecture

The system 3500 architecture, as shown on the facing page, illustrates the internal layout of the 3500 system. It also shows external devices necessary to make the lidar system completely self-contained.

The 3500 system is available in two basic versions, Model 3500C and 3500M. Basically, the 3500M is designed for DMA applications while the 3500C is designed for Camac applications. Either model is field upgradable. Depending on the model purchased, different add-on features will be necessary for a complete package. Two shopping lists are furnished.

MODEL 3500M

3921 Dual Floppy Disc Accessory
with Fortran

3931 Printer/Plotter

MODEL 3500C

3921 Dual Floppy Disc Accessory
with Fortran

DMA Data Memory Module

MCA Firmware

3931 Printer/Plotter

Light Pen

ALSO

(2) 3521 Multi-Channel Scalers

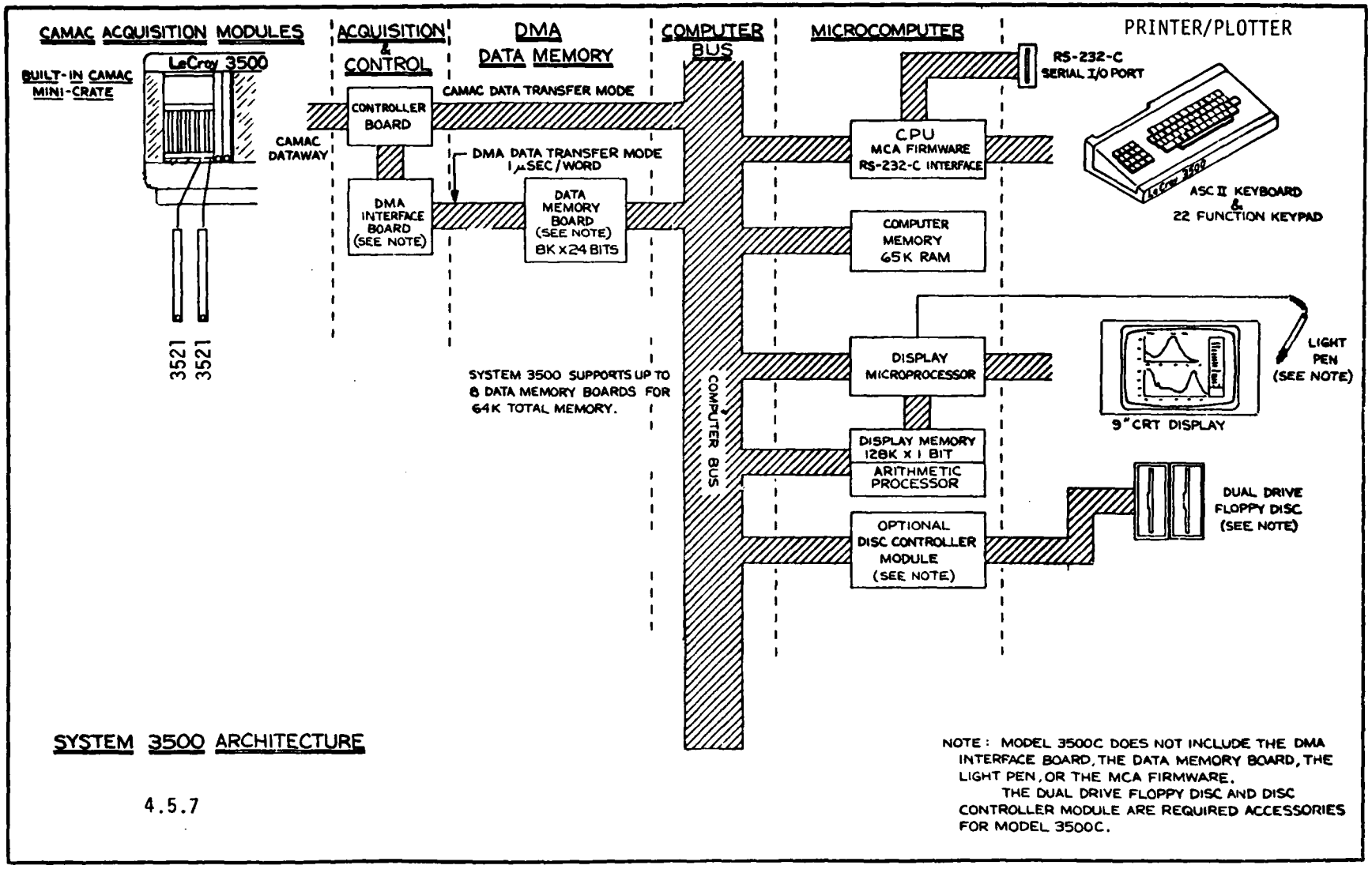

SYSTEM 3500 ARCHITECTURE

4.5.7

NOTE: MODEL 3500C DOES NOT INCLUDE THE DMA INTERFACE BOARD, THE DATA MEMORY BOARD, THE LIGHT PEN, OR THE MCA FIRMWARE.
THE DUAL DRIVE FLOPPY DISC AND DISC CONTROLLER MODULE ARE REQUIRED ACCESSORIES FOR MODEL 3500C.

4.5.8 Maintenance

Since the control system will be completely solid state there should normally be no need for maintenance. It may however be advisable, to assure prcper operation, to periodically check the frequency of the system clock and the different delays between signals.

Again, since the LeCroy is mostly solid state, little or no maintenance should be required. The two exceptions to this are the floppy disc and printer/plotter, which should be maintained as suggested by the manufacturer.

4.5.8 MAINTENANCE

- Solid state electronic requires little maintenance

- 1-2 month interval

  Check

  - System clock
  - Delay variables

- LeCroy System

  - No maintenance required on solid state equipment
  - Maintain floppy disc as required by manufacturer
  - Maintain printer/plotter

4.5.9 Control Console

Depicted on the opposite page is a conceptual drawing of the Control Console including the LeCroy dual floppy disc device. A minimum of external control will ensure simple and error free operation.

The controls include 5 thumbwheel switches which will be used to set the total number of laser shots per lidar run, the beginning channel for the medium altitude signal, the high altitude signal, the energy signal, and finally the last channel to be addressed per opportunity. Also included is a power on/off switch, a stop/start button, and a reset button.

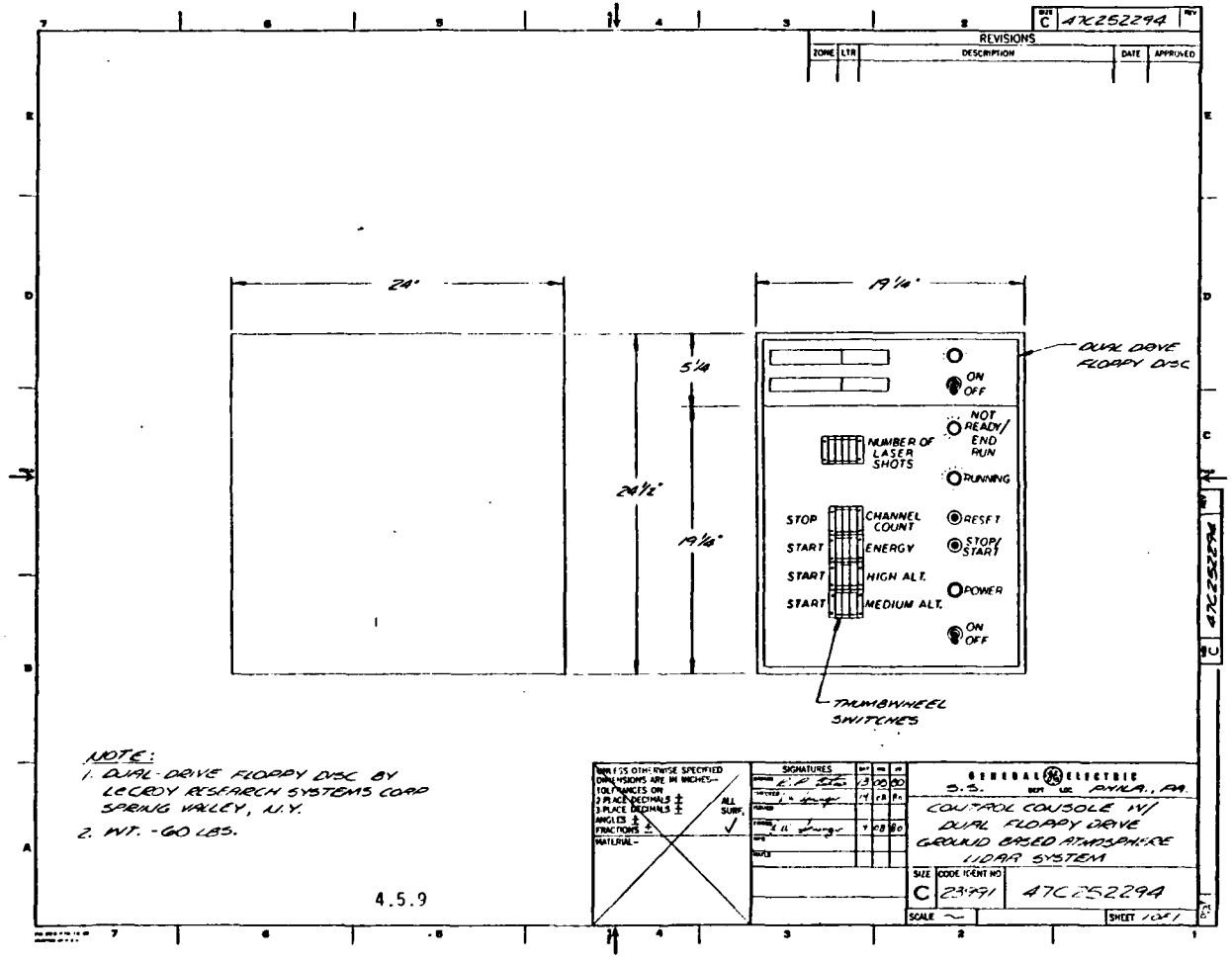
SIZE C 47C252294 REV
REVISIONS
ZONE LTR DESCRIPTION DATE APPROVED
24"
19 1/4"
5 1/4
24 1/2"
19 1/8"
DUAL DRIVE FLOPPY DISC
ON OFF
NOT READY/ END RUN
RUNNING
NUMBER OF LASER SHOTS
STOP
START
START
START
CHANNEL COUNT
ENERGY
HIGH ALT.
MEDIUM ALT.
RESET
STOP/ START
POWER
ON OFF
THUMBWHEEL SWITCHES
NOTE:
1. DUAL-DRIVE FLOPPY DISC BY LECROY RESEARCH SYSTEMS CORP SPRING VALLEY, N.Y.
2. WT. -60 LBS.
4.5.9
UNLESS OTHERWISE SPECIFIED DIMENSIONS ARE IN INCHES
TOLERANCES ON
2 PLACE DECIMALS ±
3 PLACE DECIMALS ±
ANGLES ±
FRACTIONS ±
MATERIAL -
ALL SURF.
SIGNATURES
GENERAL ELECTRIC
S.S. DEPT. LOC. PITTSFIELD, PA.
CONTROL CONSOLE W/ DUAL FLOPPY DRIVE
GROUND BASED ATMOSPHERE LIDAR SYSTEM
SIZE C
CODE IDENT NO 23791
47C252294
SCALE
SHEET 1 OF 1

4.6 Operational Requirements

Well before the lidar run while the roof opening is still closed, if possible the receiver telescope and laser beam expander ambient temperature should be adjusted to match the outside temperature anticipated for the time of the lidar run. Given the large thermal equilibrium time for the telescope, this thermal pre-conditioning will greatly reduce the required open-roof time and will probably allow lidar runs to start earlier in the evening. Similarly, if the Varian PMT is not normally stored in a fully cooled condition, its special cooled housing will require two hours to come to PMT operating temperature.

Any time the laser is optically adjusted or personnel are potentially exposed to the laser beam, proper protective laser goggles should be worn. Laser goggles are commercially available which will protect the user from both of the non-visible laser wavelengths (1064 and 355 nm), while providing relatively good transmission in the visible including the 532 nm (green) laser line. In this case, the user must still be careful to avoid excessive exposure to the laser green output.

Since the optical components inside the laser head come to thermal equilibrium with both the room and the considerable optical power in the head, the laser optimum internal alignment is a function of stable average output power. That is, the laser head final alignment can be made only after the laser warms up and its output stabilizes, and then laser alignment will be maintained only as long as room temperature and laser output are held constant. Thus, if the laser is switched from automatic repetition to remote control by the lidar shutter, the shutter speed must already be adjusted to result in the same laser repetition rate. To maintain laser alignment and output, the laser operation and repetition rate must continue without change or interruption as subsequent lidar runs are made.

4.6 OPERATIONAL REQUIREMENTS

A. Well Before Lidar Run
- Expose telescope and beam expander to expected outside temperature
- Adjust system focus to anticipated outside temperature
- Equilibration of laser and detection assembly to normal room temperature

B. ≥2 Hrs. Before Lidar Run
- Cool PMT-6 (see Section 4.4)
- Check transmitter receiver alignment (see Section 6.0)

C. ≥30 Min. Before Lidar Run
- Start laser as per manufacturer instructions (wear protective goggles)
- Turn on all electronics
- With PMT shutters closed, note PMT dark current
- Adjust altitudes and Run time limits
- Initialize LeCroy System as per manufacturers instructions
- Connect laser output monitor to scope
- When laser stabilizes (15-30 min.)
  - Observe green & UV outputs on scope
  - Optimize outputs (see laser manual)
  - Continue to operate laser
  - Block laser output beam
- Start rotating shutters
- Open roof cover
- Remove Lidar optical covers
- Open PMT shutters and note sky background reading
- Check shutter speed

D. Lidar Run
- Make sure roof and air spaces are all clear
- Unblock laser beam
- Switch laser from "Auto" to "Remote" and immediately start Lidar Run
- As ground truth calibration (sounding) data is taken, make a Lidar calibration run
- Between adjacent Lidar Runs, continue operating laser at same repetition rate
- Continue making Lidar Runs as desired

E. Lidar Shut-Down
- Block laser beam and turn off laser
- Turn off rotating shutters and close PMT shutters
- Replace optical cover
- Close roof opening
- Turn off all remaining electronics

4.7 Drawing List

4.7.1 Mechanical Drawing Index

A list of preliminary design drawings, that define all mechanical subsystems of G-BALS, is shown on the facing page. Reduced copies of all the original issues are included throughout this report for completeness to facilitate the reader's overall understanding of G-BALS. Some portions of the reduced copies are not completely legible due to the size reduction required to accommodate a report size page. The reader should therefore refer to the original full size issue which is provided under separate cover.

4.7 DRAWING LIST

4.7.1 MECHANICAL DRAWING INDEX

	TITLE	DRAWING NUMBER
1.	INSTALLATION	47J252275
2.	TELESCOPE	47C252276
3.	TELESCOPE SUPPORT FRAME	47D252277(1)
4.	LASER AND BEAM EXPANDER SUPPORT FRAME	47D252278(1)
5.	ALIGNMENT SCHEMATIC	47D252279
6.	DETECTOR SECTION	47J252280
7.	BEAM EXPANDER	47B252281
8.	LASER HEAD SCHEMATIC	47B252282
9.	TRANSMITTER (45^{o} TURNING) MIRROR	47A252283
10.	CONTROL CONSOLE WITH DUAL FLOPPY DRIVE	47C252294
11.	INSTALLATION TEMPERATURE ZONES	47B252295
12.	LASER HEAD	47B252296
13.	LASER HEAD POWER SUPPLY	47B252297
14.	MOUNTING STAND - 45^{o} MIRROR	47C252298(1)
15.	DETECTOR SECTION VERTICAL HEIGHT ADJUSTMENT DETAIL	47D252299
16.	WINDOW/ENERGY MONITOR	47B250324

NOTES:

(1) These drawings depicting structural detail are shown on the following pages. The remaining drawings are shown throughout Section 4.0 as reduced copies of the original issues.

(2) A complete set of original issue drawings are provided under separate cover. Therefore, the large size drawings that appear in this report as 8½ x 11 inches in size, can be examined in greater detail by referring to the original issues.

4.7.1.1 Telescope Support Frame

Drawing 47D252277 depicts the telescope support frame assembly. This assembly is constructed entirely of 6061-T6 aluminum alloy structural members and an aluminum plate. The assembly consists of a 1" thick top mounting plate (item 2) supported by a welded base structure. The base structure is to be made up of angles welded together to form a top and base frame (items 3 thru 10); these two frames will be basically identical. They will be joined by welding uprights. These uprights consist of two types. One type is a formed face post (item 12) with a tee post (item 11) welded to the inside corner for stiffness (see a typical corner detail on the drawing). The other posts will be standard structural angles (item 13) used at the three square corners of the frame. Both types of posts, as well as the top and bottom frames, will have a series of mounting holes along their front faces for the attachment of closure panels (item 17). The structure will be stiffened by the addition of cross braces (items 15 and 16) which may be welded or bolted in place as required. The top plate will have a reinforcing ring (item 14) welded to its bottom side around the 34 inch diameter opening.

The top plate will be attached to the base frame with a minimum of twelve bolts. The base structure will also have a number of holes in the floor angles for anchoring the entire structure to the floor. The top plate will also have three equally spaced mounting holes on a 38.00"B.C. for the attachment of the telescope structure (Dwg. 47E252276) plus three equally spaced mounting holes on a 8.75"B.C. for the attachment of the transmitter (45^{o} turning) mirror assembly (Dwg. 47A252283).

The entire structure including the top plate will measure 48" W x 58" D x 57½" H and weigh approximately 307 pounds.

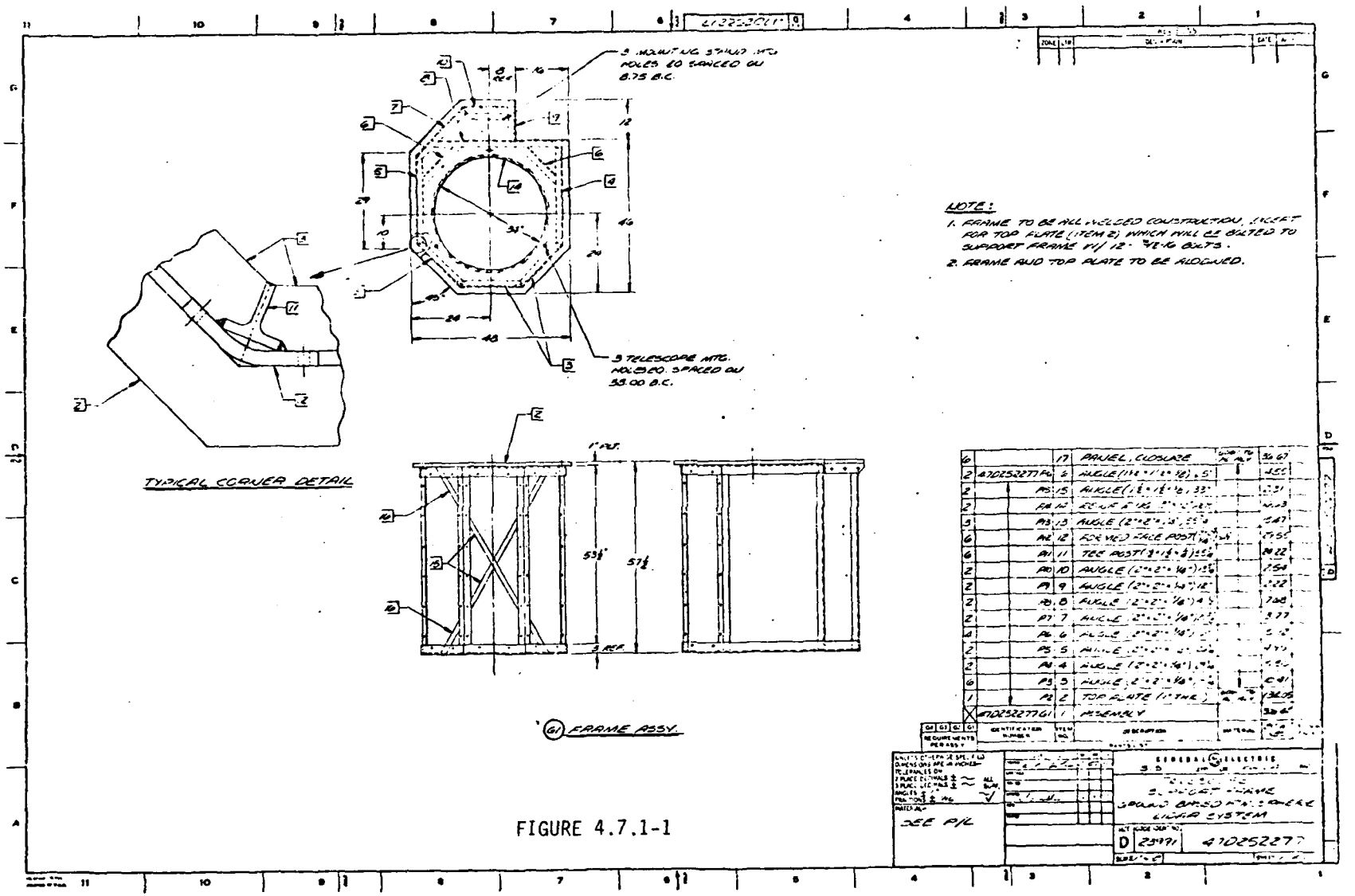
3 MOUNTING STUD MTG. HOLES TO BE SPACED ON 8.75 B.C.
3 TELESCOPE MTG. HOLES TO BE SPACED ON 33.00 B.C.
NOTE:
1. FRAME TO BE ALL WELDED CONSTRUCTION, EXCEPT FOR TOP PLATE (ITEM 2) WHICH WILL BE BOLTED TO SUPPORT FRAME W/ 12 - 3/4-16 BOLTS.
2. FRAME AND TOP PLATE TO BE MACHINED.
TYPICAL CORNER DETAIL
53 1/4"
57 1/2"
(61) FRAME ASSY.
SEE P/L
GENERAL ELECTRIC
SPACECRAFT ANTENNA
SQUARE BASED MONOPOLE
LINEAR SYSTEM
D
23971
47025227

FIGURE 4.7.1-1

4.7.1.2 Laser and Beam Expander Support Frame

Drawing 47D252278 shows the support frame for the laser and beam expander. The support frame assembly is constructed entirely of 6061-T6 aluminum alloy. The assembly consists of a top mounting channel (item 2) which was selected for its stiffness and is 12 inches in width. The vertical support members (item 4) and the base members (item 3) are also fabricated from structural channels. The frame, due to its height, is further stiffened with the use of structural angle cross braces (items 5 thru 10). Each base member is supported on two leveling pads (item 13).

The entire structure will be fabricated in two sections to facilitate handling. One section will be 6'9" long and the other 6'3"; both will be 26" wide x 57½" high. Each section will weigh about 102 pounds. The two sections will be joined by splices (item 14). After assembly the two sections will be 13'0" long and weigh approximately 203 pounds. Both sections will be of welded construction to insure a rigid structure.

The top channel and mounting surface will have mounting holes for attaching the laser, beam expander and window/energy monitor. One end of the channel will have a series of seven mounting holes to attach this support frame to the telescope support frame (Dwg. 47D252277).

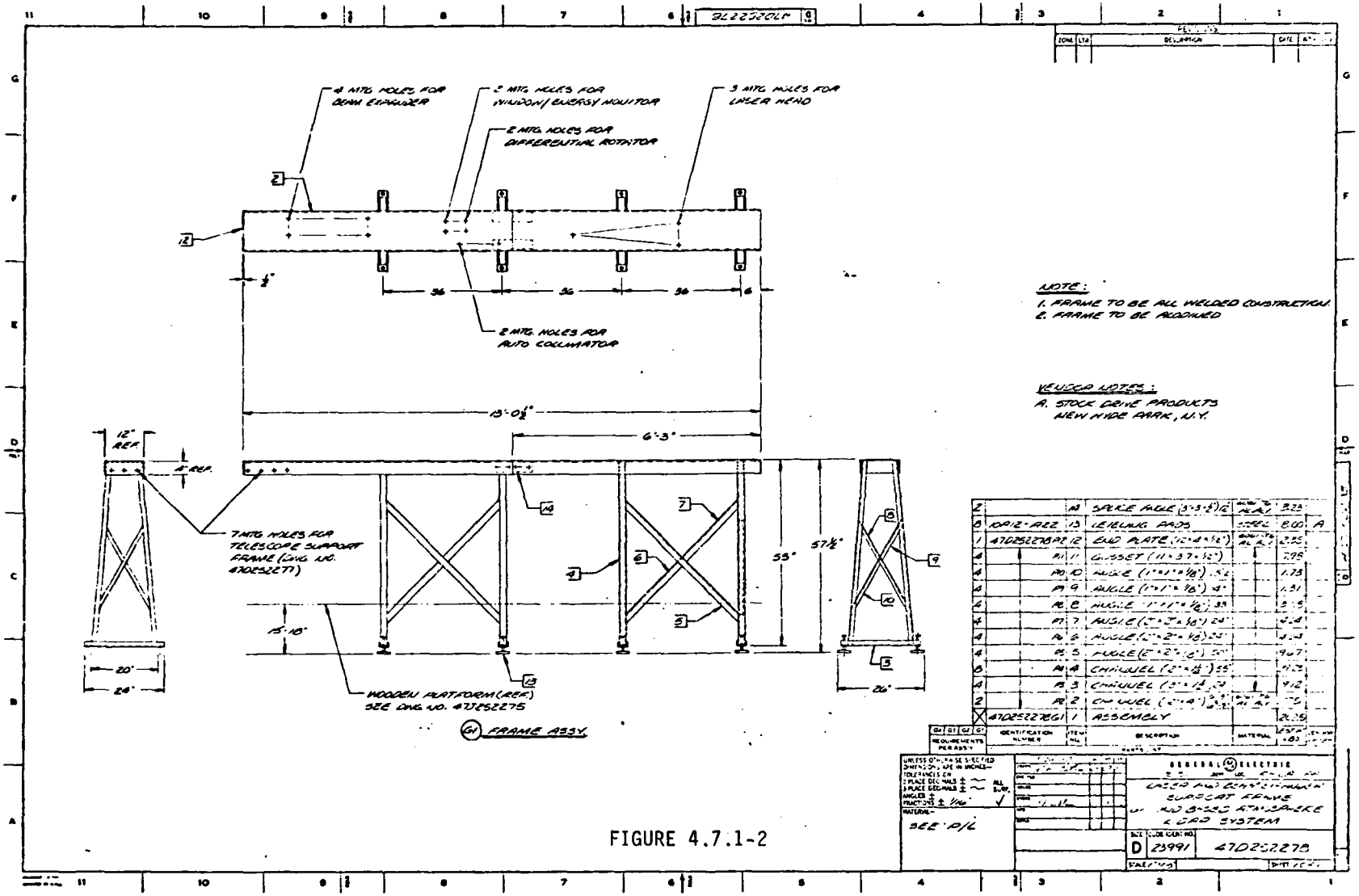
4 MTG HOLES FOR BEAM EXPANDER
2 MTG HOLES FOR WINDOW/ ENERGY MONITOR
2 MTG HOLES FOR DIFFERENTIAL ROTATOR
3 MTG HOLES FOR LINEAR HEAD
2 MTG HOLES FOR AUTO COLLIMATOR
36
36
36
6
13'-0½"
6'-3"
12" REF.
4" REF.
7 MTG HOLES FOR TELESCOPE SUPPORT FRAME (DWG. NO. 47D252271)
55"
57½"
15'-10"
20"
24"
WOODEN PLATFORM (REF.) SEE DWG NO. 47D252275
FRAME ASSY.
NOTE:
1. FRAME TO BE ALL WELDED CONSTRUCTION.
2. FRAME TO BE ACCURATE
VENDOR NOTES:
A. STOCK DRIVE PRODUCTS NEW HYDE PARK, N.Y.
GENERAL ELECTRIC
LASER AMPLIFIER ALIGNMENT SUBSCAT FRAME
47D252278
D
23991

FIGURE 4.7.1-2

4.7.1.3 Transmitter (45^{o} Turning) Mirror Mounting Stand

Drawing 47C252298 shows the mounting stand for the transmitter mirror shown on Drawing 47A252283. The assembly is constructed entirely of 6061-T6 aluminum alloy, 0.25 inch thick plate. It consists of a top plate, two side plates, a base plate, front plate, and two(2) rear gussets. The top plate is to be positioned at $45^{o} \pm 1^{o}$ to the base plate. The welded assembly will measure 11.00" wide x 10.00" deep x 11.25" high. The base plate will have three(3) (0.281"dia.) mounting holes for attachment to the telescope support frame (Dwg. 47D252277). The top plate also has three(3) mounting holes for the attachment of the mirror and mirror cell assembly. See Drawing 47A252283 for details.

Total weight of the assembly is approximately 10.5 pounds.

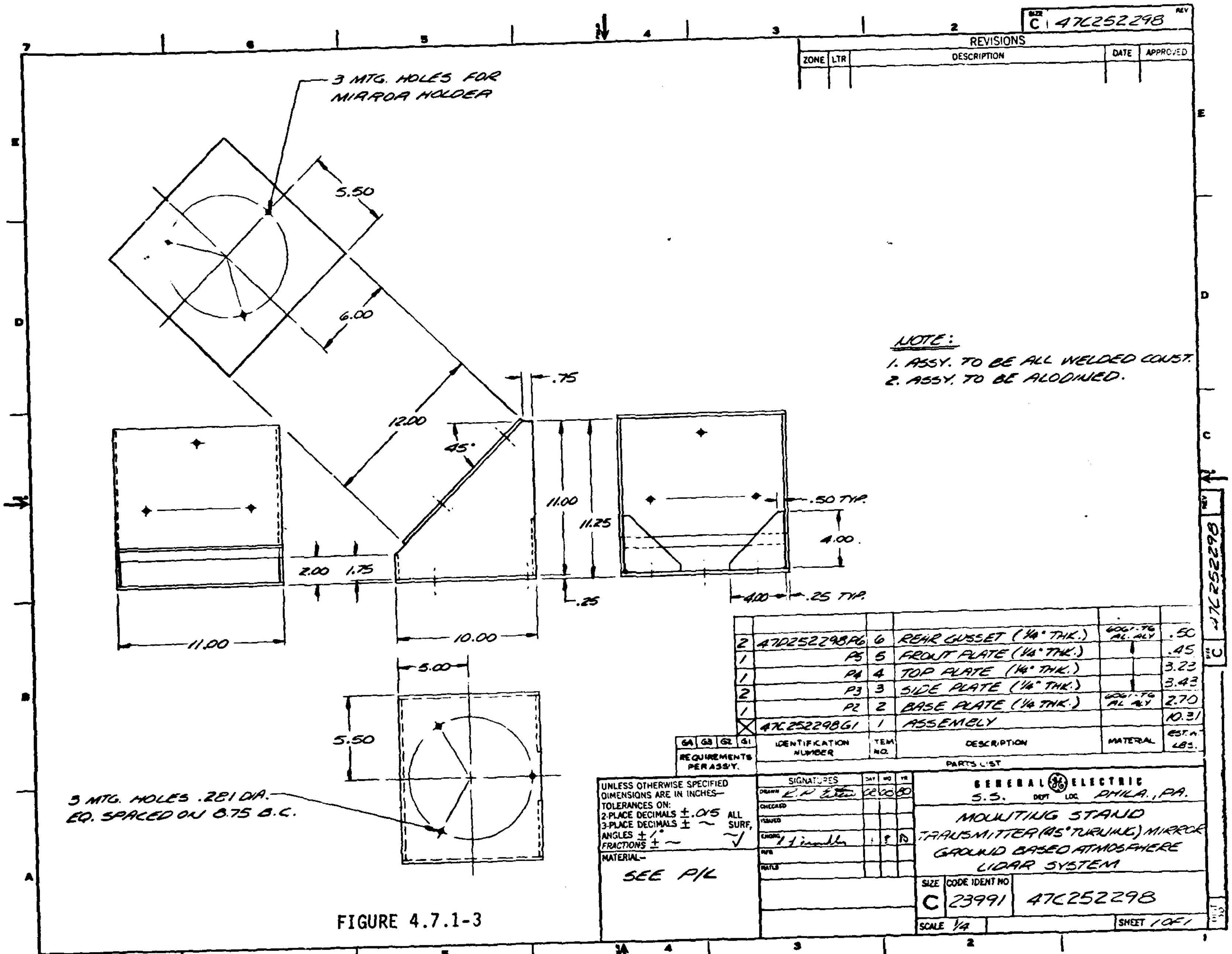

C 47C252298
REVISIONS
ZONE LTR DESCRIPTION DATE APPROVED
3 MTG. HOLES FOR MIRROR HOLDER
5.50
6.00
12.00
45°
.75
11.00
11.25
.25
2.00 1.75
10.00
11.00
.50 TYP.
4.00
4.00 .25 TYP.
5.00
5.50
3 MTG. HOLES .281 DIA. EQ. SPACED ON 8.75 B.C.
NOTE:
1. ASSY. TO BE ALL WELDED CONST.
2. ASSY. TO BE ALODINED.
2 47D252298P6 6 REAR GUSSET (1/4" THK.) 6061-T6 AL ALY .50
1 P5 5 FRONT PLATE (1/4" THK.) .45
1 P4 4 TOP PLATE (1/4" THK.) 3.23
2 P3 3 SIDE PLATE (1/4" THK.) 3.43
1 P2 2 BASE PLATE (1/4 THK.) 6061-T6 AL ALY 2.70
47C252298G1 1 ASSEMBLY 10.31
G4 G3 G2 G1 REQUIREMENTS PER ASSY. IDENTIFICATION NUMBER ITEM NO. DESCRIPTION MATERIAL EST. WT LBS.
PARTS LIST
UNLESS OTHERWISE SPECIFIED DIMENSIONS ARE IN INCHES— TOLERANCES ON: 2-PLACE DECIMALS ±.015 3-PLACE DECIMALS ± ~ ANGLES ±1° FRACTIONS ± ~ ALL SURF.
MATERIAL— SEE P/L
SIGNATURES
GENERAL ELECTRIC
S.S. DEPT LOC PHILA., PA.
MOUNTING STAND TRANSMITTER (45° TURNING) MIRROR GROUND BASED ATMOSPHERE LIDAR SYSTEM
SIZE C CODE IDENT NO 23991 47C252298
SCALE 1/4 SHEET 1 OF 1

FIGURE 4.7.1-3

4.7.2 Electrical Drawing Index

A list of preliminary design drawings, that define all electrical subsystems of G-BALS, is shown on the facing page. Reduced copies of some of the original issues are included throughout this report. A complete set of all electrical drawings, which are at the original full size issue, are provided under separate cover.

4.7.2 ELECTRICAL DRAWING INDEX

	TITLE	DRAWING NUMBER
1.	SHUTTER SYNC SHAPER & DELAY CIRCUIT (2 SHTS.)	47B252284
2.	SYSTEM CLOCK SCHEMATIC	47C252285
3.	ENERGY DIGITIZER	47B252286
4.	ADDRESS CONTROLLER (2 SHTS.)	47B252287
5.	SYSTEM BLOCK DIAGRAM	47C252288
6.	MULTIPLEX CONTROLLER (2 SHTS.)	47C252289
7.	ENERGY MONITOR	47B252290
8.	SYSTEM CONTROLLER	47E252291
9.	SYSTEM TIMING DIAGRAM	47C252292
10.	SIMPLIFIED SYSTEM BLOCK DIAGRAM	47B252293

NOTE: A complete set of original issue drawings are provided under separate cover.

4.8 SYSTEM WEIGHT BREAKDOWN

	DESCRIPTION	WEIGHT
1.	TELESCOPE SUPPORT FRAME	307
2.	LASER & BEAM EXPANDER SUPPORT FRAME	203
3.	TELESCOPE	1,300
4.	BEAM EXPANDER	47
5.	TRANSMITTER (45^{o} TURNING) MIRROR	29
6.	ELECTRONICS RACK	375
7.	LASER HEAD	85
8.	DETECTOR SECTION	184
9.	CONTROL CONSOLE (LeCROY)	100
10.	WORK TABLES	180
11.	CHAIR	32
12.	FILE CABINET	151
13.	PARTITION	100
14.	PROTECTIVE COVER	40
15.	AIR PLENUM	300
16.	ANTENNA	150
17.	QUARTZ WINDOW ASSEMBLY	20
18.	WOODEN PLATFORM	300
19.	CONTROL CONSOLE (G.E.)	60
20.	DETECTOR SECTION VERTICAL HEIGHT ADJUSTMENT DEVICE	94
	TOTAL WEIGHT	4,057 LBS.

5.0 SAFETY

5.0 SAFETY

For the ground-based lidar system (G-BALS), hazards can be divided into two major groups, electrical and optical.

Electrical hazards result from the presence of some fairly high voltages, with standard high voltage electrical precautions being sufficient. In some cases such as the laser Pockels cell Q-switch and power supply, the high voltage is limited to such low current and charge as to present relatively little danger.

The photomultiplier tube (PMT) power supplies and the laser primary power supply (for flashlamps) present more significant dangers, with the laser flashlamp electrical system presenting by far the greater hazard. With a capability of 200 joules/pulse at 10 pps, the laser power supply is capable of at least one amp average at 1900 V. To help protect the laser user from inadvertently contacting the laser primary high voltage, the laser manufacturer says the laser system is interlocked to turn off and dump the flashlamp power supply and capacitors if power is lost, if high voltage connectors are removed, or if the laser head cover is removed.

5.0 SAFETY

TYPES OF HAZARDS

- Electrical
- Optical

ELECTRICAL HAZARDS

- Follow normal electrical safety precautions for high voltage equipment
- High voltage sources
  - PMTs and their power supplies

    five at 3000 VDC max (10 ma max)
    one at 6000 VDC max (20 ma max)
  - Laser primary power supply (for flashlamps)

    1900 V. max pulsed at 10 pps
    200 joules max per pulse (100/unit)
  - Laser Q-switch and power supply

    4000 VDC max
    Very low current capability
- Laser primary power supply turns off and dumps if:
  - High voltage connectors removed
  - Laser head cover removed
  - Lose power or switch off

5.1 Optical Hazards

The output of a high powered laser (especially when Q-switched) contains very high power densities of radiation. Due to the collimated nature of laser radiation, these high power densities of radiant energy can be transmitted for long distances through a clear atmosphere. Thus, when using lasers, the user must take precautions to avoid radiation injuries, particularly to the eye.

The eye is the most sensitive part of the body to laser or any other optical radiation. This is primarily because the eye can focus the laser radiation to even higher power densities on the retina. In this way the power density on the retina can be about 10^5 times greater than on the cornea or skin. Any damage to the retina is especially serious if it happens to involve the macula, the retinal region which is the center of vision and has the greatest resolution. The safe limit for ocular exposure to short pulse visible lasers is considered to be 10^{-7} joules/cm^2 on the cornea of an unaided eye with the pupil wide open (7 mm).

In order for radiation to be concentrated on the retina, the ocular media must be transparent to the radiation. The eye has a significantly high transmittance from about 0.3-1.4 microns, this range being much greater than the visual response range of 0.4-0.7 micron. Thus, even invisible radiation can be focused on the retina and cause damage.

With at most a few milliwatts of cw output power, the HeNe alignment laser (see Section 4.1.2) falls into Bureau of Radiological Health (BRH) Class II or IIIa. The minor hazards are such that a person should not stare into a Class II or IIIa laser beam, and should not view into a Class IIIa laser beam with an optical instrument.

The lidar's main Nd:YAG laser is Class IV for all output wavelengths. Such output intensities will cause severe injury to the eye if one looks into the beam or a specular reflection of the beam. For this laser class, a diffuse reflection may also be hazardously bright, and the direct beam may burn the skin. The various indoor and outdoor precautions shown on the facing page are designed to avoid these hazardous situations.

The type laser goggle referred to in Section 4.6 is obtainable from Glendale Optical Company as Model LGS-NDGA. As indicated in Section 4.6, this goggle will protect the user from the non-visible 355 nm and 1064 nm laser outputs, but not the 532 nm (green) laser output. We have not identified any laser goggle which protects against all three laser outputs and still allows the wearer to see. Thus caution is always necessary.

5.1 OPTICAL HAZARDS

The Eye is Main Concern

- Eye is 100,000 times more sensitive than skin.
- Wavelengths 250 to 1400 nm.

Intense Light Sources

- Laser output is primary hazard.
- Laser flashlamp is secondary hazard.

HeNe Alignment Laser

- BRH class II or IIIa.
- Do not look into beam.
- Do not view unattenuated beam with instruments.

Nd:YAG Laser for G-BALS Lidar

- BRH class IV for all output wavelengths.
- After beam expander, outputs are still class IV.

Nd:YAG Laser Indoor Precautions

- Do not allow laser beam to strike skin.
- Wear proper laser goggles when in presence of laser beam.
- Do not look into laser beam without special protection.
- Keep laser beam covered when possible.
- Laser head interlocks prevent unintentional operation of laser with cover removed.

G-BALS Laser Outdoor Precautions

- Prevent access to vicinity of roof opening.
- Direct beam only to high elevation angles.
- Do not beam into low level dense clouds.
- Interrupt operation when aircraft near beam.
  - Can visual monitor through co-aligned binoculars plus handy shut-off switch
  - Can use aircraft-surveillance radar

5.2 Range-Safety Radar

It is desirable to have a non-visual method to detect aircraft approaching the lidar laser beam, and allow interruption of the laser output. A small radar transceiver system can perform this function.

Some conditions for use of any such radar system include the detection of aircraft within several degrees of the lidar laser beam, use only during clear weather, a clear weather range of at least 10 to preferably 15 km, and both size and cost which are reasonably small. It would appear that these conditions can best be met with a boresighted (to the lidar system) non-scanning X-band radar system of perhaps 50 kW peak power and several degrees beam width.

For G-BALS, a surplus military radar can be adapted for use as the described range safety system. If it is necessary to purchase and modify a commercially available radar system, aircraft and small airport radar systems should be considered.

Visual monitoring of the sky may still be advisable because a small radar system, such as described, may not detect aircraft or balloons which are non-metallic, very small, or at very high altitude.

5.2 RANGE-SAFETY RADAR

Purpose

- Monitor sky for aircraft near laser beam.
- Turn off laser when detect aircraft.

Desired Radar Characteristics

- Clear weather characteristics only.
- X-band radar.
- About 50 kw peak pulsed output.
- About 5-10 degree beam width.
- Radar non-scanning.
- Boresight with lidar.
- Free (surplus) or low cost.

Radar Candidates

- Modify/adapt available military radar.
- Modify/adapt small airport radar.
- Modify small commercial weather radar.
- AFGL to identify available surplus radar.

Radar Shortcoming

- Small low power radar may not detect aircraft or balloons which are:
  - very small
  - non metallic
  - very high altitude (>40,000 feet)

6.0 ALIGNMENT

6.0 ALIGNMENT

6.1 Lidar Transmitter:Receiver Alignment

It is desirable that the lidar transmitter:receiver alignment method be accurate, fast, simple, and entirely indoors. The suggested method which fulfills these desires involves two steps for aligning the lidar transmitter to the receiver by means of (1) a stationary ("fixed") autocollimator and (2) a special optical jig. Reference mirrors allow a check at any time on the stability of system alignment.

6.0 ALIGNMENT

6.1 LIDAR TRANSMITTER: RECEIVER ALIGNMENT

ALIGNMENT GOALS

- MINIMIZE COST AND COMPLEXITY
- ACCURATE TO 2 ARC SEC (.01 MRAD)
- FAST AND CONVENIENT
- REQUIRES NO MORE THAN TWO PEOPLE
- ALIGNMENT POSSIBLE ANY TIME AND IN ANY WEATHER
- ALIGNMENT REFERENCE FOR IMMEDIATE CHECK BY ONE PERSON, EVEN DURING LIDAR RUN

ALIGNMENT OVERVIEW*

I) LASER TRANSMITTER: FIXED AUTOCOLLIMATOR (A/C) ALIGNMENT (ADJUST FIXED A/C)

II) FIXED AUTOCOLLIMATOR: RECEIVER ALIGNMENT (ADJUST TRANSMITTER 45° MIRROR)

III) MONITORING REFERENCE MIRRORS VIA FIXED A/C (ADJUST REFERENCE MIRRORS)

*REFERENCE ALIGNMENT SCHEMATIC DRAWING 47D252279 (FIGURE 6-1).

6.2 Alignment Schematic

Figure 6-1 shows the general layout of lidar transmitter elements relative to each other and to the lidar receiver, as well as how the various alignment aids are positioned.

The autocollimator (A/C) located between laser and beam expander is always left in position, and is referred to elsewhere as the fixed autocollimator ("fixed A/C"). Both it and the expanded laser beam use the same adjustable beam-directing ("45^{o} turning") transmitter mirror. A special optical test jig can be temporarily placed in the telescope tube wall and rotated to either of two positions for use with a second removable A/C ("A/C-2"). Finally for alignment only, the receiving system field stop is to be back-illuminated with a frosted lamp which is removed when not in use. Reference mirrors are fixed to both the top and bottom of the telescope.

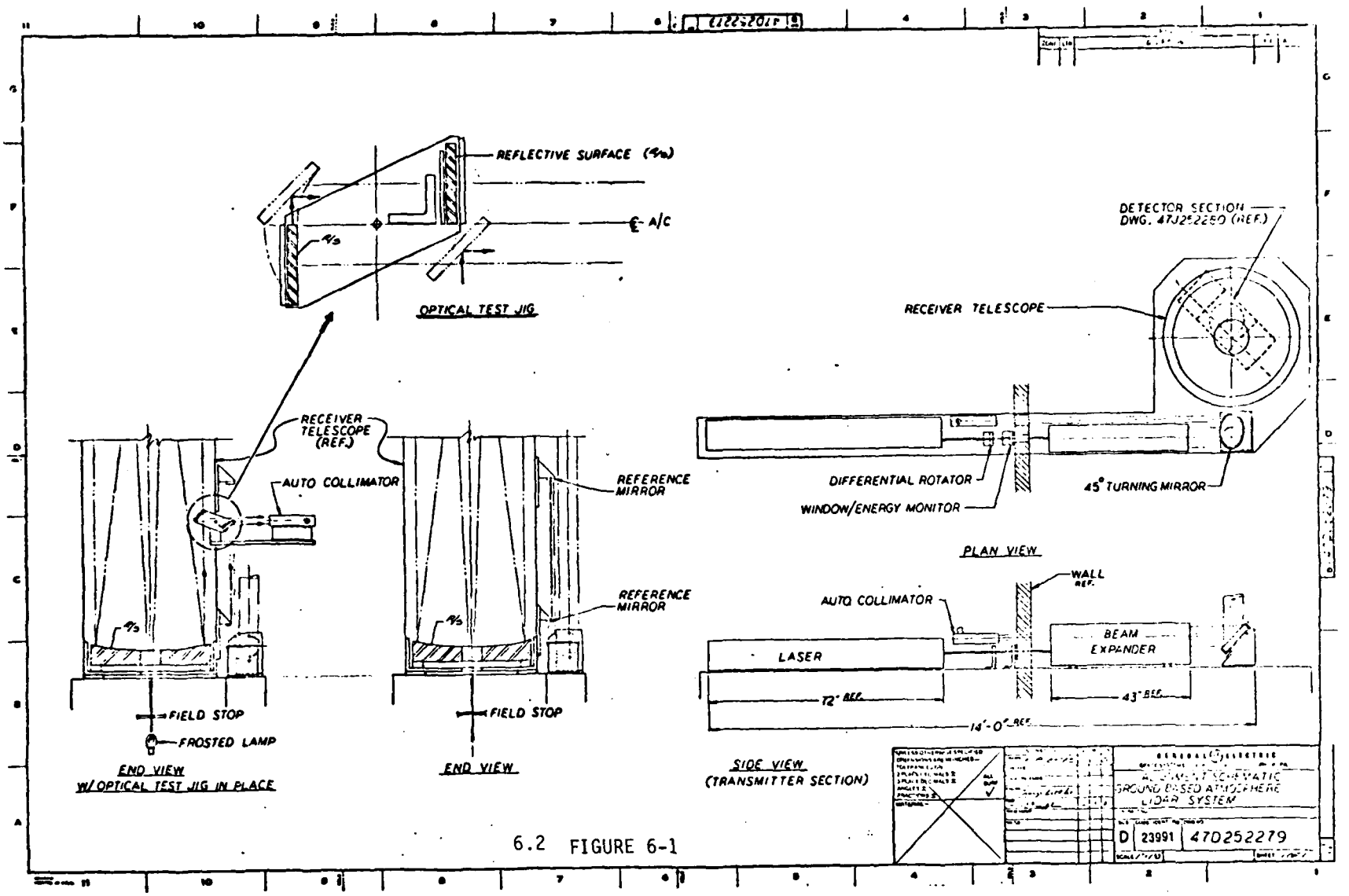
REFLECTIVE SURFACE (95%)
℄ A/C
OPTICAL TEST JIG
DETECTOR SECTION
DWG. 47J252250 (REF.)
RECEIVER TELESCOPE
RECEIVER TELESCOPE (REF.)
AUTO COLLIMATOR
REFERENCE MIRROR
REFERENCE MIRROR
DIFFERENTIAL ROTATOR
WINDOW/ENERGY MONITOR
45° TURNING MIRROR
PLAN VIEW
WALL REF.
AUTO COLLIMATOR
LASER
BEAM EXPANDER
72" REF.
43" REF.
14'-0" REF.
FIELD STOP
FROSTED LAMP
END VIEW
W/ OPTICAL TEST JIG IN PLACE
FIELD STOP
END VIEW
SIDE VIEW
(TRANSMITTER SECTION)
SCHEMATIC
GROUND BASED ATMOSPHERE
LIDAR SYSTEM
D 23991 47D252279

6.2 FIGURE 6-1

6.3 Laser Transmitter:Fixed Autocollimator Alignment

The purpose of this procedure is to align the fixed autocollimator (A/C) with the laser beam as it exits from the beam expander. Since the HeNe alignment laser beam (inside the main laser head) does not penetrate to the main laser output opening, it is necessary to align the fixed A/C with respect to the main laser output beam by some method such as detailed on the facing page.

When the large corner cube is positioned between the laser beam and fixed A/C beam as per step (6.3 B5) on the facing page, it is necessary to also include attenuating filters to reduce the expanded laser beam intensity by several orders of magnitude to an intensity which is safe for viewing through the fixed A/C. The safety hazard which would result from filter failure during such observations (step 6.3 B6) can be completely eliminated by substituting a simple Vidicon or other electronic viewer in place of the eye for looking into the fixed A/C while it receives the attenuated laser beam.

An alternate method not presented on the facing page is to reflect the expanded laser beam exactly back on itself with a large flat mirror to which the fixed A/C is subsequently adjusted. A 1 mm hole in an opaque plate at the laser head output opening will assist the observation and adjustment of the reflected laser beam back upon itself. This alignment method may not be sensitive enough to permit the desired alignment accuracy.

The alignment adjustment of this Section 6.3 should be relatively stable due to the compact and sturdy physical structure holding the laser head, fixed A/C and the beam expander.

6.3 LASER TRANSMITTER: FIXED AUTOCOLLIMATOR ALIGNMENT

A) BASELINE CONFIGURATION (REF. DRAWING 47D252279, FIGURE 6-1)

1) TRANSMITTER

a) INCLUDES LASER PLUS BEAM EXPANDER
b) BOTH COMPONENTS FIXED

2) FIXED AUTOCOLLIMATOR (A/C)

a) LOCATED SO A/C OUTPUT BEAM IS $\leq$1 INCH FROM AND PARALLEL TO EXPANDED LASER BEAM
b) HAS ANGULAR ADJUSTMENT IN AZIMUTH AND ELEVATION

3) SPECIAL TEST ITEMS

a) SPECIAL HIGH DENSITY FILTERS TO ATTENUATE LASER BEAM
b) LARGE CORNER CUBE PRISM

B) PROCEDURE

1) CENTER LASER BEAM IN ENTRANCE AND EXIT APERTURES OF BEAM EXPANDER

2) PLACE FILTERS (A3a) IN LASER BEAM

3) POSITION CORNER CUBE (A3b) ON-AXIS WITH FIXED A/C

4) INTERNALLY ADJUST A/C RETICLES, IF NECESSARY, SO THEY CENTER ON EACH OTHER

5) POSITION CORNER CUBE (A3b) BETWEEN EXPANDED LASER BEAM AND FIXED A/C BEAM

6) COMPARE FIXED A/C AXIS WITH EXPANDED LASER BEAM AXIS

a) EXTERNALLY ADJUST FIXED A/C SO LASER SPOT CENTERS ON A/C RETICLE
b) FIXED A/C AXIS IS NOW PARALLEL TO EXPANDED LASER BEAM AXIS

7) TURN OFF LASER, REMOVE CORNER CUBE AND LASER FILTERS

6.4 Fixed Autocollimator:Receiver Alignment

This procedure permits adjustment of the laser beam-directing ("45° turning") mirror such that the fixed A/C (and thus expanded laser beam) is aligned with respect to the lidar receiver telescope field-of-view. As detailed on the facing page and illustrated in Figure 6-1, the procedure makes use of a second autocollimator (A/C-2), a special optical test jig, and temporary back-illumination of the receiver telescope field stop. This procedure (Section 6.4 opposite) is easily and rapidly repeated, allowing a check of transmitter:receiver alignment.

An alternate receiver:fixed A/C (or laser beam) alignment method not presented on the facing page, is through temporary conversion of the receiving telescope into an autocollimator by temporary insertion of suitable optics at its field stop. Then either the fixed A/C or the transmitter laser beam can be aligned to the receiver telescope via a large flat mirror (common to all beams) and the transmitter adjustable ("45° turning") mirror. If transmitter adjustment is made using the laser beam itself rather than the fixed A/C, then it may be necessary to use the alternate method (discussed at the end of Section 6.3 text) for aligning a flat mirror perpendicular to the laser beam.

6.4 FIXED AUTOCOLLIMATOR: RECEIVER ALIGNMENT

A) BASELINE CONFIGURATION (REF. DRAWING 47D252279, FIGURE 6-1)

1) TRANSMITTER INCLUDES

a) LASER
b) BEAM EXPANDER
c) FIXED AUTOCOLLIMATOR (A/C)
d) 45^{o} BEAM DIRECTING ("TURNING") MIRROR

2) RECEIVER INCLUDES RECEIVING TELESCOPE WITH FIELD STOP (FS)

3) SPECIAL TEST ITEMS

a) ANOTHER AUTOCOLLIMATOR (A/C-2)
b) OPTICAL TEST JIG WITH ADJUSTABLE FLAT MIRRORS (SEE FIG. 6-1)
c) BACK-LIGHTING LAMP FOR RECEIVER FS (PRODUCES RECEIVER TELESCOPE "BEAM")

B) PROCEDURE

1) OPTICAL TEST JIG ADJUSTMENT

a) PLACE OPTICAL JIG TO INTERCEPT BOTH THE FIXED A/C BEAM AND PART OF THE TELESCOPE BEAM
b) LOCATE A/C-2 TO VIEW THE OPTICAL JIG
c) ROTATE OPTICAL JIG SO ITS MIRRORS REFLECT A/C-2 BACK ON ITSELF
d) OBSERVING A/C-2 IMAGES, ADJUST OPTICAL JIG MIRRORS SO THEY ARE MUTUALLY PARALLEL (IMAGES COINCIDE)

2) ADJUSTMENT OF 45^{o} BEAM DIRECTING MIRROR

a) ROTATE OPTICAL JIG TO REFLECT BOTH THE TELESCOPE BEAM AND FIXED A/C BEAM INTO A/C-2
b) IN A/C-2, NOTE IMAGE OF ILLUMINATED FS AND IMAGE OF FIXED A/C RETICLE PATTERN
c) ADJUST 45^{o} BEAM DIRECTING MIRROR UNTIL RETICLE IMAGE IS PROPERLY LOCATED WITH RESPECT TO FS IMAGE
d) LIDAR TRANSMITTER IS NOW ALIGNED TO RECEIVER

3) REMOVE OPTICAL JIG AND FS LAMP

6.5 Adjustment and Use of Reference Mirrors

With the transmitter:receiver alignment so easily made as described in Sections 6.3 and 6.4, it may not be considered necessary to have still another method to check for stability of alignment. However, the reference mirror method described on the facing page and illustrated in Figure 6-1 does have the advantage of allowing an immediate check, at any time, of transmitter: receiver relative orientation, even during lidar runs.

Referring to Figure 6-1, the lower reference mirror intrudes only perhaps 1/3 the way into the fixed A/C extended aperture. The rest of the fixed A/C aperture is to be used for either the optical jig (Section 6.4) or the upper reference mirror (when the optical jig is removed).

6.5 ADJUSTMENT & USE OF REFERENCE MIRRORS

PURPOSE (SEE REF. DRAWING 47D252279, FIGURE 6-1)

REFERENCE MIRRORS ALLOW CONVENIENT CHECKING FOR RELATIVE MOVEMENT BETWEEN RECEIVER TELESCOPE AND LASER TRANSMITTER.

PROCEDURE

1. FIXED AUTOCOLLIMATOR (A/C) APERTURE SIMULTANEOUSLY VIEWS TWO REFERENCE MIRRORS VIA 45^{o} BEAM DIRECTING MIRROR.

2. IF NECESSARY, ADJUST EACH REFERENCE MIRROR TO OPTIMIZE ITS FIXED A/C IMAGE LOCATION (RECORD LOCATIONS).

3. IF LIDAR COMPONENTS SHOULD MOVE, REFERENCE IMAGES WILL SHIFT IN FIXED A/C.

4. IF SUCH AN IMAGE SHIFT IS DETECTED, THEN LIDAR SYSTEM ALIGNMENT SHOULD BE CHECKED AS ALREADY DESCRIBED.

5. FIXED A/C REFERENCE IMAGES CAN BE CHECKED AT ANY TIME, EVEN WITH LIDAR OPERATING.

7.0 CALIBRATION AND TEST

7.0 CALIBRATION AND TEST

7.1 Lidar Calibration

The lidar system plus lower atmosphere (below 20 km) are to be jointly calibrated by making lidar measurements of 20 km altitudes and above, while "ground" truth measurements of atmospheric density are made at two differing altitudes above 20 km. These ground truth measurements can be obtained with either rocket or balloon-borne instruments, as long as both measurements are obtained close enough in time and space to the lidar measurement to be applicable.

Ground truth reference measurements are needed at two altitudes because the probable presence of significant haze backscatter during calibration requires combining the two range equations (one for each lidar wavelength, see Section 11.1) to eliminate the unknown haze scatter coefficients. Now with one combined equation containing two calibration constants (one for each wavelength), reference (ground truth) data are needed from two altitudes to permit a solution. The two reference altitudes should have significantly different atmospheric density, but negligible attenuation between them.

Since the combined lidar plus lower atmosphere (<20 km) calibration is valid only as long as the lower atmosphere integrated absorption is constant, the calibration may have to be repeated each night. However, if the lower atmosphere integrated transmittance could be monitored at the lidar wavelengths, then the lidar calibration constants could be corrected for changes in atmospheric transmittance, and the calibration remain valid for extended periods of time.

It is here suggested that the atmospheric total transmittance can be monitored by measurement of star intensities using a special small pointable telescope complete with detector and lidar wavelength filters. If the intensities of several stable stars are measured during a lidar calibration run, then later reference to any of those stars will permit correction of the lidar calibration constants for changes in atmospheric transmission. It is here assumed that while star intensity is affected by the total atmosphere (from ground level on up), essentially all the attenuation changes are due to the lowest 20 km. Also, as star elevation changes during the night and/or season, correction must be made for non-vertical slant path effects on transmittance.

7.0 CALIBRATION AND TEST

7.1 LIDAR CALIBRATION

PURPOSE

- EVALUATE LIDAR SENSITIVITY AND THUS RANGE EQUATION CALIBRATION CONSTANTS.

CONCEPT

- LIDAR RUN, PLUS "GROUND" TRUTH MEASUREMENTS AT $\geq$ 20 KM ALTITUDE.

DETAILS

- NEED REFERENCE ATMOSPHERIC DENSITY DATA AT TWO ALTITUDES OF $\geq$20 KM.
- OBTAIN REFERENCE DATA FROM BALLOON/ROCKET FLIGHT MEASUREMENTS.
- MONITOR LASER OUTPUT AT EACH WAVELENGTH (SEE LATER).
- STORE LIDAR RUN DATA UNTIL REFERENCE DATA AVAILABLE.
- USE SPECIAL CALIBRATION SOFTWARE TO EVALUATE LIDAR CALIBRATION CONSTANTS.
- RESULTING CALIBRATION CONSTANTS ARE VALID UNTIL LOWER ATMOSPHERE (<20 KM) TRANSMITTANCE CHANGES.

7.2 Laser Output Monitor

To compensate for any variations in laser output, lidar system calibration and lidar data reductions require normalization of lidar data with respect to laser energy. This laser energy monitor supplies not only the output energy of each laser pulse at both 355 nm and 532 nm, but also the time-zero for each lidar system shot.

As detailed in Section 4.2.3, the type of energy monitor design proposed here employs the measurement of light internally scattered from the laser beam by the material of a window. This window also serves to transmit the laser beam while blocking air flow between indoor and outdoor thermal regions.

7.2 LASER OUTPUT MONITOR

PURPOSE

- PROVIDE LASER ENERGY AT EACH WAVELENGTH FOR LIDAR DATA NORMALIZATION.

CONCEPT

- MEASURE INTERNALLY SCATTERED LIGHT FROM WINDOW IN LASER BEAM.

DETAILS

- LOCATE WINDOW AT WALL BETWEEN LASER HEAD AND BEAM EXPANDER.
- MEASURE WINDOW-SCATTERED LASER LIGHT AT 355 NM AND 532 NM WAVELENGTHS WITH TWO SILICON PHOTODIODES.
- USE BANDPASS FILTERS TO ISOLATE EACH WAVELENGTH AND REJECT FLASHLAMP LIGHT.
- TIME OF MONITOR OUTPUT ESTABLISHES LIDAR TIME ZERO.
- INTEGRATED OUTPUT OF EACH DETECTOR PROVIDES LASER ENERGY PER SHOT AT EACH WAVELENGTH.

7.3 Photomultiplier Tube Stability Check (Optional)

Although the photon-counting mode of detection employed here reduces the effect of photomultiplier tube (PMT) gain variations on lidar signal level, PMT's are still subject to very slow changes in sensitivity as well as faster sensitivity changes due to overloading or large temperature variations. Thus it may be desirable to have the capability for checking the stability and relative sensitivity of the six lidar PMT's. As detailed on the facing page, such sensitivity checks can be obtained while weakly illuminating all PMT's from a common stabilized light source. Since the silicon photodiode forms a relatively stable sensor, it is a good candidate for sampling and stabilizing the common light source.

The moderate thermal control of the lidar receiver detection section is to be provided by the recommended air-conditioned indoor environment (see Section 4.0.4) present around the detector section.

7.3 PHOTOMULTIPLIER TUBE (PMT) STABILITY CHECK (OPTIONAL)

PURPOSE

- PROVIDE RELATIVE MEASURE OF DETECTION SECTION PMT SENSITIVITIES
- CHECK DAILY REPRODUCIBILITY OF PMT SENSITIVITIES

CONCEPT

- PROVIDE STABILIZED COMMON LIGHT SOURCE TO ALL PMT DETECTORS

DETAILS

- WEAKLY ILLUMINATE ALL PMT'S FOR PHOTON COUNTING DETECTION
- USE NORMAL DATA HANDLING ELECTRONICS
- USE FIBER OPTIC GUIDES FROM ONE SOURCE TO ALL PMT'S
- SOURCE CAN BE A FILAMENT LAMP OR A GREEN LED
- USE BANDPASS FILTER TO SELECT/PURIFY WAVELENGTH AND THUS REMOVE COLOR TEMPERATURE EFFECTS
- USE SILICON PHOTODIODE TO MONITOR SOURCE INTENSITY
- STABILIZE SOURCE OUTPUT VIA FEEDBACK FROM PHOTODIODE TO CONTROL THE SOURCE CURRENT
- PROVIDE MODERATE THERMAL CONTROL OF THE RECEIVER DETECTION SECTION

8.0 CLEANLINESS AND MAINTENANCE

8.0 CLEANLINESS AND MAINTENANCE

8.1 G-BALS System Maintenance and Precautions

With large aligned optical systems such as G-BALS, environmental shock and vibration should be limited to relatively low levels if system alignment is to be preserved.

Photomultiplier tube (PMT) detectors can easily show some loss of sensitivity or even be damaged if they are turned on while exposed to normal light levels. Even exposure to such light levels with the high voltage off can increase PMT dark signal for up to hours. Thus it is necessary to always turn off the PMT high voltage during exposure to non-signal light, and to keep them dark starting a few hours before use. Since the VPM-152S PMT should be stored at under $20^{o}C$, it is probably best to leave its cooled housing turned on (cooled) at all times.

The presence of deionized water in the laser head and control unit means that the ambient temperature must be kept above freezing. To prevent accumulation of optically absorbing and/or electrically conducting impurities, the laser manufacturer (Quantel International) recommends changing the deionized water at three month intervals. In general, Quantel feels that this type laser should be able to operate for at least 100,000 shots without needing service. When such service is needed, it is likely to involve touching up internal alignment, and/or blowing dust off the laser optical surfaces using a special "duster" gas (see Section 8.2), and/or changing the laser flashlamps. Be sure to read the entire laser manual before attempting anything.

8.0 CLEANLINESS AND MAINTENANCE

8.1 G-BALS SYSTEM MAINTENANCE AND PRECAUTIONS

VIBRATION

- Normal lab environment OK
- Excessive vibration/shock can mis-align optics

PHOTOMULTIPLIER TUBE DETECTORS

- Light level
  - Never expose to non-signal light when voltage on
- Temperature
  - Store VPM - 152S detector at <20°C
  - Recommend VPM - 152S cooled housing be left on

LASER

- Storage temperature
  - Internal water must not freeze
  - Storage temperature =+1°C to +40°C
- Water replacement
  - Replace internal deionized water each 3 months
- Cleanliness of optics in laser and laser beam
  - Dirt and dust effects
    reduce lidar signal
    absorbed heat damages surfaces
  - Never touch optical surfaces
  - Blow dust off optics (special gas)
  - Do not disturb dust on nearby surfaces

OTHER OPTICS

- Take precautions to keep clean
- Special care needed to clean optics

8.2 Cleaning Delicate Optical Surfaces

The presence of dust or films on optical surfaces causes loss of light and resulting system signal, and also increases scattered light. If intense laser beams are involved, the resultant heating of such dirt can actually damage or destroy optical elements. Thus cleanliness is necessary.

The best way to have clean optics is to keep dirt away through use of protective structural design and dust covers. Never touch optical surfaces with bare skin because even "clean" skin leaves deposits. Never blow with the breath at optical surfaces or touch them with any material not made for fine optics. Never try to dust or blow off nearby surfaces, as the disturbed dust may settle on a critical surface.

To clean any optical surface of dust, first try a jet of commercially available optical duster gas available in cans. If the dust resists such gas jets or if the surface has a dirt film, then try a commercially available optics liquid cleaner (or purest alcohol), but without any rubbing. Very light wiping with special optics cloth or paper plus the special liquid cleaner should be attempted only when the gentler methods fail.

8.2 CLEANING DELICATE OPTICAL SURFACES

DESIRE FOR CLEAN OPTICS

- UV absorption by "transparent" deposits
- Dust intercepts and scatters light
- Dust and deposits absorb laser beam energy
  - Heat absorption can bake dirt in (bonding)
  - Local heat transfer to optic (stress)
  - Explosive vaporizing can damage (shock)

PRECAUTIONS TO KEEP OPTICS CLEAN

- Use roof cover for building
- Equipment dust covers
- Never touch optical surfaces, especially in laser beam
- Do not blow dust from nearby surfaces

FRAGILITY OF OPTICAL COATINGS

- They scratch easy, do not rub or dust
- Do not touch with skin
- Al (LiF) is the most fragile to be used (PM)

HOW TO CLEAN MOST "HARD" COATINGS

a) First try jet of "duster" gas

b) Next try
   - Spray or flow optics cleaner over surface
   - Drain and air dry
   - Repeat (a) above

c) Next try
   - Wiping liquid cleaner (b) with special optics cloth
   - Rinse and dry as in (b) above
   - Repeat (a) above to remove lint

9.0 FACILITY AND GSE REQUIREMENTS

9.0 FACILITY AND GSE REQUIREMENTS

9.1 Facility and Ground Support

AFGL facility electrical interface requirements will be necessary for G-BALS after installation on a designated site. During non-operational (storage) periods of G-BALS, a power draw of 2 amps at 115 VAC will be required to provide active cooling for one photomultiplier tube (PMT) in the detection assembly. The permissable temperature limits for this one PMT are $-100^{o}C$ to $+20^{o}C$. During G-BALS operational periods, 208 VAC, 3 phase at 25 amps will be required to operate the laser subsystem. Three separate 115 VAC circuits at 20 amps each will be utilized for all the remaining subsystems. A recommendation is made for an isolation transformer installation to minimize electromagnetic interference (EMI) on the sensitive PMT signal lines.

An engineering type laboratory environment is recommended for the G-BALS building/site to preclude structural shock and vibration phenomena from affecting all subsystems and subsequent data collection during operational periods. Examples of shock and vibration that are detrimental to G-BALS are large tracks and trains passing by the G-BALS facility. Measurements should be made if an existing freight or passenger elevator operates within the same building to determine acceptable vibration levels.

Cooling water, ambient temperatures, relative humidity, and ground support equipment are also listed on the facing pages.

9.0 FACILITY AND GSE REQUIREMENTS

9.1 FACILITY AND GROUND SUPPORT

ELECTRIC POWER REQUIREMENTS

- Storage

  115 VAC at 2 amps (PMT cooler)

- Operation

  208 VAC, 3 phase, 25 amps (laser) } via isolation transformer to minimize EMI
  Three 115 VAC circuits, 15 to 20 amps each } via isolation transformer to minimize EMI

SHOCK AND VIBRATION

- Storage: Not exceed normal laboratory levels
- Operation: "Quiet" environment

COOLING TAP WATER

- Storage: 0.2 gal/minute (PMT cooler)
- Operation: 2.2 gal/minute at $\leq$ 20°C

AMBIENT TEMPERATURE

- Storage
  - Telescope and beam exp. section: -30°C to +50°C
  - Indoor (laser, detection, electronics): +1° to +40°C
- Preceding and during runs
  - Period starts several hours before runs
  - Telescope and beam exp. section:
    outdoor temp. anticipated and actual during runs
  - Indoor: +10°C to +35°C ($\pm$ 2°C)

    Temperature must be constant $\pm$2°C

    Temperature preferably same each time

INDOOR RELATIVE HUMIDITY: 8% to 80% at all times

LOCAL THERMAL TURBULENCE (SEE NEXT PAGE)

GROUND SUPPORT EQUIPMENT NEEDED

- 1-2 good oscilloscopes (power requirements assume solid state design)
- 1 good autocollimator

9.2 Effect of "Thermals" on Site Requirements

In reference to the possibility of installing the lidar system on the roof of an existing building, atmospheric thermal effects from typical large buildings may compromise the performance of this lidar system. Such "thermals" are particularly likely to cause problems in the winter when a heated building is much warmer than nighttime ambient, and during early night in the summer when the building roof is still hot from the day's sun. If the structure is well insulated and painted all white, these problems may be reduced to an acceptable level. Alternatively, it may be advisable to use a small white isolated building (an "observatory").

Although the seeing requirements are not as stringent as those for normal astronomical measurements, the lidar field of view (fov) and thus laser beam divergence must be kept relatively small in order to limit the sky background signal level. These needs in turn require "seeing" to be such that a star image will stay entirely within 5 arc seconds of its average fov location. The ability of any given site to meet these needs can be easily and cheaply checked by setting up a well-mounted small but long focal length telescope and observing star image stability (in arc seconds) over a period of time at various seasons, types of weather, and times of the night. Although such a small telescope would not have an aperture which matches the lidar receiver telescope, the angular range of star image jitter would indicate the suitability of the site for the large lidar system.

9.2 ATMOSPHERIC THERMAL TURBULENCE FROM BUILDING

EFFECT OF LOCAL "THERMALS"

- Spreads laser beam
- Degrades telescope field of view (fov)
- Diverts beam relative to telescope fov
- Partial loss of lidar signal (wrong results)

TURBULENCE LIMITS FOR G-BALS

- Estimate 5-10 X those allowable for astronomy

CAUSE OF NIGHT LOCAL THERMALS

- Building night temperature different from ambient
- Especially severe certain seasons and weather

VARIABLES INFLUENCING NIGHT LOCAL THERMALS

- Building size and shape
- Building color, insulation and internal temperature
- Atmosphere day/night temperature differential
- Lack or presence of preceding day sun/clouds
- Immediate surroundings
  - Asphalt
  - Bare ground
  - Grass
  - Trees

SELECTION OF LIDAR SITE AND STRUCTURE

- Can do thermal analysis
- Or can do site tests on star image stability
  - Use small telescope (6-8 inch diameter)
  - Tests cover all seasons
  - Tests cover all applicable weather
- Roof of large building vs. isolated small site

10.0 TRANSPORTABILITY

10.0 TRANSPORTABILITY

To move the G-BALS lidar from one (fixed) site to another requires disassembly of all equipment to major subsections, the use of a crane or lift at both old and new sites, and use of a moving van or truck for transportation. The new site also will require a specially constructed or adapted building and all facilities. Finally, the entire lidar system must be re-assembled and re-aligned.

To make any future large lidar system aimable will require a heavy duty swivel/tilt lidar mount, an improved stiffer laser head base plate (not now available from the laser manufacturer), and preferably a shorter receiving telescope design than at present.

To make this G-BALS or any future lidar system reasonably mobile will require the entire system to be mounted on one or possibly two large trailers. As with the present G-BALS design, the transmitter and receiver should be in an openable portion of the trailer, while the laser, detection assembly, and electronics require some thermal or climate control. If the lidar is to be aimable, then special bracing is needed for travel. If portable electric power is desired, it probably should be located on its own trailer to reduce vibration and noise at the lidar. Finally, it is desirable to supply indoor heated storage for the optics and electronics trailer. If outdoor storage is necessary, then externally supplied electric power must be continuously available to power in-trailer heating and air conditioning units.

10.0 TRANSPORTABILITY

LIDAR SYSTEM DESIGN PRESENTED HERE

- Fixed site
- Fixed orientation (vertical)
- Requirements for moving the Lidar System
  - Disassemble equipment to major subsystems
  - Disassemble support structure to major sections
  - Need crane or lift
  - Moving van or truck
  - New site
  - New building/housing
  - Facilities
  - Ground support equipment
  - Reassemble entire system
  - Re-align optics

FUTURE MOBILE G-BALS

- Mount lidar on large trailer or two
- Swivel/tilt mount for transmitter/receiver optics
  - Aimable system for wider coverage of atmosphere
  - Specially orient, brace and cover optics for storage/travel
  - Need special stiffer design for laser head
  - Prefer shorter, lighter telescope design
- Trailer design
  - Air conditioned section for electronics and personnel
  - Uncoverable section for transmitter/receiver
  - Laser head and detection assemblies need thermal control
- Desire indoor storage for optics trailer
- May need portable power
- All above mobility features increase system cost

11.0 TRADE STUDIES

11.0 TRADE STUDIES

These trade studies were performed early in the contract period, and were originally presented during the mid-contract review. The ground-based atmospheric lidar system (G-BALS) conceptual design was then based on these trade studies which are presented here for completeness.

11.1 Theory

11.1.1 Lidar Equations for Photon Counting Detection

The expression which relates the lidar receiver output N_s to the lidar system parameters and atmospheric conditions is called the range equation and is shown on the facing page. A complete listing of mathematical symbols for all of the facing page equations is to be found as Section 11.1.2.

We see that while the backscatter cross sections Q_b vary as $1/\lambda^4$ and approximately $1/\lambda$ for molecular and aerosol scatter, respectively, N_s varies as $1/\lambda^3$ and approximately constant for molecular and aerosol scatter, respectively. As a result, a measure of lidar efficiency (E_m) for measuring Rayleigh scatter (and thus gas density) is defined as a function of only the appropriate variables, λ, T, QE, and E_f.

11.0 TRADE STUDIES

11.1 THEORY

11.1.1 LIDAR EQUATIONS FOR PHOTON COUNTING DETECTION

$N_s = [\Pi/8h)]\ (d/r)^2\ k_b\ \lambda_s\ U\ E_o T_i T_s$ photons/sec detected

where

$r = c\ t/2$

For Rayleigh/Mie (aerosol) scatter ($\lambda_i = \lambda_s$)

$$k_b = n\ Q_{rb} + m\ Q_{mb} = K_r\ n\ \lambda^{-4} + K_m\ m\ \lambda^{-a} \quad (a \approx 1)$$

For Raman scattering ($\lambda_i \neq \lambda_s$)

$$k_b = n_g\ Q_{gb} = K_g\ n_g\ \lambda_s^{-4}$$

Thus for wavelength and laser evaluations for gas density measurements where $\lambda_s \approx \lambda_i$

$$N_s = K(\lambda^{-3}\ T^2\ E_o)\ U = K\ E\ U$$

where K = constant

λ = wavelength

T = atmospheric transmittance to range r

E_o = system efficiency = $QE \cdot E_f \cdot E$(optics)

QE = photomultiplier tube quantum efficiency

E_f = bandpass filter efficiency

U = laser output energy

$$E_m = \lambda^{-3} \cdot T^2 \cdot QE \cdot E_f$$

11.1.2 Mathematical Symbol Definitions

The facing page shows a complete listing of definitions for all the mathematical symbols used in Section 11.1.1 as well as elsewhere in Section 11.0.

11.1.2 MATHEMATICAL SYMBOL DEFINITIONS

c	velocity of light
d	aperture diameter of lidar receiver
E	efficiency
E_f	bandpass filter optical efficiency (transmittance)
E_o	lidar efficiency
E_m	lidar measurement efficiency
h	Planck constant
H	geopotential altitude
k_b	backscatter coefficient
K	constant
K_g	a Raman backscatter constant
K_m	an aerosol (Mie) backscatter constant
K_r	a Rayleigh backscatter constant
m	aerosol density
n	atmosphere total number density
n_g	total number density of gas component g
N_s	number of photons per second detected (counted)
QE	detector quantum efficiency
Q_{gb}	Raman backscatter cross section for gas g
Q_{mb}	aerosol (Mie) backscatter cross section
Q_{rb}	Rayleigh backscatter cross section of atmosphere
r	range
t	time
T	atmospheric transmittance to range r
T_i	atmospheric transmittance at λ_i
T_s	atmospheric transmittance at λ_s
U	laser output energy
λ	wavelength
λ_i	incident wavelength
λ_s	scattered wavelength
α	lidar receiver full angle field of view
B_f	spectral band pass of narrow band filter

11.2 Commercially Available Pulsed Lasers

Table 11.2-1 lists the best visible and near-visible outputs in joules/sec commercially available from pulsed lasers. This listing is limited to lasers operating at 100 pps maximum so as to allow time between each shot for lidar signal return, background measurement, and all data acquisition.

Anticipating the results of Sections 11.3 and 11.4, the Nd:YAG(SHG) and Nd:YAG(THG) lasers listed are both Quantel International Model YG-482CM. At present, this laser is claimed to have outputs of 1500 mJ/pulse when Q-switched (1064 nm wavelength), 650 mJ/pulse at 532 nm and 700 mJ/pulse at 1064 nm when frequency-doubled, and 220 mJ/pulse at 355 nm, 400 mJ/pulse at 532 nm, and 450 mJ/pulse at 1064 nm when frequency-tripled. These outputs are all for laser pulse rates of 10 per second.

11.2 COMMERCIALLY AVAILABLE PULSED LASERS

TABLE 11.2-1
MAXIMUM USEFUL OUTPUTS FROM SOME
COMMERCIALLY AVAILABLE PULSED LASERS*

TYPE PULSED LASER	LASER WAVELENGTH (NM)	MAX OUTPUT/SEC (100 PPS MAX)	
		PPS	U(j/sec)
Ho/YLF	2060	10	0.75
Er/YLF	1730	10	0.05
Nd/YAG	1064	10	20
Nd/glass	1060	.033	0.5
Er/YLF	850	10	0.5
Fluorine	713	$\leq$100	$\sim$0.1
Ruby	694	1	3
Dye* (rhodamine)	$\sim$600	12	$\sim$ 2
Nd/YAG (SHG)	532	10	6.5
Dye* (coumarin)	$\sim$500	12	$\sim$ 2
N_2^+	427	$\leq$100	$\sim$0.1
Nd/YAG (THG)	355	10	2.2
XeF eximer	351	$\leq$100	5
Ruby (SHG)	347	1	0.3
N_2	337	$\leq$100	0.5
XeCl eximer	308	$\leq$100	7
Nd/YAG (FHG)	266	10	1.1
KrF eximer	249	$\leq$100	11

*Notes: Wavelength range = 300-2000 nm
Pulse widths <400 ns
Dye lasers are coaxial flashlamp-pumped

11.3 Lidar Wavelength and Laser Trade

Figure 11.3-1 shows a plot, vs. wavelength, of $1/\lambda^3$ atmospheric vertical transmittance squared (T^2), bandpass filter typical transmittance (E_f), best available detector quantum efficiency (QE), the product of those factors (E_m, see Section 11.1.1), and laser:efficiency products $E_m \cdot U$. For this plot, U is defined as joules/second, not joules/shot. The (S), (M), or (A) along each section of the QE curve refers to the photomultiplier tube (PMT) cathode type used. Laser points are generally shown as circles, except triangles are used for frequency-doubled laser configurations and squares are use for frequency-tripled laser configurations.

The best pair of $E_m \cdot U$ points from a single laser are found to be at 355 nm and 532 nm as obtained from Quantel International Model YG-482CM in the frequency-tripled configuration.

Figure 11.3-1

11.3 LIDAR WAVELENGTH AND LASER TRADE

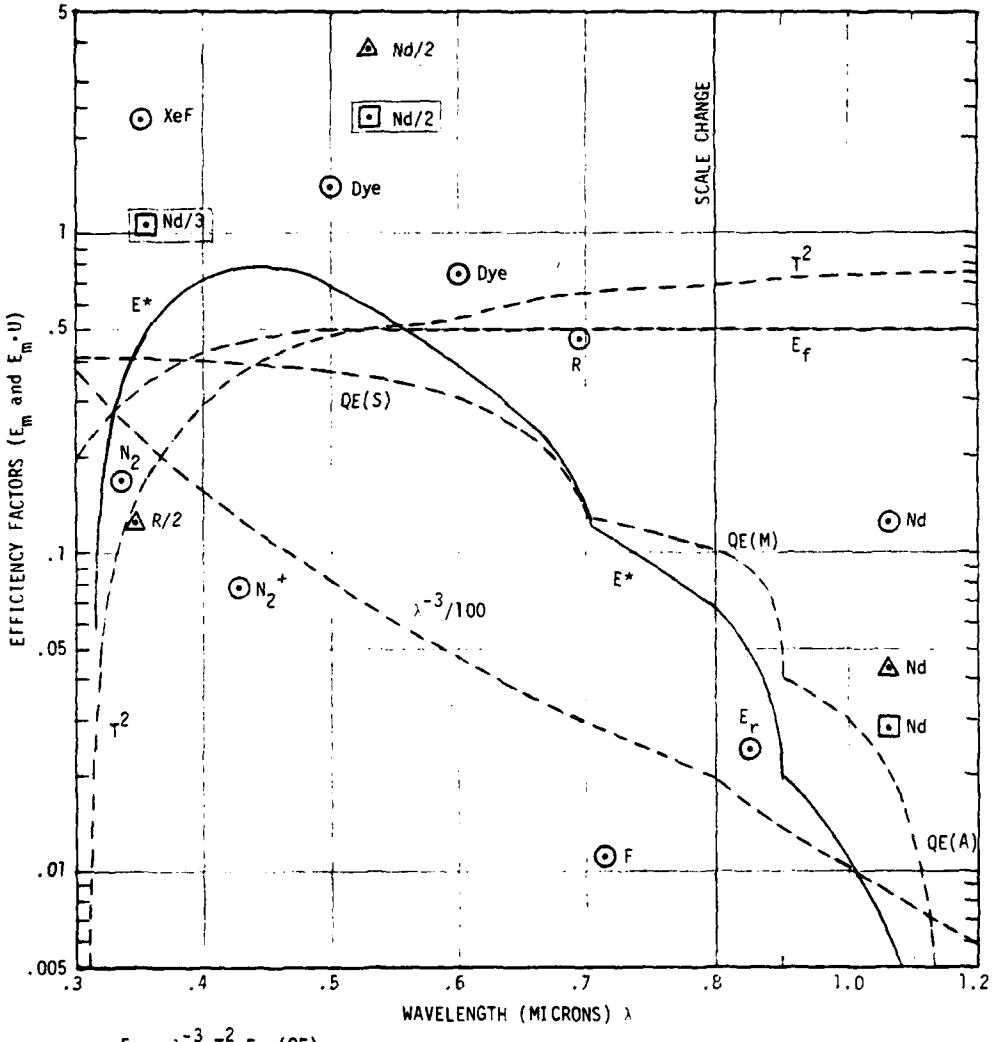

$E_m = \lambda^{-3} T^2 E_f (QE)$

Laser Points = E_m · U

= Selected laser

11.4 Baseline Definition Comparison of Lidar Systems

Table 11.4-1 compares the performance of several one-laser and two-laser combinations of Rayleigh/rotational Raman and two-color Rayleigh lidar systems employing Quantel International Model YG-482CM neodymium:YAG lasers. This performance comparison is relative to the Raman lidar system for which the reference cost is $X, and the reference signal altitude (H) is assumed to be 100 km for which a signal count level N_s is obtained (see Section 11.1). For all non-Raman lidar systems, that lidar signal altitude is calculated which yields the same N_s; and also the approximate cost differential is estimated. Note that the altitudes H are for comparison purposes only, with actual altitudes of performance dependent on specific design details (covered elsewhere).

The selected lidar is the single-laser two-color Rayleigh type system operating at 532 nm and 355 nm. This system yields nearly the highest average altitude of performance, and at a relatively small cost penalty.

TABLE 11.4-1

11.4 BASELINE DEFINITION COMPARISON OF LIDAR SYSTEMS

Type Lidar	Laser Output λ(nm)	Laser Output U(mj/pulse)	Max. Alt.* H (km)	Est. Cost ($)	
Ray/Rot. Ram (one laser)	532	650	100 (ref.)	X (ref.)	
	(~532)	-	71.5		
Two Color Rayleigh (one laser)	1064	700	78.5	X + 10K	
	532	650	100.0		
	1064	450	76.0	X + 10K	
	355	220	93.25		
	532	400	97.5	X + 10K	Selected
	355	220	93.25		Selected
Two Color Rayleigh (two lasers)	1064	1500	82.5	X + 100K	
	532	650	100.0		
	1064	1500	82.5	X + 100K	
	355	220	93.25		
	532	650	100.0	X + 100K	
	355	220	93.25		

*All altitudes H are calculated to yield the same N_s, where

$$N_s \propto E_m U n/H^2$$

11.5 Shutter Trade-Offs

Since low altitude lidar signals are many orders of magnitude stronger than for the high altitudes desired, a high altitude ground-based lidar system may easily expose some of its detectors to signal levels which cause at least slow recovery of sensitivity and perhaps also increased dark count, detector afterpulse effects, and possibly even detector damage. Photomultiplier tube (PMT) protection can be provided by mechanical shutters if fast and durable enough, electro-optical "shutters" if they have suitable optical properties, and electronic off-gating in the PMT.

Pockels cell shutters often have a marginal on/off ratio (relative to the need) and require polarized light, causing excessive loss of unpolarized light. The frustrated total internal reflection (FTIR) electro-optical shutter avoids this disadvantage, but it has too short an active period (on or off) and also has too poor an on/off ratio.

(continued)

11.5 SHUTTER TRADE-OFFS

A. Phenomenon

1. Low altitude scatter will overdrive PMT's
2. Excess signal lasts 100-200 microseconds

B. Resulting Problems

1. Possible afterpulsing
2. Slow recovery of sensitivity and dark count
3. Possible damage to PMT

C. Possible Protection Methods

1. Mechanical shutters
   Reverse motion types (slow, wear)
   Continuous motion type (wheel)
2. Electro-optical shutters
   Pockels cell (polarizers and lossy)
   FTIR
3. Electronic off-gate of PMT

D. FTIR Electro-Optical Shutter

1. Short activation period (100-300 ns max)
2. Poor on/off ratio (about 13 db)

(continued)

11.5 Shutter Trade-Offs (continued)

All PMT's can be off-gated by pulsing selected dynodes or the cathode, but charge distributions can slowly change on internal insulating surfaces, resulting in problems with slow recovery. This characteristic plus the question of cathode recovery must be fully checked and perhaps improved before success can be assured for the G-BALS application.

Mechanical rotating wheel shutters can be made fast enough and have good durability. However, the necessary high rotational speeds require attention to mechanical dynamics. Also, timing of lidar shots must be dependent on shutter wheel position.

The rotating wheel shutter system is chosen for the ground-based atmospheric lidar system because it has perfect extremes of on and off, and with careful design it will perform well without significant development time or risk.

11.5 SHUTTER TRADE-OFFS (CONT'D.)

E. Off-Gated PMT

1. Off-gate via dynodes or cathode
   - Any PMT
   - Good on/off ratio (40 db)
   - Cathode not protected if via dynodes
   - Relaxation effects on sensitivity
2. Off-gate via cathode internal grid
   - Better gating characteristics
   - Few PMT choices, expensive
   - Available PMT's too noisy or slow for this application

F. Rotating Wheel Shutters

1. Moving parts (rotation)
2. Wheel position must determine lidar t_o
3. Minimal risk/development

G. Shutter Choice for GBALS

Rotating wheel shutter

11.6 Comparison of Photomultiplier Tubes

Table 11.6-1 lists several photomultiplier tubes (PMT's) with promising characteristics for use as G-BALS detectors. Since the photon-counting detection technique has been selected (see Sections 12.2 and 12.5), some of the characteristics listed are of special interest for such techniques. Also, all PMT's listed are of electrostatic focused design so as to preserve the fast rise times needed to permit high count rates.

The PMT's selected for G-BALS are the Varian Model VPM-152S for highest altitude use at 532 nm, and the RCA Model 8850 for lower sensitivity (lower altitude) uses at 532 nm and all uses at 355 nm. The Varian PMT was selected primarily for its very high quantum efficiency in the green, while the RCA 8850 PMT was selected for its good compromise between cost, quantum efficiency, room temperature dark current, GaP first dynode for good photon-counting characteristics, and its high allowable anode output.

11.6 TABLE 11.6-1. COMPARISON OF PHOTOMULTIPLIER TUBES (PMT)

Brand	Model	Cathode				Dark Counts/Sec.		First Dynode Matl.	Anode Max. Avg. Output (ma)	Volts for Gain = 10^7	Special Equipment Needed[b]
		Type	Size (mm)	Quantum Eff. (typ.) 355 nm	530 nm	Room Temp.	-20°C				
EMI	9863B	MA	9 diam	21%	12%	400	5E	BeCu	0.2	2300	C
EMI	9893B	BA	9 diam	26%	10%	40	-	BeCu	0.2	2300	None
Hamamatsu	R1332	BA	46 diam	25%	10%	?	?	GaAsP	0.1	2000E	M
"	R1333	MA	46 diam	3.5%	12%	?	800	GaAsP	0.1	2100	C&M
"	*R943-02*	*GaAs*	10 x 10	20%	13%	?	10	CuBe	.001	1600[a]	C
"	928P	MA	8 x 24	21%	11%	1500	20E	Alk. Sb	0.1	1000	C
RCA	8850*	BA	46 diam	32%	10%	170	-	GaP	0.2	1900	M
"	8852	MA	46 diam	<2%	8%	20,000	200E	GaP	1.0	2000	C&M
"	C31034A-02	GaAs	7.6 x 23	35%	23%	?	12	BeO	10^{-4}	1800[a]E	C
Varian	VPM-152S*	GaAsP	5 diam	40%	35%	5000	10	BeO	0.05	6000[a]	$&C

Notes: All PMT's listed have rise time of 3 ns or less.

MA = multialkali
BA = bialkali
E = estimated
* = tubes selected for G-BALS

a) For gain = 1×10^6
b) C = cooled housing with AR coated double windows
M = aperture magnet to reduce dark current
$ = very expensive PMT

11.7 Design Options for Two-Color Lidar

Three different designs have been considered for the two-color Rayleigh type ground-based atmospheric lidar system (G-BALS).

As summarized in Table 11.7-1, Option A is simplest and cheapest, but would require three lidar runs totalling 35 minutes to cover the full 20-100 km altitude range. Options B and C would both cover the full altitude range in 15 minutes. Option C would have the greatest stability of alignment and allow the smallest receiver field-of-view (of advantage for daytime runs), but also has the lowest optical efficiency and highest development risk.

Option B has been selected as meeting the design goals with the best compromise between optical efficiency, cost, and risk.

The remainder of this Section 11.7 shows optical block diagram concepts for various sub-assemblies of Options A, B, and C.

TABLE 11.7-1

11.7 DESIGN OPTIONS FOR TWO COLOR LIDAR

CHARACTERISTICS	OPTIONS		
	A	B	C
System Description			
Transm/rec. tel.	separate	separate	combined
No. of detectors	2	6	6
Data Multiplexing	*No?*	Yes	Yes
Performance			
Optical efficiency:			
at 355 nm (UV)	1	0.90	0.75
at 532 nm (green)	1	0.89	0.71
Total Oper. time (min)	35	15	15
Rec. fov limits	-	-	smallest
Alignment stability	-	-	best
Cost Impact			
Optical matls. diff.	reference	+13K	+21K
Data handling	simpler?	-	-
Fab/Ass'y/Test	cheapest	-	-
Complexity	low	mod.	high
Technological Risk	low	low med.	high
Option Selected		x	

11.7.1 Optical Arrangement for Options A and B

Figure 11.7-1 indicates the transmitter concept and the overall transmitter-receiver arrangement for both Options A and B. The reason for the specified orientation of the detector section is discussed in Section 4.4.2.

The symbols used in this and all remaining conceptual block diagrams are defined below for Options A, B, and C (Figures 11.7-1 through 11.7-4).

BS	Beam Splitter
DL	Detector Lens
DM	Dichroic Mirror (UV-Reflecting)
F	Filter
F1	UV Narrow Band Filter
F2	Green Narrow Band Filter
FS	Field Stop
L	Lens
M	Mirror
M5	Receiver PM
M6	Receiver SM
NF	Neutral Density Filter
PM	Primary Mirror
PMT	Photomultiplier Tube Detector
SM	Secondary Mirror
UV	Ultraviolet
W	Window (for Laser Monitor)

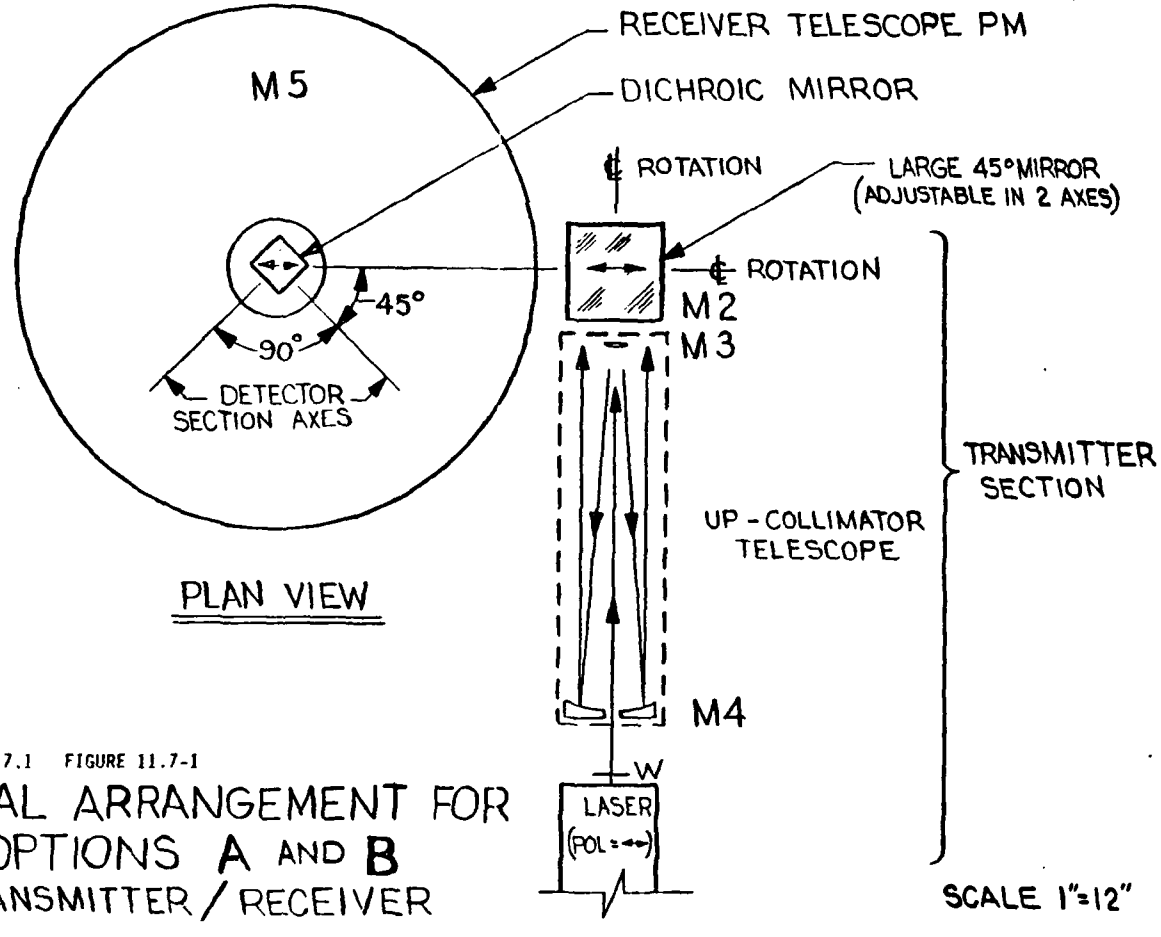

11.7.1 FIGURE 11.7-1

OPTICAL ARRANGEMENT FOR OPTIONS A AND B TRANSMITTER / RECEIVER

11.7.2 Detector Section of Option A

Figure 11.7-2 shows the lidar detector section of Option A to have only one PMT detector for each lidar wavelength, and thus to measure only one altitude range at a time. Neutral density filters NF1 and NF2 must be changed to shift to another altitude range.

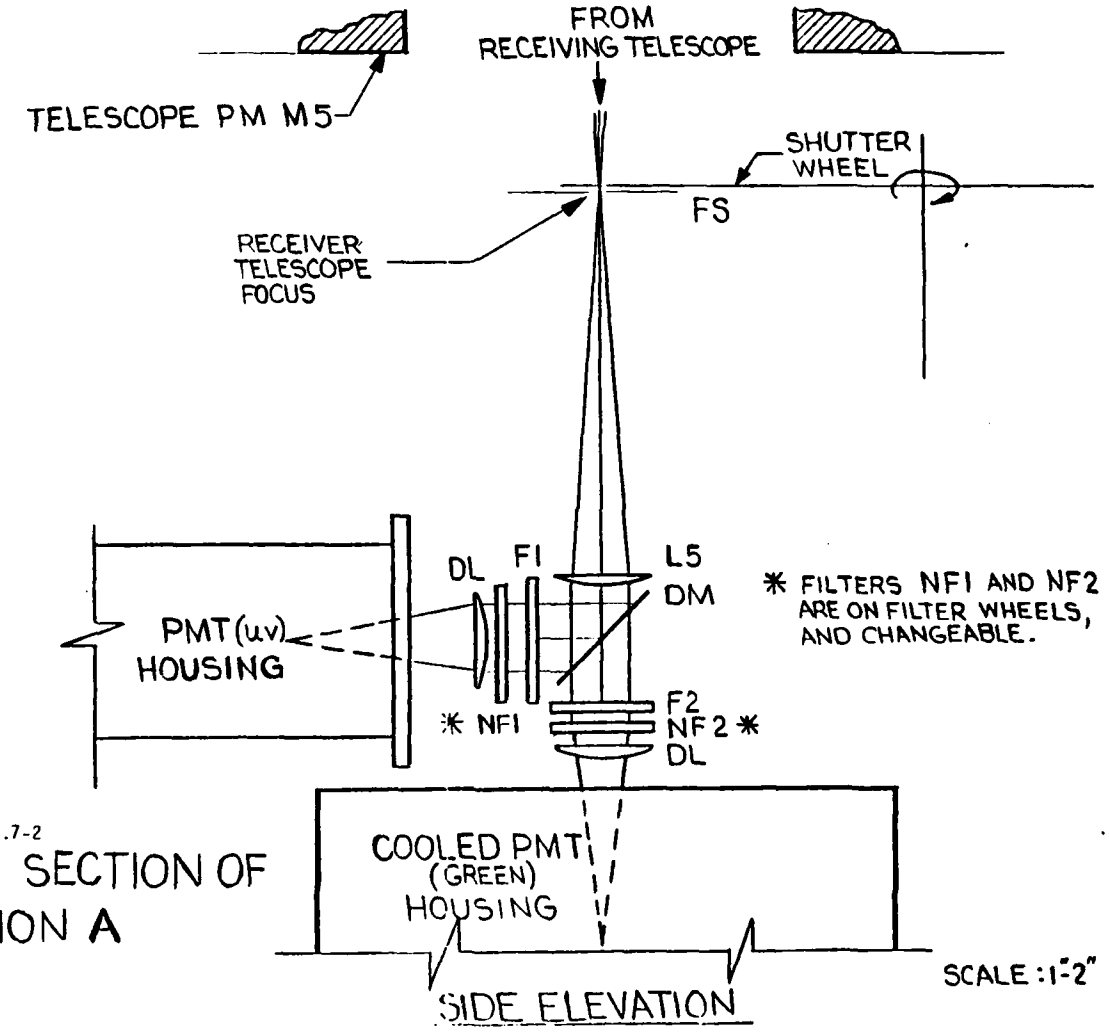

11.7.2 FIGURE 11.7-2

DETECTOR SECTION OF OPTION A

11.7.3 G-BALS Options B and C Detector Region

Figure 11.7-3 shows the lidar receiver's detector section for Options B and C. In addition to the dichroic mirror DM for separating the green and near-UV wavelengths, this design also employs beam splitters BS to unequally apportion the return signal at each wavelength between three PMT detectors so as to cover the full 20-100 km altitude range in one shot. Also, the design includes two rotating shutter wheels mounted on a common shaft and mutually oriented so that all detectors are blocked from lidar return signals originating well below 20 km, while the two most sensitive detectors are blocked from signals originating below about 50 km.

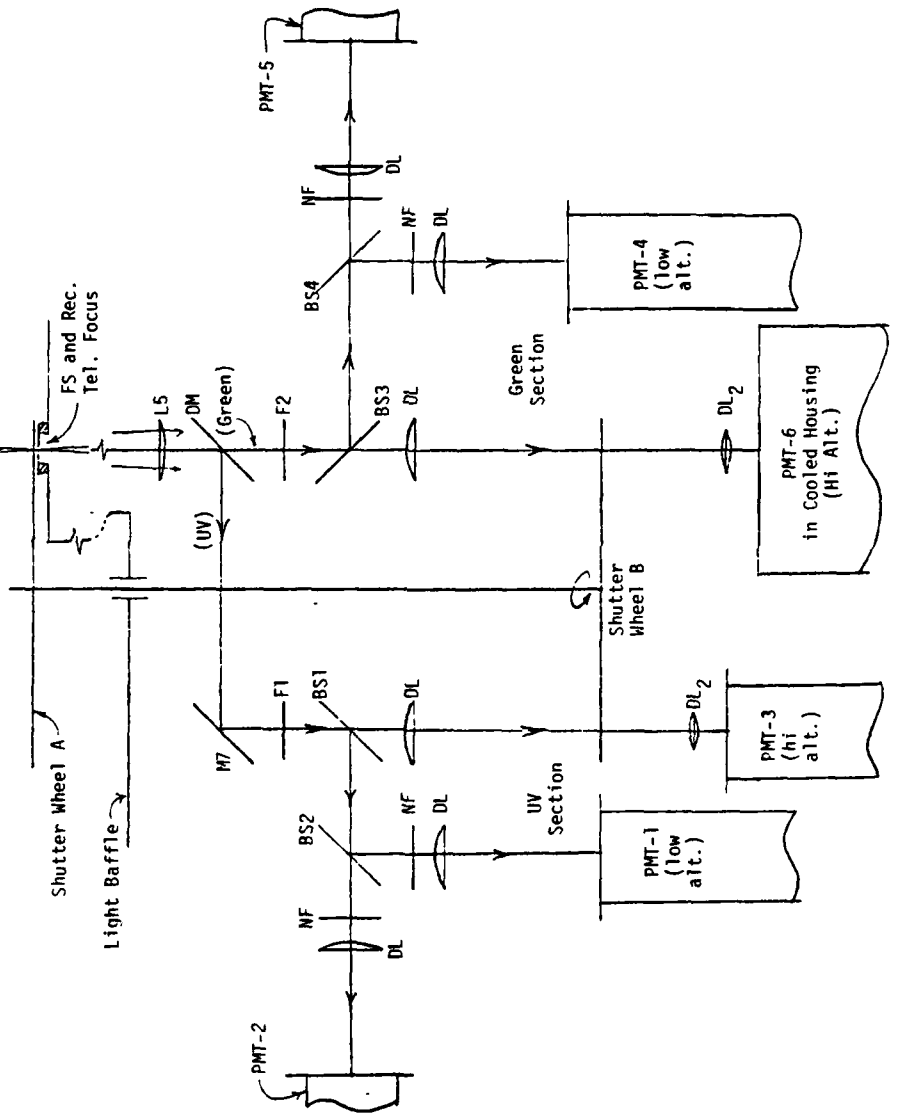

11.7.3 FIGURE 11.7-3. GRALS OPTIONS B&C DETECTOR REGION

11.7.4 G-BALS Option C: Laser Output/Optical Switch Region

Figure 11.7-4 shows the lidar transmitter:receiver design concept for Option C. The heart of this option is the use of an FTIR optical switch to allow the telescope to function as both the lidar transmitter up-collimator and also as the lidar receiving telescope. From field stop FS and on, the detector section concept is as already shown in Figure 11.7-3.

In this Figure 11.7-4 design concept, shutter wheel A also serves to block the laser light path after the laser light pulse and during the lidar detection period. This prevents any laser flashlamp residual glow from scattering into the very light-sensitive detector section. The laser output beam is down-collimated to a smaller diameter so as to reduce the laser shutter closing time.

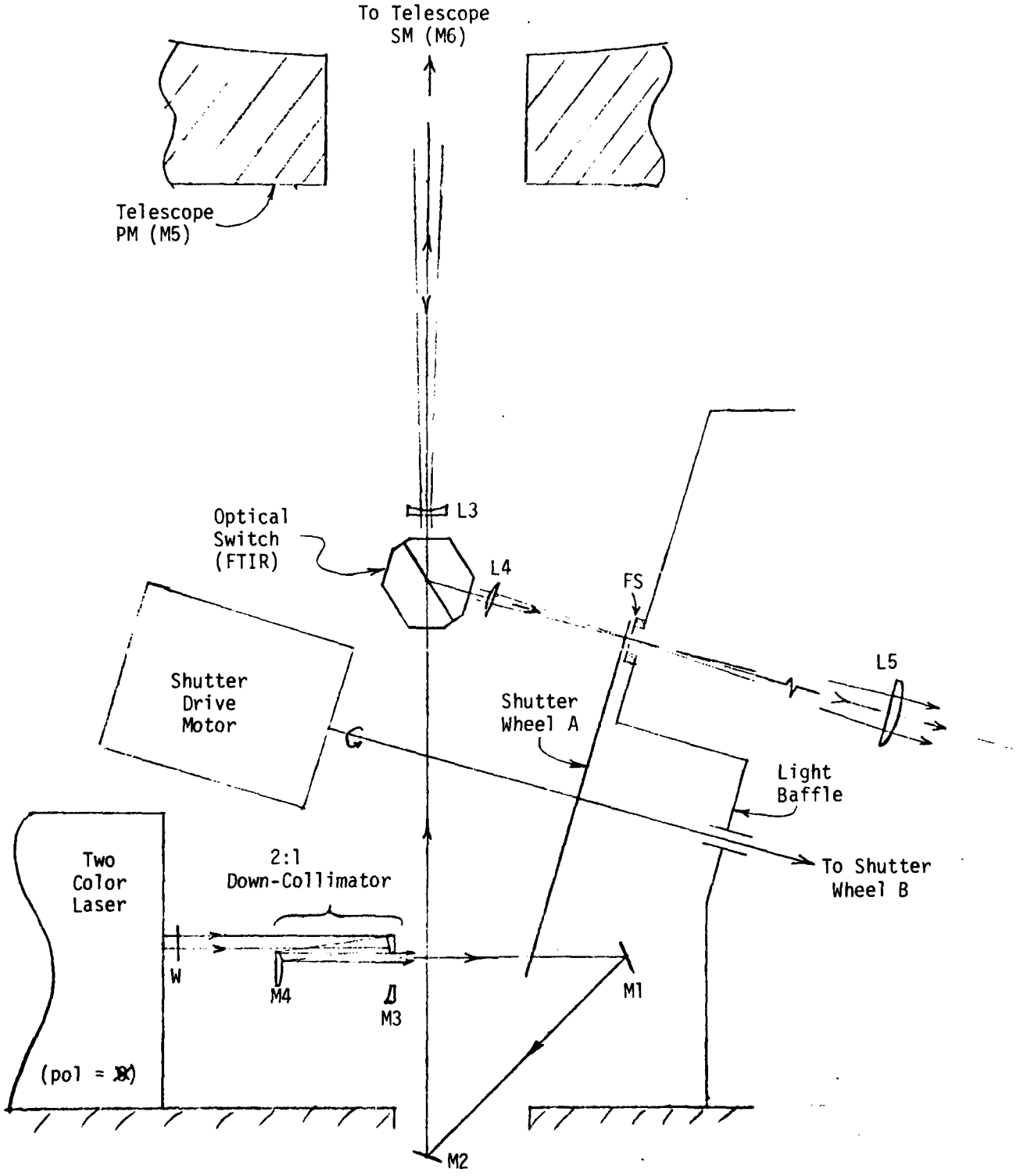

11.7.4 FIGURE 11.7-4. GBALS OPTION C: LASER OUTPUT/OPTICAL SWITCH REGION

11.8 Receiver Telescope

11.8.1 Maximum Measurement Altitude vs Telescope Aperture

Figure 11.8-1 shows a plot of maximum measurement altitude vs Option A telescope aperture. Assumptions not shown on the figure include use of the LOWTRAN-3B atmosphere and atmospheric optical characteristics, a 2.5 km range resolution, 9000 shots (15 minutes) measurement period, and nine background measurements per lidar shot (see Sections 11.1, 12.1, and 12.2). For application to Options B and C, the vertical scale of Figure 11.8-1 should be multiplied by 1.06 and 1.18, respectively.

It is seen from Figure 11.8-1 that to obtain moonlit night lidar signals with S/N = 10 from 100 km altitude requires a receiver telescope diameter of 1.87 m (73.6 in.), 1.98 m (78.0 in.), and 2.21 m (86.7 in.) for Options A, B, and C, respectively. If the maximum altitude requirement is relaxed to 95 km, then the equivalent required telescope diameters are 0.88 m (34.6 in.), 0.93 m (36.7 in.), and 1.04 m (40.9 in.) for Options A, B, and C, respectively.

11.8 RECEIVER TELESCOPE
11.8.1 MAXIMUM MEASUREMENT ALTITUDE VS TELESCOPE APERTURE
FIGURE 11.8-1

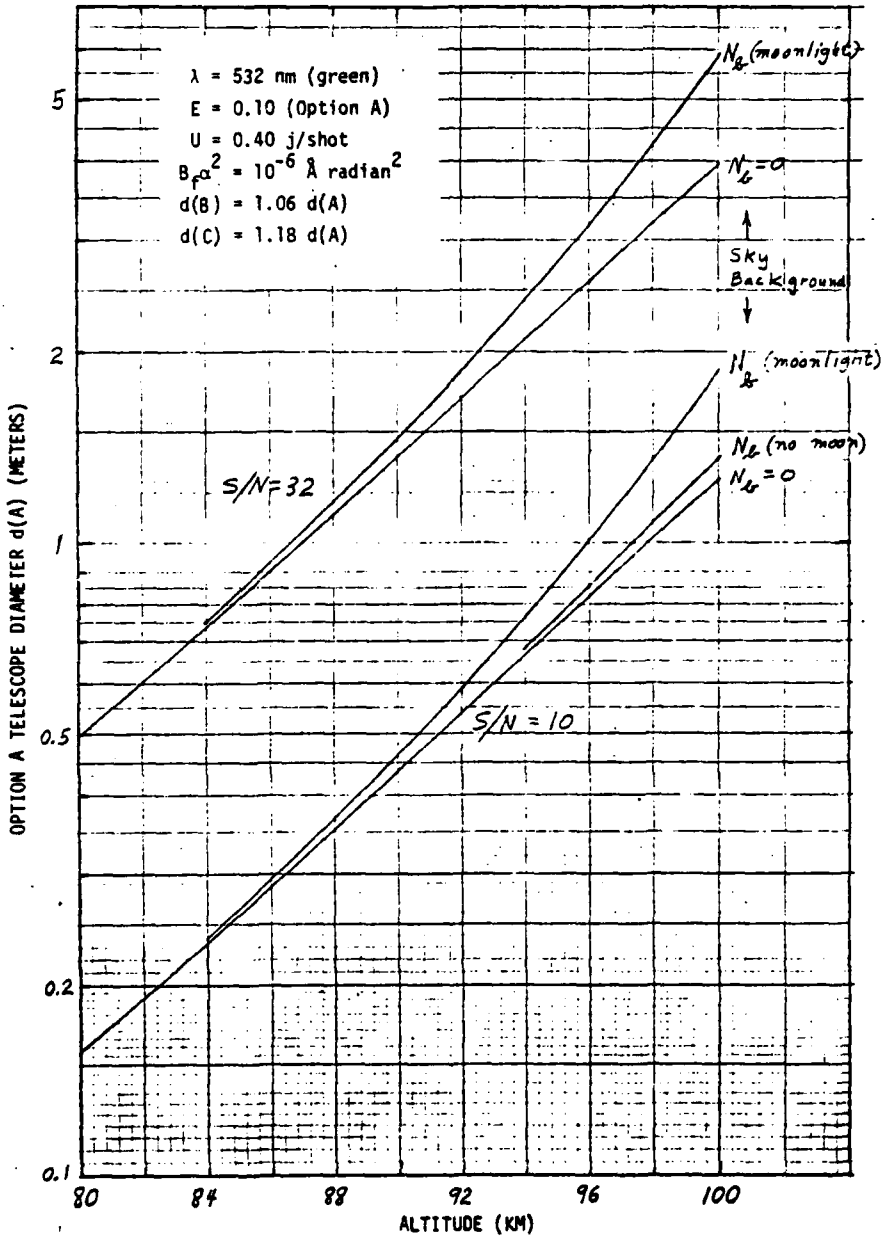

11.8.2 Telescope Definition

The receiver telescope requirements as listed on the facing page are significantly more relaxed than needed for astronomical use. Yet due to the need to limit even night-time background levels, the lidar system field-of-view will be about 0.2 mrad (Options A and B), leading to the resolution requirement shown.

Discussions with optical fabricators confirm that the Dall-Kirkham compound reflector is the most cost-effective telescope design that meets the listed criteria. The selection of a 36-inch aperture is largely based on limiting the long delivery time and large expense of this major cost item.

11.8.2 TELESCOPE DEFINITION

Criteria

Same focus both wavelengths (UV & green)
Large collecting area ($\gtrsim$ 1 m^2)
Maximum fov = .001 radian diameter
Resolution = 5 arc sec (.025 mrad)
Effective fl = 20 m max
Good optical efficiency (coatings)
Minimize cost (design)
Reasonable length and access
Use is vertical orientation only

Telescope Types

Refractors
Simple reflectors
Compound reflectors with corrector plate
    Maksutov - Cassegrain
    Schmidt - Cassegrain
Compound reflectors (without corrector plate)
    True Cassegrain
    Ritchey - Chretien
    Dall - Kirkham
Segmented reflectors

Tentative Selection

Dall Kirkham compound reflector
    Primary mirror = Pyrex or metal
    Secondary mirror = zero expansion glass or Pyrex
Estimated cost and delivery
    36" diameter PM (.66 m^2), \$X, 8 mo delivery (tel. size selected)
    48" diameter PM (1.17 m^2), \$2X, 18 mo delivery
    60" diameter PM (1.82 m^2), \$4X

11.9 Control Electronics Trade Study

The basic requirements of the Control Electronics are to synchronize the events in the Lidar system with the shutter wheel, decide how shutter opportunities should be used (laser shot, background shot or nothing), count the number of events and compare it with a preset value, provide timing for the complete data acquisition system and supply the proper delays for different control signals.

There are three candidates which could possibly fulfill the requirements, a dedicated micro-processor, a system employing the internal processor of the LeCroy, and finally hardwired logic.

In this particular situation there are two primary considerations; one is the speed of the system and the second the cost of the system.

At present the upper limit on micro-processor speed is about 4 MHz. This is the internal clock frequency of the device and many clock pulses are necessary to execute one command, the exact number being determined by the particular device. For any sort of decision or control function there must be a long series of commands. This series of commands, termed the program, could easily take milli-seconds to execute. Also, to realize the maximum speed of the device, the program would have to be written in machine language as opposed to a high level language such as basic or Fortran. Programming in machine language is very time consuming even for the experienced programmer. One of the main reasons for considering a micro-processor-based system is its flexibility to change; if it requires an expert to re-program this device then this flexibility cannot be fully realized.

The price of a system is affected by the cost of the hardware, time to assemble it, and the time to make it functional. Although parts count and therefore labor would be lowest for a micro-processor based system, experience has shown programming the device greatly outweighs the cost of the former two items.

The LeCroy, being a micro-processor based system,suffers from the same deficiencies with the additional one of not being a dedicated system.

Considering hardwired logic, using TTL, one can realize speed on the order of tens of nano-seconds. This speed is of great importance in a Lidar system, where every nano-second means approximately 1/2 foot of range information. The flexibility of the system can be made adequate for present and future needs, and because of its simplicity anyone will be able to operate it. The complexity of the system can be kept to a minimum and therefore the parts count reasonably low.

For the reasons outlined above the decision was made to go with a hardwired system.

11.9 CONTROL ELECTRONICS TRADE STUDY

BASIC REQUIREMENTS

- Synchronize system to shutter wheel
- Make decisions (laser/background shot)
- Act as counter
- Provide timing
- Provide delays

CANDIDATES/OPTIONS

- Dedicated micro-processor
- LeCroy System
- Hardwired logic

CONCLUSION

- Use hardwired logic

REASONS

- Speed
- Flexibility adequate
- Cost
- Programming micro-processor difficulty (machine language)

AD-A091 955 DESIGN STUDY FOR GROUND-BASED ATMOSPHERIC LIDAR SYSTEM (U) GENERAL ELECTRIC CO PHILADELPHIA PA SPACE DIV R L FRANKLIN ET AL. 29 SEP 80 AFGL-TR-80-0264 3/3

UNCLASSIFIED F19628-80-C-0062 F/G 4/1 NL

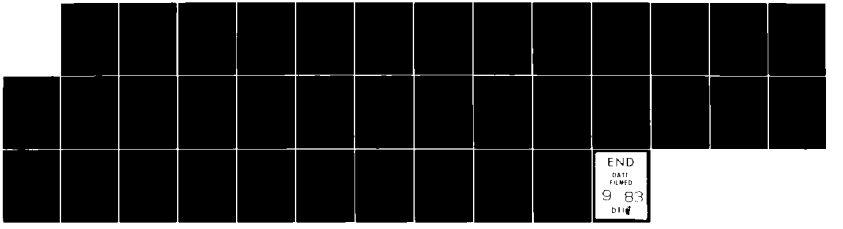

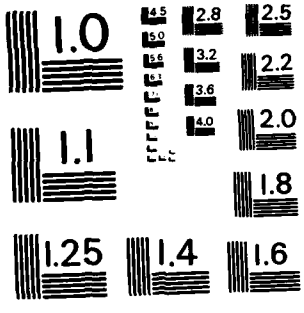

12.0 PERTURBATIONS AND INTERFERENCES

12.0 PERTURBATIONS AND INTERFERENCES

Perturbations and interferences can be considered as including many effects, such as optical material problems, atmospheric refraction and absorption, atmospheric haze and clouds, and background radiation.

Depending on type and design, pulsed lasers can readily emit peak power densities in excess of 10^8 watts/cm^2. Such power densities can damage some optical materials, causing degradation of system output and eventual failure. The proper selection of specially prepared optical materials plus the use of special laser grade dielectric coatings (both reflective and anti-reflective) routinely allows the use of such power densities for extended periods without damage.

One potential source of atmospheric perturbation is atmospheric refraction of the incident and scattered lidar radiation. Since the atmospheric refractive index varies with altitude, pointing the lidar in a non-vertical direction will result in bending of the incident beam as well as reverse bending of any return signal. It would seem that the main effect of such refraction would not be the loss of or error in signal, but rather a small error or deviation in pointing (measurement location). Since lidar measurements are to be made vertically, these small errors will not apply.

The lower atmosphere shows strong continua or band absorption at less than 2000 Å and at many wavelengths in the infrared. In the infrared the best atmospheric "windows" are spectrally located at <0.75 micron, 1.0-1.1 microns, 1.2-1.3 microns, 1.5-1.75 microns, 2.05-2.35 microns, 3.5-4.0 microns, and 8.5-11.0 microns. Ozone shows a very strong absorption (Hartley band) through the wavelength interval 2000-3000 Å, which tapers off (Huggins band) from 3000 Å to negligible absorption above 3450 Å. Ozone also has a very weak and diffuse absorption (Chappius bands) which peaks near 5900 Å and becomes negligible outside the range of 5000-7000 Å. The existence of these ozone band systems in the upper and middle atmosphere then requires us to further limit the previously identified visible/ultraviolet window to 0.345-0.75 micron, with the 0.5-0.7 micron region needing a little extra data reduction when used for very long range lidar.

(continued)

12.0 PERTURBATIONS AND INTERFERENCES

INEFFICIENCY AND DAMAGE OF OPTICS

- Laser peak power density = 100 MW/cm^2
- Use best optical materials
- Use best optical coatings

ATMOSPHERIC REFRACTION

- Slight pointing error if lidar not vertical
- Error correctable

ATMOSPHERIC ABSORPTION

- Blocks or limits lidar range
- Principle absorbing molecules are

  Water Vapor (IR)

  Carbon Dioxide (IR)

  Oxygen (Far UV)

  Ozone (UV, visible)

- Atmospheric "windows"
  - Several located at 0.34 - .75μ, 1.0-1.1μ, and beyond
  - At low altitudes, visible/UV window extends to 0.2μ

(continued)

12.0 PERTURBATIONS AND INTERFERENCES - CONTINUED

In the non-absorption or low absorption regions of the atmosphere, the principle extinction process is due to both gas and particulate (haze) scattering. Haze scatter also increases same-wavelength lidar return signals, although the G-BALS lidar data reduction will correct for haze at altitudes (Z) greater than 20 km. As discussed in Section 7.0, haze or other attenuation originating at $Z < 20$ km also affects the lidar signals but is compensated for by the sounding type lidar calibration. Thus either the lidar must be re-calibrated when low altitude transmittance changes, or else such transmittance must be monitored and the calibration constant corrected.

Generally, lower level clouds are essentially opaque and will terminate the useful lidar return. However, cirrus or higher altitude clouds often have albedos as low as 0.1, and thus can transmit most or much of a collimated light beam. Consequently, while such a cloud dominates the lidar return from within the cloud, through suitable data manipulation it may be possible to recover atmospheric density information from the weakened lidar return from the far side of such a cloud.

12.0 PERTURBATIONS AND INTERFERENCES - CONTINUED

HAZE (AEROSOLS AND PARTICULATES)

- Causes extra attenuation and scatter for lidar
- Low altitude (Z <20 km) haze
  - Effect is included in lidar calibration
    (calibration uses sounding meas. at >20 km)
  - Must re-calibrate when <20 km haze changes
  - Or monitor 0-20 km transmittance and correct calibration
- High altitude (Z >20 km) haze
  - Effect not included in lidar calibration
  - Haze effect to be corrected in lidar software
  - Need lidar with two or more wavelengths

CLOUDS

- Dense clouds prevent distant measurements
- Tenuous clouds
  - May permit far-side lidar measurements
  - Cloud base at <20 km
    Measurements possible
    Need simultaneous lidar re-calibration
    Reduced range beyond cloud
  - Cloud base at >20 km
    Measurements possible without re-calibration
    Reduced accuracy and range beyond cloud

12.1 Background Radiation

Any sky background adds to the desired signal, which then increases signal noise and decreases the signal-to-noise ratio (S/N). Even if the receiver field-of-view (fov) excludes all direct sources of background radiation, any atmospheric scattering will direct some light into the receiver fov from sources positioned outside the fov.

If the sky radiance (brightness) is known for the particular combination of atmospheric scatter and light source, then the number of sky background photons detected per second (N_b) can be calculated as

$$N_b = [10^7\pi^2/(16hc)]I_s\lambda Bd^2\alpha^2E$$

Here, I_s is the sky radiance at wavelength λ, B is receiver spectral bandpass (FWHH), d is lidar receiver diameter, α is the full angle fov of the lidar receiver, and E is lidar receiver efficiency including the detector. In the infrared at over three microns wavelength, another significant source of cw background radiation which must be considered is thermal emission from the earth's surface, air, and clouds.

Signal to background and thus S/N ratios can be optimized by both increasing signal and decreasing background. For most lidar systems, background can be altered through control of fov, filter bandpass, and time gate width, while signal level can be altered via the laser output energy per pulse.

12.1 BACKGROUND RADIATION

BACKGROUND EFFECTS

- Adds to desired signal
- Increases signal noise
- Decreases signal: Noise ratio (S/N)

SKY BACKGROUND SOURCES

- Direct sources
  - Atmospheric thermal emission (IR only)
  - Sun
  - Moon, stars
  - City lights
- Scattered direct source light
  - Gas (Rayleigh plus Raman) scattering
  - Haze (Mie) scattering
  - Clouds (multiple Mie scattering)

SKY BACKGROUND INTENSITY

- Highly variable
- Increases with haze
- Increases with gas density (decreasing Z)
- Increases with ambient light level
  - Clear moonless night sky (Int $\approx$ I)
  - Clear full moon-lit night sky (Int $\approx$ 10I)
  - Clear day sky (Int $\approx 10^7$ I)

BACKGROUND DISCRIMINATION METHODS

- Small field-of-view
- Narrow bandpass optical filter or spectrometer
- Time gate for signal period only
- Background sample and subtraction
- Increase lidar laser intensity

12.2 Lidar Signal Noise

Both the desired lidar signal and any cw background signal obtained from the lidar detector system contain random fluctuations or noise which depend on the background level, the type of detector used, the system bandpass, and the temperature, current, and resistance of critical elements. All detection systems yield thermal (Johnson) noise, quantum detectors yield shot noise, and semiconductors yield current noise. Significant noise originates from not only the radiation detector, but also from the load resistor and any preamplifier. It is the total effect of all this noise in the lidar and background signals which limits the system range and sensitivity of measurement.

Lidar systems operating in the near infrared, visible, and ultraviolet spectral regions usually use photomultiplier tube detectors due to their relatively high quantum efficiencies and relatively noise-free high gain. As a result, high sensitivity photomultiplier tubes can detect individual photons when illuminated by low light levels. In this case, the primary noise is due to the statistical fluctuations in arrival of the individual photons (yielding shot noise). Thus assuming Poisson statistics, the standard deviation variation or noise count, N, in a specific time (lidar range) interval is

$$N = \sqrt{S}$$

Here, S is the average count from the sum of signal counts N_s, background counts N_b, and detector dark counts N_d.

As shown at the bottom of the facing page, S/N in the presence of background can be improved by averaging over several background measurements for each signal measurement. The S/N improvement resulting from this technique becomes greater as background becomes larger relative to the signal.

12.2 LIDAR SIGNAL NOISE

PRIMARY NOISE SOURCES

- Shot noise (random, statistical)
- Thermal (Johnson) noise
  - Thermal fluctuations of resistor electrons
  - Load resistors
  - Amplifiers
- Current noise
  - Charge carrier trapping
  - Semi conductor detectors only

PHOTOMULTIPLIER TUBES

- Photoemissive sensor
- Near-ideal large internal gain
- Thermal noise negligible
- Shot noise dominates

SHOT NOISE

- Standard dev. of signal count (N) = $\sqrt{S}$

  where

  $$S = N_s + N_b + N_d$$

- Signal only

  $$S/N = \sqrt{N_s}$$

- Signal (N_s) plus background (N_b) and dark current (N_d)

  $$S(tot.)/N = (N_s + N_b + N_d)^{1/2}$$

- After subtracting background and dark current

  $$S(N_s)/N \approx (S - N_b - N_d)/(N_s + 2N_b + 2N_d)^{1/2}$$

- If subtract N_b and N_d averaged n times

  $$S(N_s)/N \approx (S - N_b - N_d)/[N_s + (N_b + N_d)(n + 1)/n]^{1/2}$$

12.3 High Altitude Performance and Background Discrimination of Design G-BALS

Table 12.0-1 lists some lidar design characteristics at both operating wavelengths, followed by the highest altitudes for which the system 532 nm signal degrades to S/N = 32 and then S/N = 10.

The various design characteristics of Table 12.0-1 were assembled and/or derived from the data and specifications detailed in Section 4.0. This highest altitude range resolution of 2.40 km results from the choice of 16 microseconds time resolution (0.150 km/microsecond), which in turn results from 2 microsec/channel minimum increments in the data acquisition and storage system (Section 4.5.4). All differences between these lidar system characteristics and those assumed for the telescope trade-off plot of Figure 11.8-1 were used to calculate on "equivalent d(A) aperture". When this equivalent d(A) aperture is applied to Figure 11.8-1, we obtain the altitudes of Table 12.0-1 for which the design system signal/noise ratios reach 32 and 10.

TABLE 12.0-1

12.3 HIGH ALTITUDE PERFORMANCE AND BACKGROUND DISCRIMINATION OF DESIGN G-BALS

DESIGN CHARACTERISTICS

Wavelength (nm)	532	355
Laser output (joules/pulse)	0.40	0.22
Transmitter optical efficiency	0.96	0.96
Receiver and detection, efficiency	.119	.0614
Filter bandpass (A FWHH)	25	50
Receiver fov diameter (radians)	2 E-4	
Range resolution (km)	2.40	
Time resolution (μsec)	16	
No. laser shots/measurement	9000	
No. background samples/shot	10 (1-15)	
Telescope aperture (diameter)	.914 m (36")	
Telescope effective aperture (diameter)	.882 m (34.7")	

HIGH ALTITUDE PERFORMANCE

Equivalent d(A) aperture* for Fig. 11.8-1	.924 m	
Design altitudes* from Fig. 11.8-1		
Altitude for S/N = 10 (km)		
Moonlit night	95.7	-
Dark night (no moon)	97.0	-
Altitude for S/N = 32 (km)		
Moonlit night	86.3	-
Dark night	86.5	-

*All differences between Figure 11.8-1 and final design are used to calculate an equivalent aperture for use of Figure 11.8-1 to show performance of actual design.

12.4 Typical Background and Signal Levels

Table 12.0-2 shows the results of some design lidar system signal counts (N_s), dark counts (N_d), background counts (N_b), and resulting signal-to-noise ratios (S/N) as obtained from the appropriate beam splitter:PMT combination appropriate for each of three altitudes. The lidar design characteristics are again the same as for Table 12.0-1 except where the characteristics vary with the photomultiplier tube (PMT) detector and thus altitude interval of interest. As with all previous lidar calculations, the LOWTRAN-3B model atmosphere and atmospheric optical characteristics were used. The S/N values of Table 12.0-2 are calculated using the last $S(N_s)/N$ equation of Section 12.2, with n = 10 background plus dark count samples per laser shot. In Table 12.0-2, NA means not applicable.

The S/N results of Table 12.0-2 show good values for all clear night conditions. Daytime background signal levels are calculated to be so high as to exceed the count rate capabilities of the highest altitude detectors (PMT-3 and PMT-6), and to approach the random count rate limits of the intermediate altitude detectors (PMT-2 and -5). However, the noise statistics are such that useful daytime measurements can be made at relatively low altitudes (PMT-1 and PMT-4), and perhaps even to intermediate altitudes.

It should be noted that PMT-1 and PMT-4 are used for the altitude range of 20 to about 35 km, PMT-2 and PMT-5 are used for 35 km to perhaps 50 km, and PMT-3 and PMT-6 are used from 50 km on up. The exact altitudes for PMT switching have not been worked out, but can be easily chosen and set (see Section 4.5.9) as G-BALS operating experience dictates.

TABLE 12.0-2

12.4 TYPICAL BACKGROUND AND SIGNAL LEVELS

Wavelength (nm)	532			355		
Altitude (km)	80	40	20	80	40	20
PMT # (Fig. 4.0-1)	6	5	4	3	2	1
Receiver & Detection Eff.	0.119	0.00380	1.25E-4	0.0614	0.00279	1.23E-4
Range Resol. (Δr km)	2.40	1.20	0.60	2.40	1.20	0.60
Measurement Time (min)	15	10	5	15	10	5
Tot. Time/Δr (Σt, ms)[a]	144.1	48.0	12.0	144.1	48.0	12.0
Signal Counts						
N_s #/μsec	0.0240	0.674	2.66	0.00680	0.262	1.19
N_s #/(Σt)	3465	32370	31900	979	12570	14260
Detector Dark Counts						
N_d #/μsec	1E-5	2E-5	2E-5	2E-5	2E-5	2E-5
N_d #/(Σt)	1.44	0.96	0.24	2.88	0.96	0.24
Dark Night Background						
Sky Radiance[b]	3E-14			2E-14		
N_b #/μsec	4.58E-5	1.46E-6	4.82E-8	2.11E-5	9.57E-7	4.22E-8
N_b #/(Σt)	6.61	0.0704	5.79E-4	3.04	0.0460	5.07E-4
S/N	58.8	180	179	31.2	112	119
Moonlit Night Backgr.						
Sky Radiance[b]	2.5E-13			2E-13		
N_b #/μsec	3.82E-4	1.22E-5	4.02E-7	2.11E-4	9.57E-6	4.22E-7
N_b #/(Σt)	55.1	0.586	0.00482	30.4	0.460	0.00507
S/N	58.3	180	179	30.7	112	119
Clear Day Sky						
Sky Radiance[b]	2.9E-7			$\sim$2E-7		
N_b #/μsec	443.5	14.16	0.466	210.6	9.57	0.422
N_b #/(Σt)	6.39E+7	6.80E+5	5595	3.04E+7	4.60E+5	5068
S/N	NA	36.6	164	NA	17.5	101

Notes: a) Assuming 10 shots/second

b) Sky radiance units = W $\mathring{A}^{-1}$ cm^{-2} sr^{-1}

12.5 Comparison of PMT Output Measurement Methods

The facing page table qualitatively compares the relative merits of photomultiplier tube (PMT) photon-counting systems and PMT current or charge-measurement systems. For G-BALS, the need for very high altitude lidar measurements dictates emphasis on night measurements and other low interference characteristics. These needs, then, indicate use of the photon counting technique as chosen.

12.5 COMPARISON OF PMT OUTPUT MEASUREMENT METHODS

	Photon Counting	Current and Charge Measurements
Widest dynamic range	-	X
Daytime measurements	-	X
Night measurements	X	-
Lowest dark signal	X	-
Best S/N	X	-
Most suitable sensitivity	X	-
For Lidar Detection Systems		
High altitude night measurements	X	-
Mid-altitude night measurements	X	X
High altitude day measurements	-	-
Mid-altitude day measurements	-	X

13.0 SECONDARY OBJECTIVES

13.0 SECONDARY OBJECTIVES

13.1 Particulates and Aerosols (Haze)

The lidar equations of Section 11.1 show the backscatter coefficients to vary as $1/\lambda$ and $1/\lambda^4$ for Mie (haze) scattering and Rayleigh (gas) scattering, respectively. If photon-counting techniques are used, lidar sensitivity to the two types of scattering are then independent of wavelength (λ) and proportional to $1/\lambda^3$, respectively. Unfortunately, photon-counting detection becomes less efficient in the near infrared, and normally not feasible beyond 1100 nm.

If the atmospheric gas density is known, then the gas (Rayleigh) scattering is easily and accurately calculated, allowing a simple lidar measurement to be used for determination of the haze (Mie) backscatter coefficient. As measurement range increases, the haze scatter attenuation must also be accounted for using the nearer range results and theoretical or experimental relations between backscatter and attenuation. The uncertainties in the backscatter: attenuation ratio produce an accumulating backscatter coefficient error as lidar range increases.

If the atmospheric gas density is not initially known, then the combined gas plus haze scatter effects are best unfolded (separated) by making lidar measurements at two or more wavelengths. A two-color lidar system (such as G-BALS) emits two laser wavelengths which are very different, measures the Rayleigh plus Mie scatter at each wavelength, and then uses their different wavelength-dependence to separate the effects during data reduction. A differential absorption lidar (DIAL) system emits two laser wavelengths which are nearly the same except one coincides with an atmospheric major gas absorption line. Since now the haze effects are about the same at both DIAL wavelengths, the atmospheric dens.ty can be obtained, and this information then allows calculation of the haze scatter component from the off-line data. Finally, a Raman lidar system uses only a single wavelength laser light source, but measures the light scattered at not only the laser wavelength (Rayleigh plus Mie scatter), but also measures the much more weakly Raman-scattered light at the displaced wavelength corresponding to a major gas constituent of the atmosphere. Since the Raman-scattered lidar signal contains no haze scattered component while the laser wavelength scatter signal does, a proper data analysis provides both gas density and haze scatter coefficients.

(continued)

TABLE 13.1-1

13.1 PARTICULATES AND AEROSOLS (HAZE)

Haze Scatters Light and Limits Visibility

- Causes Mie-type scattering.
- o Interferes with lidar measurement of gas density.

Optimize Wavelength for Haze Scatter

- Short wavelength (λ)
  - Largest Mie effect (λ^{-1})
  - But gas scatter increases faster (λ^{-4})
- Long wavelengths
  - Poor lidar performance (equipment)
  - Mie effect small (λ^{-1})

Use of Lidar to Measure Haze

- Use simple lidar if gas density known.
- Otherwise use two wavelengths
  - Two-color lidar (G-BALS)
  - Differential Absorption Lidar (DIAL)
  - Raman lidar

Lidar Yields Haze Backscatter Coefficient

- Coefficient results from density data reduction
- Coefficient is function of many parameters
  - scatterer concentration
  - scatterer size distribution
  - scatterer particle shape
  - scatterer refractive index
  - scatterer absorption
  - scatterer layering

Depolarization of Backscattered Light

- Atmospheric gas shows little depolarization.
- Haze shows variable depolarization.
  - No depolarization from spheres (aerosol)
  - Much depolarization from ice crystals
  - Depolarization depends on particle variables, especially shape

(continued)

13.1 Particulates and Aerosols (continued)

If some lidar technique, such as G-BALS, provides Mie (haze) backscatter coefficients, it may be further desired to characterize the haze which produces the scatter. As seen in Table 13.1-1, so many haze parameters influence the backscatter coefficient that many lidar wavelengths must be used or many parameter assumptions must be made to allow conclusions about the haze concentration or type.

Depolarization measurements may be useful for qualitatively distinguishing between spherical (including water aerosol) and highly non-symmetric (including water ice) haze particulates.

As presently configured, the G-BALS lidar can be easily modified to provide depolarization information, although with the loss of some sensitivity and thus range. Also, two complete separate runs would have to be made for this information, with the angle of a polarizing filter re-adjusted for each run. This G-BALS modification consists of mounting a high quality polarizing filter in or near the lidar detection section above the dichroic mirror. A mounting location for such a filter has already been provided on the same base that holds the detector section collimating lens (item 10 of Figure 4.4-1). If depolarization measurements were of primary interest, more extensive changes might be made to speed the measurements, but then the atmospheric density measurements would be compromised.

TABLE 13.1-1

13.1 PARTICULATES AND AEROSOLS (HAZE) - CONTINUED

Conclusion

- Simple lidar systems provide limited qualitative information about haze particles.
- G-BALS
  - Provides haze backscatter coefficient
  - Haze particle information is limited
  - Can modify system to provide depolarization information

13.2 Species Concentrations

The measurement of minor species concentrations by lidar must depend on a wavelength-sensitive phenomenon which affects the lidar signal and is peculiar to the species of interest, gas "a". This can be accomplished by Raman lidar and if certain conditions are met, also by differential absorption lidar (DIAL) and resonance Raman lidar.

Since Raman lidar does not depend on any special relationship between lidar output and gas "a", it is generally applicable to species measurements. Also, calibration is simple to maintain because it is only necessary to measure the ratio between two lidar signals, one being the vibrational Raman signal for gas "a", and the other being the vibrational Raman signal from a constant major atmospheric component such as nitrogen. Unfortunately the vibrational Raman scatter cross sections are very small (about 0.001 of Rayleigh values), which combined with the very small atmospheric density of minor species, results in lidar ranges limited to a few kilometers or less. Rotational Raman wavelength shifts are generally too small to separate minor species signals from major species signals.

As described in Section 13.1, DIAL uses spectral line absorption by gas "a". Although dye lasers can be made to cover the visible and near UV with fairly high output energies, a suitable gas "a" absorption line may or may not exist depending on the spectrum of gas "a". Because gas absorption lines are very narrow, especially at high altitudes, the on-line laser output must have a known narrow line shape and a precisely controlled wavelength. Another complication is that the gas "a" line shape and therefore local absorption coefficient will vary with altitude due to variations in Doppler and collision broadening. Although this lidar method can show high sensitivity to a particular gas species, good range and range resolution are usually not both simultaneously possible.

There is a general relationship between DIAL penetration distance, R, and range resolution, Δr. For the concentration of an absorbing gas "a" to be measurable, its absorptivity over the range interval Δr must be at least several percent. If the round trip transmission over Δr is 0.90, the round trip transmission through an absorber thickness of $20\Delta r$ is $(0.90)^{20} = 0.12$. Thus, for those cases where gas "a" is localized near the lidar maximum range where the non-absorbed received signal is already small, Δr is limited to perhaps 5% of

(continued)

TABLE 13.2-1

13.2 SPECIES CONCENTRATIONS

Lidar Methods

- Vibrational Raman lidar
- Differential Absorption Lidar (DIAL)
- Resonance lidar

Vibrational Raman Lidar

- Generally applicable
- Allows ratio type measurement
- Scatter cross sections are small
- Requires most powerful lasers
- Limited range for minor species

DIAL

- Requires two adjacent laser wavelengths
- Need laser line:gas absorption line match
- Must control laser wavelength
- Narrow laser line shape
- Absorption line varies with altitude
- Often poor range or range resolution

Resonance Lidar Methods

- Scatter cross sections are increased
- Need laser line:gas strong absorption line match
- Must control laser wavelength
- Narrow laser line shape
- Scatter enhancement may vary with altitude

Conclusion for Minor Species Measurement

- Vibrational Raman Lidar
  - generally applicable
  - limited range
- DIAL and resonance lidar methods
  - good potential range
  - special conditions are difficult to meet
- G-BALS
  - Can be modified for Raman measurements
  - Results in limited range for minor species

13.2 Species Concentrations (continued)

the localized gas "a" thickness. At closer ranges, Δr could be <5% of gas "a" thickness. For those cases where gas "a" is uniformly mixed throughout the atmosphere, a small Δr requirement severely limits the maximum range of measurement. Similarly, a required large maximum range limits Δr to large values.

By combining the spectral coincidence requirement of DIAL with the measurement technique of Raman lidar, Raman scatter cross sections can be selectively enhanced to make resonance Raman measurements possible. Similarly, resonance fluorescence lidar may be possible in special cases. Although resonance lidar methods may now permit better range and range resolution than for DIAL, the laser/(gas "a") spectral match requirements and laser line control requirements are at least as difficult to meet as for DIAL systems. The resonance enhancement and fluorescence characteristics of any gas "a" must be fully determined before resonance lidar methods can be seriously considered.

As presently configured, G-BALS does not give species information. It could be most easily converted to a vibrational Raman lidar system by optimizing the laser output for either 532 nm or 355 nm, substituting a different dichroic mirror DM (see Figure 4.0-1) and different filters FG and FU, perhaps re-coating or replacing mirrors FM and SM, and perhaps changing some or all of the beam splitters BS and neutral filters NF. Such a modification will allow the measurement of minor species to only a few kilometers or less, depending on species and concentration.

13.3 Gas Temperature

Atmospheric temperatures can be obtained by many of those lidar techniques which allow the measurement of atmospheric species, specifically DIAL and especially Raman lidar (but now preferably rotational Raman). That is, any lidar method which can measure spectral features can obtain band or line shapes or line ratios, all of which depend, at least partly, on gas temperature.

Within the range limitations of Raman lidar, it probably can provide the best measure of gas temperature.[1,2] Here rotational Raman scatter measurements are preferred over vibrational Raman due to the larger scatter cross sections of rotational Raman and the better temperature sensitivity of rotational Raman at low (room) temperatures. In principle, the thermal information is obtained by making lidar measurements at only two different spectral locations on the same air rotational Raman branch (Stokes or anti-Stokes). However as discussed by Cohen et al.,[2] it is also advisable to measure the Rayleigh plus Mie scatter intensity to allow correction for filter "leakage". Since only relative intensities are needed, calibration is simplified and stable, and the results are not sensitive to haze. It should be possible to measure gas temperatures to better than $1^{o}K$.

As always, the DIAL method[3-5] requires two, or for temperature measurements at least three, laser output wavelengths, each of which must be very accurately controlled in wavelength. Kalshoven and Korb[5] are constructing a DIAL system to measure atmospheric temperature (and density) using the oxygen A-band absorption system in the far red and near infrared. For more comments on DIAL, see Section 13.2.

Another method for obtaining atmospheric temperatures is via atmospheric density measurements (such as are to be obtained from G-BALS), and then to relate atmospheric density to temperature assuming that the upper atmosphere follows the ideal gas law and is in hydrostatic equilibrium.[6] Hauchecorne and Chanin[6] claim to obtain temperature accuracies of 1 to $15^{o}C$ depending on altitude, up to the maximum limit of their Rayleigh:Mie lidar. A concern here is that density and temperature are not obtained independently.

(continued)

13.3 GAS TEMPERATURE

Lidar Methods

- Rotational Raman lidar
- Differential absorption lidar (DIAL)
- Via atmospheric density lidar measurements

Rotational Raman Lidar

- Basis: Air Raman band shape
- Simultaneously measure three wavelengths (λ)
  - Rayleigh signal
  - Rotational Raman (RR) small λ shift
  - Larger λ shift from same RR branch
- Needs only relative intensities
- Not influenced by haze
- Temperature accuracy $1^{o}K$ (est.)
- Altitudes to perhaps 50 km

DIAL

- Basis: temperature-sensitive line ratios or shapes
- Can use oxygen A-band (far-red)
- Needs 2 or 3 controlled laser wavelengths
- Typical DIAL requirements for laser

Atmospheric Density Lidar Systems

- Rayleigh/Mie lidar (G-BALS)
- or Raman lidar
- Basis: calculate temperature from density results
  - assume hydrostatic equilibrium
  - assume ideal gas law
- Temperature accuracy 1^{o} to $15^{o}K$ (70 km)

Conclusions for Gas Temperature

- Temperature from design G-BALS via density
  - Est. accuracy 1^{o} to $20^{o}K$
  - Est. altitudes to 95 km
- If modify G-BALS for rotational Raman lidar temperatures
  - Est. accuracy about $1^{o}K$
  - Est. altitudes to 50 km

13.3 Gas Temperature (continued)

As indicated above, the present G-BALS design will provide the atmospheric density data to allow calculation[6] of atmospheric temperatures to altitudes of about 95 km with an accuracy of perhaps 1 to 20°K (estimated). Alternately, the G-BALS lidar can be modified for the rotational Raman measurement of temperature with an accuracy of about 1°K and to a maximum altitude of perhaps 50 km (estimated). The modification of G-BALS to Raman measurements is briefly described at the end of Section 13.2, although the replacement part specifications are different for the rotational Raman measurements described here.

References

1) John Cooney, J. Appl. Meteor. 11, 108 (1972).

2) A. Cohen, J. Cooney, and K. Geller, Appl. Opt. 15, 2896 (1976).

3) James Mason, Appl. Opt. 14, 76 (1975).

4) I. Barton and J. Marshall, Optics Letters 4, 78 (1979).

5) J. Kalshoven and C. Korb, NASA Technical Memorandum No. 79538 (U.S. GPO, Washington, DC, 1978).

6) A. Hauchecorne and M. Chanin (submitted to Geophysics Research Letters).

13.4 Winds

Doppler and correlation lidar techniques show promise for the remote active measurement of wind velocity.

In the reference beam-Doppler (RBD) technique, the Doppler shift of light scattered from particles in a gas is measured by heterodyning it against unshifted "reference" light from the same source (laser). In a single ended arrangement (lidar) this technique is sensitive only to the velocity component parallel to the direction of observation. Furthermore, RBD requires a light source with coherence length comparable to the working distance, which eliminates most pulsed lasers. These characteristics reduce the potential of the RBD technique for meteorological measurements.

In the differential Doppler (DD) (or cross-beam) technique, two beams of laser light are projected so as to intersect at the measurement region. Light scattered from one beam by a moving particle will experience a different Doppler shift than light scattered from the second beam, because of the different directions of propagation of the two beams. The two components of light automatically heterodyne at any light detector. Alternatively, the signal frequency may be explained as arising from the motion of the particle through the interference pattern (fringes) created by the intersection of the two beams. These explanations have been shown to be equivalent. In a single ended configuration, the DD technique is sensitive to velocity components perpendicular to the direction of observation. Furthermore, the DD technique does not require beams of long coherence length, and can be implemented with pulsed lasers to provide discrimination against background light. Direction information can be obtained, for example, by using a third beam or rotating the two incident beams. Unfortunately, the fringe spacing for upper atmosphere lidar use (1-10 cm), combined with likely wind speeds will require use of a cw laser or very rapidly pulsed laser. Also, the large ranges of interest here (>20 km) require signals from many particles (clouds) which are probably larger than the fringe spacing.

In the optical correlation technique two parallel beams of light are projected upwards. The time dependence of scattering from particles in one beam is correlated with scattering from the other beam. The correlation analysis provides a measure of time required for propagation of fluctuations from one

(continued)

13.4 WINDS

Reference Beam Doppler Lidar

- Heterodyne with local oscillator
- Velocity measured along lidar axis
- Critical optical alignments
- Very difficult with pulsed lidar (coherence, delay)

Differential Doppler (Cross-Beam) Lidar

- Laser output split to two beams
- Measure velocity where beams intersect (fringes)
- Velocity measured perpendicular to lidar axis
- Need cw or rapid pulsed laser source
- Upper atmosphere phenomena too large?

Optical Correlation Lidar

- Need two laser beams (no intersection)
- Make repeated lidar measurements, both beams
- Look for correlation of signal variations
- Velocity measured perpendicular to lidar axis
- Repetitively pulsed lidar is OK
- May need short integration periods

G-BALS Use

- Optical correlation techniques possible
- One wavelength sufficient
- Need second laser beam
- Considerable modification of detection section
- Alternately, use a second G-BALS
- Sensitivity uncertain

beam to the other, which yields a measure of wind velocity perpendicular to the line of sight. Direction information is obtainable by rotating the orientation of the beams.

The G-BALS lidar appears to be most compatible with the optical correlation wind measurement method. Conversion of the designed system to such a capability would require optimizing the laser for green output only, splitting the green output to two collimated non-overlapping beams, and then greatly modifying the field stop and detection section so both beams are separately observed and recorded. However, the physical size and velocity of upper atmospheric phenomena may instead require the laser beams to be so far apart that two separate lidar systems are needed, each with a single beam.

APPENDIX A

SHUTTER WHEEL ASSEMBLY DYNAMIC ANALYSIS

APPENDIX A

SHUTTER WHEEL ASSEMBLY DYNAMICS ANALYSIS

See Drawing 47J252280 (Item 4)

The shutter wheel assembly being the only moving part in the detector section requires some special design due to its rotational speed (approx. 7000 rpm). The shutter wheel assembly is made up of two 11.00" dia. x 0.090" discs joined by a 1.00" dia. x 0.065" wall tube 24.63 inches long. All parts are 304 S.S. Each end is supported on a radial/thrust ball bearing (item 34). At the top of the detector section the shutter wheel assembly is driven by means of a timing belt from a motor (item 30) mounted to the rear of the detector section.

Drag and Power

First we consider the drag induced on the two 11" dia. shutter wheels rotating at 7000 rpm in air at 68^{o}F.

$$\text{Power} = C_m \, (0.5 \, \rho a^5 \, w^3) \, \frac{\text{ft-lb}}{\text{sec}}$$

$$C_m = 0.146 \, R^{-1/5}$$

$$\text{Reynolds No.} = R = \frac{w \, a^2 \, \rho}{\mu}$$

w = angular velocity, rad/sec

ρ = mass of gas per unit volume

a = radius, ft

μ = coefficient of viscosity

C_D = drag coefficient of cylinder

C_m = drag coefficient of disc

ℓ = length, feet

$$R = \frac{w \, a^2 \, \rho}{\mu}$$

$$= \frac{733 \text{ rad/sec } (0.4583 \text{ ft})^2 \, (0.002378 \text{ slugs/ft}^3)}{0.38 \times 10^{-6} \text{ slugs/ft-sec}}$$

$$R = 963{,}456$$

$$C_m = 0.146 \, R^{-1/5}$$

$$= 0.146 \, (963{,}456)^{-1/5}$$

$$C_m = 9.281 \times 10^{-3}$$

$$\text{Power} = Cm\ (0.5\ \rho a^5\ w^3)\ \frac{\text{ft-lb}}{\text{sec}}$$

$$= 9.281 \times 10^{-3}\ (0.5)(0.002378)(0.4583)^5\ (733)^3$$

$$\text{Power} = 87.869\ \text{ft-lb/sec}$$

$$HP = \frac{(87.869\ \text{ft-lb/sec})(60\ \text{sec/min})}{(33{,}000\ \text{ft-lb/min})}$$

$$\underline{HP = 0.1598\ \text{per disc}}$$

Total horsepower required to overcome wheel drag is 2(0.1598) or 0.32 HP.

Drag induced on the shaft due to rotating at 7000 rpm in air at 68^oF(1) is similarly calculated.

$$R = \frac{w\ a^2\ \rho}{\mu}$$

$$= \frac{733(0.04167)^2\ (0.002378)}{0.38 \times 10^{-6}}$$

$$R = 7{,}963.61$$

$$C_D = 0.008$$

$$\text{Power} = C_D\ \pi\ \rho a^4\ w^3\ \ell$$

$$= (0.008)\ \pi\ (0.002378)(0.04167)^4 (733)^3\ 2.08$$

$$\text{Power} = 0.1476\ \text{ft-lb/sec}$$

$$HP = \frac{0.1476(60)}{33{,}000}$$

$$\underline{HP = 2.68 \times 10^{-4}}$$

This value is so low it can be ignored.

To provide a margin of safety a 1/2 horsepower motor is recommended for driving the shutter wheel assembly.

Shaft Resonance

Using $C/10^4 = 31.73$ for a hinged-hinged beam and radius of gyration for a tube $K = 0.707\ r = 0.707(0.5) = 0.3535$ in., we find the natural frequency of the 1" dia. shaft to be 220 cps, or the allowable rpm - 220 C/sec (60 sec) = 13,200 rpm. Since this is greater than the 7000 rpm operating speed the shaft is more than adequate.

Bearing Loads

The loads on the two bearings will be very low as can be shown:

$$P = f_p \times \frac{Q}{R} = \text{Load}$$

f_p = belt tension factor = 5

$$Q = \frac{63{,}000 \times \text{H.P.}}{N} \text{ lb-in}$$

R = pulley pitch radius = 0.764 in.

N = shaft speed = 7000 rpm

H.P. = horsepower = 0.5

$$Q = \frac{63{,}000 \times \text{H.P.}}{N}$$

$$= \frac{63{,}000 \times 0.5}{7{,}000}$$

$$Q = 4.5 \text{ lb-in}$$

$$P = \frac{Q}{R}$$

$$P = \frac{4.5 \text{ lb-in}}{0.764 \text{ in}}$$

$$P = 5.89 \text{ lb (use 5.9 lb)}$$

Therefore:

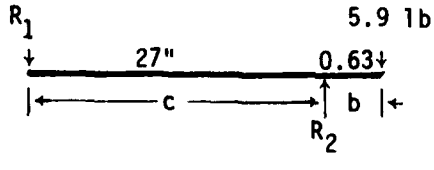

R_1 and R_2 are bearing reactions

$$R_1 = P\,\frac{b}{c} = 5.9\,(\frac{0.63}{27.0})$$

$$\underline{R_1 = 0.138 \text{ lb}}$$

$$R_2 = P\,(\frac{b+c}{c}) = 5.9\,(\frac{0.63 + 27}{27})$$

$$\underline{R_2 = 6.038 \text{ lb}}$$

At 7000 rpm the bearings (item 34) will take a 90 lb radial load which is well above our maximum load of 6 lb. The thrust load will be equal to the weight of the shutter wheel assembly which is 9.0 lb. The bearing thrust load capacity is 50% of its radial load capacity or 45 lb which is also greater than the 9 lb applied thrust load.

Shutter Wheel Stress

The stress induced in the discs due to rotation is:

a) Radial Stress

$$\sigma_{r\ max} = \frac{3 + \mu}{8}\ \frac{pw^2(b-a)}{g}$$

μ = Poisson's ratio = 0.305

p = weight of material per unit volume - 0.285 lb/in^3

g = acceleration due to gravity = 386 in/sec^2

a = inside radius = 1.0 in

b = outside radius = 5.50 in

w = angular velocity = 733 rad/sec

$$\sigma_{r\ max} = \frac{3 + 0.305}{8}\ \frac{(0.285 \text{ lb/in}^3)(733 \text{ rad/sec})^2(5.5-1)}{386 \text{ in/sec}^2}$$

$$\underline{\underline{\sigma_{r\ max} = 3{,}319 \text{ PSI}}}$$

b) Tangential Stress[3]

$$\sigma_{t\ max} = \frac{3 + \mu}{4} \frac{pw^2}{g} \left(b^2 + \frac{1 - \mu}{3 + \mu} a^2\right)$$

$$= \frac{3 + 0.305}{4} \frac{(0.285\ lb/in^3)(733\ rad/sec)^2}{386\ in/sec^2}$$

$$\left[(5.5\ in)^2 + \frac{1 - 0.305}{3 + 0.305} (1^2)\right]$$

$$\underline{\sigma_{t\ max} = 9{,}984\ PSI}$$

Both values of radial and tangential stress are well below the allowable value of 30 KSI for 304 S.S. and therefore safe.